TRANSMISSION OF ELECTROMAGNETIC WAVES BY DISCRETE RANDOM MEDIA

by

LAWRENCE MAXWELL MONARI

A dissertation submitted to the Graduate Faculty in Physics in partial fulfillment of the requirements for the degree of Doctor of Philosophy, The City University of New York.

1973

This manuscript has been read and accepted for the Graduate Faculty in Physics in satisfaction of the dissertation requirement for the degree of Doctor of Philosophy.

May 11, 1973
date

Irving Lerner
Chairman of Examining Committee

May 15, 1973
date

Marvin H. Mittleman
Executive Officer

Leo Diesendruck

Ferdinand Shore

George Papanicolaou

Marvin Mittleman
Supervisory Committee

The City University of New York

Abstract

TRANSMISSION OF ELECTROMAGNETIC
WAVES BY DISCRETE RANDOM MEDIA

by

Lawrence Maxwell Monari

Adviser: Professor Irving Lazar

A simple one-dimensional model for transmission of electromagnetic waves in a stratified random medium is investigated experimentally. The model consists of a stack of randomly separated plane parallel dielectric slabs having nearly identical thicknesses. The mean power transmission coefficients of the stack are compared with the values predicted by Papanicolaou's approximation, the first order Born approximation, and the exact solution of Maxwell's equations. The radiation is normally incident and plane polarized. The wavelength is approximately 5 mm.

Measurements of the mean power transmission coefficient made on another more complex model are compared with values predicted by the Papanicolaou approximation and the Born approximation for a plane stratified dielectric medium. This model consists of a stack of randomly separated plane-parallel dielectric slabs; a single long thin conducting strip is mounted on each slab. The strips are aligned parallel and in line with one another. The radiation is normally incident and plane polarized with the electric field vector parallel

to the strip axis.

Equipment to automatically generate random slab configurations and measure power transmission coefficients is also described.

PREFACE

Electromagnetic waves have been used in the past century to probe natural processes to determine the laws governing their behavior. Many processes occurring in nature are random. Attenuation in the original direction of propagation is a typical characteristic of wave interactions with matter. Indeed, the complex wave interaction with matter is itself a random process.

Very often a prior knowledge, of the properties of the radiation in free space and its interactions with simple fixed material configurations, allows the prediction of more complex propagation through a random medium. Transmission through plane stratified fixed dielectrics has been treated extensively by Brekhovskikh et. al and an exact means of solution derived. Transmission through a plane stratified random dielectric medium has been treated by Papanicolaou et. al and an approximate statistical means of solution developed.

The present investigation is concerned with acquiring experimental information on the mean power transmission of electromagnetic waves through both random plane stratified dielectric media and random conducting media. The work is unique in the sense that, although the medium is random, the location of each scatterer comprising the medium is known. In addition, the statistics of the medium are deterministic in that both the number and location probability

densities of the scatterers can be preset. This knowledge permits treating the scatterers comprising each configuration of an ensemble as though they were fixed, and therefore the problem lends itself more closely to solution by the exact method. Even complex geometries of fixed material arrays which cannot be solved exactly, can be done so approximately by application of asymptotic techniques such as are developed in Keller's work entitled "A Geometrical Theory of Diffraction." The approximation converges rapidly, for many problems, to what may be considered the exact solution.

For the stratified dielectric media the experimental, statistical and exact values are compared. For the conducting medium, observations concerning the similarity between the experimental values and approximate statistical predictions are made.

The rate at which data is acquired is intensified by the use of a large digital computer accessible on a time sharing basis via the telephone lines. The computer calculates, directs and controls every aspect of all the fully automatic experimental procedures. Both mechanical and electronic equipment was designed and fabricated to implement the above operations.

Acknowledgements

I am particularly grateful to Dr. Irving Lazar for the role he's played as my mentor. Through his diligence and abundant guidance this research has been successfully completed.

Dr. George Papanicolaou, faculty member at the Courant Institute of Mathematical Sciences at New York University, provided continual theoretical advice, encouragement and inspiration for this work. I join with the C.U.N.Y. Physics Department in thanking him for all he has done. His efforts are grately appreciated.

The mechanical components comprising this project were machined and assembled almost exclusively by Mr. Edward Kuhner with both expeditiousness and proficiency. He has consistently offered valuable design suggestions to reduce material costs, shorten machining time, and improve system performance. Mr. Walter Koch, who was primarily responsible for the many photographs appearing in this thesis, meticulously fabricated the complex harness arrangements and wired many of the electronic system interfile cables. In addition, he has contributed his skill to almost every other aspect of the electronics. Both he and Mr. Edward Kuhner constructed the aluminum framework which supports the mechanical equipment hanging from the laboratory ceiling. Without the assistance of Messrs. Kuhner and Koch this experiment could not have been materially developed. It was through their combined efforts that the work evolved.

Dr. Louis De Acetis provided expert advice and guidance in writing many of the computer programs, and in numerous other features of the system software. His availability for consultation on these, as well as for experimental and theoretical aspects of diffraction theory, was truly an asset.

Mr. Kenneth Pospisil furnished formal information on the use of the Xerox Sigma Seven Computer. His advice and involvement in the derivation of mathematical computer techniques together with his allowance of lengthly computer time sharing intervals during periods of data acquisition were important factors in the projects' development.

Mr. Charles Fries, who played a prime role in processing the photographs, facilitated the purchase of hundreds of items used in this project. His consciencious interaction with vendors permitted the timely physical realization of this experiment.

Dr. Shore provided guidance and suggestions on many experimental features of the experiment, especially the normalization procedures for the transmission measurements and the detection of standing waves.

Dr. Diesendruck furnished a computer program for the exact solution of the interaction of electromagnetic waves with a plane-stratified medium. This provided a more versatile much needed means to cross-check existing software methods of solution.

Dr. Marvin Mittleman provided early reference material from sources not readily accessible to the author. His thoughtful suggestions and advice were instrumental in outlining our eventual affiliation with the Courant Institute.

I wish to thank Dr. J. B. Keller, faculty member at the Courant Institute of Mathematical Sciences at New York University for supplying much appropriate referance material, and for his recommendation of Dr. George Papanicolaou as a member of my examining committee.

I wish to thank the Queens College Physics Department science assistants-Mr. John Behrens, Mr. Ralph Johnson, and Mr. Jack Kohl for the many diversified services they performed in the projects' behalf. I especially wish to thank Mr. Paul Schaedler for machining work done early in the projects' development; and Mr. Charles Spiteri, who together with Mr. Edward Kuhner constructed partitions in the anechoic chamber and have helped maintain the equipment during its use.

I wish to thank the Queens College Physics Department for appropriating the necessary funds in support of this project, and the Chemistry Department for the protective plating of various precision machined mechanical components.

Gloria Monari, my wife, judiciously typed the manuscript. Her efficacy and abiding support in this and in my overall research effort is heartfelt.

TABLE OF CONTENTS

APPENDIX

LIST OF TABLES

LIST OF TABLES

LIST OF FIGURES

LIST OF FIGURES

LIST OF FIGURES

Page

LIST OF FIGURES

LIST OF FIGURES

APPENDIX (FIGURES)

Page

SUMMARY OF PHOTOGRAPH NOTATIONS IN THE FIGURES

A - collimating aperture.

B - polystyrene slab

C - collimating aperture

D - longitudinal table

E - upper ball bushing bearing block.

F - carriage assembly mounting block.

G - picker motor

H - aluminum supporting structure

J - aluminum channel

K - picker rod

L - picker motor arm

M - collimating aperture

N - klystron power output detector

O - polystyrene slab

P - XTAL field detector pedestal

Q - 45^{o} dielectric sheet

R - detector horn

S - E-H tuner

T - micrometer slide

U - precision rack

V - rotary solenoid arm

W - rotary solenoid

X - carriage drive motor

Y - carriage potentiometer

Z - needle bearing block

AA - transmitter electronics file

BB - digital voltmeter

CC - upper control panel

DD - multiplexer electronics file

EE - lower control panel

FF - receiver electronics file

GG - solenoid & picker motor servo electronics file

HH - carriage motor servo electronics file

a - lower carriage rail

b - upper carriage rail

c - upper carriage plate

d - klystron rectangular waveguide

e - collimating aperture on parabolic mirror

f - collimating aperture for klystron power detector XTAL

g - conducting strip

h - styrofoam slab

i - horizontal plate of longitudinal table "tee"

j - vertical plate of longitudinal table "tee"

m - mounting tab

n - counterweight holes

q - mounting tab

r - rotary table assembly

t - building girder

y - crystal detector

I. Introduction

Throughout all nature there are problems of transmission and reflection from media whose properties vary in a random manner. The subject of wave propagation through a non-random or deterministic medium has been investigated by many authors.[1-6]

It is often very difficult in a physical system to measure basic parameters accurately due to the fact that the system is subject to internal or externally imposed random variations. These variations may be electrical noise, humidity, velocity, acceleration, thermal fluctuations, etc. Today there is general interest in various aspects of the propagation of electromagnetic waves through systems having random characteristics as evidenced by myriads of papers, predominately theoretical, written on the subject.[7-11]

Wave propagation in discrete random media is of considerable interest for such problems as molecular scattering of light, dielectric constant of nonpolar gases, radiative transfer and physical chemistry.

The theory of electromagnetic wave propagation in random media is concerned with linear wave motion in media whose properties have so complicated a space and time dependence that the motion can only be described statistically. The mathematical formulation of the problem leads to linear partial differential equations whose coefficients are random functions of space and time, a problem which belongs to the class of linear stochastic equations. Unfortunately, the theory of

linear partial differential equations with non-constant coefficients is still very incomplete, and for random coefficients the situation is even worse, so that at present, a rigorous theoretical study of wave propagation in random media is out of the question.[12]

In some recent papers the problem of wave transmission and reflection from a one-dimensional randomly fluctuating medium has been considered, and a statistical method of solution has been given.[13-15] The characteristic feature of this problem is the presence of a random (stochastic) term, namely, the refractive index in the governing equations. An experimental model of a random media which retains the characteristic features of wave propagation problems, but is simple enough to give a definite answer above the validity of the theoretical method, is investigated in this dissertation.

The model consists of a stack of plane parallel dielectric slabs having nearly identical thicknesses. Two different slab materials are considered i. e. styrofoam and polystyrene. The index of refraction of a styrofoam slab is approximately that of free space, and its thickness is large compared to a wavelength, i. e. 5.23 mm. The index of refraction of a polystyrene slab is large compared to that of free space, and its thickness is of the order of a wavelength. The mean power transmission of an ensemble is calculated as the arithemetic mean of the individual power

transmission measurements characterizing each random slab configuration, and plotted as a function of the length of the random medium; the length of the random medium is approximately proportional to the number of slabs comprising an ensemble. Measurements are made for both random and fixed slab positions relative to nominal slab locations. The power transmission of a slab configuration is measured for nearly normally incident plane polarized radiation by a crystal detector located in the far field, i. e. 500 wavelengths distant. The experimentally determined mean power transmission coefficients are compared with values predicted by both contemporary and classical theory, i. e. the Papanicolaou approximation, Born approximation and the exact solution of Maxwell's equations.

Measurements of the mean power transmission coefficient made on another more complex model are compared with values predicted by contemporary theory for plane stratified dielectric media. The model consists of a stack of randomly separated plane-parallel dielectric slabs; a single long thin conducting strip is mounted on each slab. The strips are aligned parallel and in-line with one another. The electric field vector is parallel to the strip axis. Although the Papanicolaou theory was not intended to treat conducting media, the theoretical predictions it affords are in good agreement with experimental measurements.

The random slab configurations were prepared by an electro-mechanical apparatus specifically designed and

constructed for this purpose. The apparatus hangs from the laboratory ceiling. It is interfaced with a digital computer, on a time sharing basis, by an electronics system. The electronics system was designed and built to permit the computer, when suitably programmed, to acquire data and run the experiment automatically.

The expression for the mean power transmission referred to in the present work as the "Papanicolaou approximation" is the result of the combined contributions of G. C. Papanicolaou, J. B. Keller and J. A. Morrison.

2. EXPERIMENTAL APPARATUS

A. Description of the Mechanical System

The mechanical system (see Figs. 1-4, 6-9, 29) is composed of two (2) sections, e. g. rotary table assembly (r) and longitudinal table assembly (D).

a) The purpose of the rotary table assembly is as follows:

(1) serves as a fixture on which the longitudinal table assembly is mounted.

(2) provides a mechanism for adjusting the angle of the longitudinal table assembly relative to the incident electromagnetic field (adjusts the angle of incidence).

The rotary table is a mechanism for adjusting the angle of the longitudinal table relative to the incident electromagnetic field. The rotary table assembly is housed in a well built into the laboratory ceiling. It is mounted on a 3 inch aluminum I-beam framework (H). The framework is suspended from the 18 inch girders which traverse the laboratory building. This structure guarantees stability of the 500 lb. longitudinal table mounted on and beneath the rotary table, and for the accompanying slabs which the longitudinal table supports. The dimensions of the rotary table and longitudinal table are roughly 2 ft. X 2 ft. X 1 ft. high, and 1 ft. X 1 ft. X 5 ft. long, respectively.

The base of the rotary table assembly is a 2 ft. X 2 ft. X 1 inch thick plate of aluminum flat ground stock. The

plate thickness was chosen to prevent flexure. A stepper motor is mounted on this base. It drives a 1" iron worm gear which in turn drives a 12.5" bronze spur gear. The worm is mounted in a thrust bearing block. The spur gear is mounted on a 2 3/4" diameter stainless steel flanged shaft. The shaft is mounted in two pre-loaded thrust bearings to minimize play. The flange has a 4" diameter. The flange turns at approximately two (2) deg./sec. when the stepper motor is driven at the highest speed. Leveling of the base and flange is accomplished by adjustment of three (3) jackscrews. The longitudinal table assembly is bolted onto the underside of the rotary table assembly 4" flange.

b) The longitudinal table assembly (D) is comprised of two major sub-assemblies.

   (1) The carriage sub-assembly rectilinearly positions the dielectric slabs relative to one-another in a configuration programmed in the central computer.

   (2) The solenoid and picker motor sub-assembly selects the number of slabs in a configuration programmed in the central computer.

The longitudinal table is composed of two 3/4" thick, 10" wide X 57" long aluminum plates (i, j) bolted together to form a "tee"; this structure provides rigidity, freedom from warping and is relatively light in weight.

The plates are made from flat ground stock to provide reference surfaces for machining and for mounting hardware.

The longitudinal table (l.t.) supports ten (10) carriage mechanisms (c). The l.t. has two sides. The layout of the l.t. is symmetrical. Five carriages are mounted on each side. This permits carriages on each side to pass one-another. Consequently, appropriately chosen scatterers hung from their respective carriages may be made to locate themselves abreast of one another.

Each carriage has two (2) precision surfaces machined onto a mounting block (F).

The slabs (B,O) are mounted on and hung from each carriage block. Therefore, as many as twenty (20) slabs can be accommodated in a stack.

The carriages, and consequently the slabs, run horizontally up and down the length of the longitudinal table. The airspace between slabs on neighboring carriages is adjusted by altering the location of each carriage.

The carriage chasis is composed of two 3/16" aluminum plates bolted together. The plates are made from flat ground stock. The outer plate provides a precision reference surface for mounting and adjustment of carriage

hardware.

The carriage servo potentiometer (Y) is mounted on the carriage chasis plate. It is a 15 turn, 10K Ohm potentiometer having a linearity of 0.01 percent. It provides a voltage analog of carriage location on the longitudinal table. Mounted on the $\frac{1}{4}$" potentiometer shaft is an anti-backlash gear. This gear meshes with a precision stainless steel rack which runs the length of the longitudinal table. The gear reduces positional errors due to gear-rack backlash.

The carriage drive motor (X) is a permanent magnet continuous duty reversible motor having an output torque of 500 oz./in. It is mounted on the outer carriage chasis plate. Mounted on the 5/16" motor shaft is a stainless steel spur gear which meshes with the longitudinal table rack. The motor provides each carriage assembly with independent positioning capability.

A rotary solenoid (W) is mounted in a rotation block (F) bolted to the inner carriage chasis plate. Rotary motion is accomplished through use of a needle bearing (Z) mounted on the outside of the lower ball bushing. The solenoids are of the 95° rotary type and have brass arms (V) mounted to their shafts. The minimum starting torque is $\frac{1}{4}$ in./lb. The solenoid allows latching of slabs out of the field by engaging the solenoid arm in an aluminum

channel (J) located on the side of the longitudinal table. The brass-aluminum material combination was chosen to prevent galling.

The ball bushings (E) are mounted in bearing blocks which are bolted to the lower carriage plate. Each ball bushing rides on a 1" precision stainless steel shaft (a, b) which runs the length of the longitudinal table. The shafts (rails) are aligned parallel to one-another. The resulting motion is virtually free of friction allowing a fast carriage servo response.

A micro-switch is mounted on each carriage. The micro-switch is actuated if the carriages collide accidentally with one-another. The micro-switches are wired in parallel with a 26V power relay. As a safety measure, to prevent gear and rack damage, if a collision occurs the relay is tripped and the system is shutdown.

The picker motor (G) is a reversible split series motor of the rotary actuator type having a torque of 500 lb./in. and travel of 90^{o}. On its $\frac{1}{2}$" splined output shaft is mounted an arm having a stainless steel pin which rides in a slot machined into another arm (L) which drives a 3/4" stainless steel rod (K). This rod runs the length of the longitudinal table and is held at the other end by a similar arm. Each arm rotates on a ball bearing, which is mounted on the lower stainless steel rail. The

picker motor, when activated rotates the picker rod (K) which rotates slabs into and out of the field. Each time the picker motor is actuated it rotates all of the slabs out of the field. Slabs are returned to the field depending on the state (on/off) of their respective rotary solenoids. These states are determined in the central computer program.

B. Description of the Electronics System

The electronics system (see Figs. 13, 29) is composed of six (6) sections, e. g. transmitter, receiver, multiplexer, solenoid, and picker servo, carriage servo and rotary table servo electronics subsystems.

a) The purpose of the transmitter electronics (AA) is as follows:

(1) scan and code measurements made by a digital voltmeter (DVM); and relay the coded measurements to a telephone modem for transmission via telephone lines to the central computer.

(2) transmit to central computer signals indicating the completion of programmed experimental operations.

Transmitter operation:

The DVM digitizes analog signals from the carriage and rotary table potentiometers. These signals are position and angle analogs for the carriages and the rotary table respectively. The DVM output is a parallel 16-bit 122'4 code. The DVM has a high impedance input (10 meg Ohms typ.) and also monitors the analog "field" and "klystron" detectors. The output voltage levels of the DVM are incompatible with the COS/MOS integrated circuits found in the transmitter ("1" = -0.6V, "0" = -28V for DVM), ("1" = +10V, "0" = 0.V for IC'S) so that interfacing circuitry is required. The transistor input-out voltage levels are

-0.6V and -28V to 0.0V and +10V respectively.

Space is conserved and versatility gained by scanning the DVM parallel-output digit by digit; the thousands, hundreds, tens and units digits are scanned sequentially in that order.

The parallel 122'4 code generated by the DVM is incompatible with the 1248 ASCii code used by both teletype and central computer. The 122'4 DVM code is converted to a 1248 code and the coded parallel information is gated to an output shift register for serial transmission.

The transmitter is coupled to a telephone modem via a driving circuit. This circuit interfaces the transmitter COS/MOS logic circuitry by providing sufficient drive current to operate the modem. The telephone modem couples the system electronics to the central computer via the telephone lines.

b) The purpose of the receiver electronics (FF) is as follows:

(1) permit entry of programmed codes (commands, instructions) from central computer, via modem.

(2) decode and store commands in a form appropriate for control of the experiment.

(3) test instructions for proper format, and reject all improper instructions such as may be due to noise.

(4) reject commands sent while any servo system is in operation.

(5) recognize servo system control codes and alert appropriate servo electronics.

(6) input analog signals from klystron power output detector and field detector; select and amplify analog signals.

Receiver Operation:

The output voltage levels of the modem are incompatible with the COS/MOS integrated circuits found in the receiver so that transistor interfacing circuitry is required. This circuitry transforms output voltages at the modem to levels suitable for driving the receiver.

The leading edge of each ASCii character sent by the central computer triggers an asynchronous clock which drives three series 8-bit (serial in/parallel out) shift registers. The clock is synchronized to drive only the central 8-bit ASCii code content of each character. Consequently, only the central 8-bit ASCii code of each character is stored in the shift registers. The total capacity of these three registers is three 8-bit characters. The content of these registers is compared, on the fly, with codes stored in two 4-bit digital comparison circuits and one 8-bit comparison circuit. The character in the first (leading register is compared, on the fly, with a character stored in the 8-bit digital

comparison circuit. The characters in the second and third registers are compared on the fly with each other in the two 4-bit digital comparison circuits. A character sequence meeting the above comparison conditions triggers an asynchronous clock which shifts the four bits of the second character into memory.

The 24-bit memory consists of three series 8-bit (serial in/parallel out) shift registers. In operation, the leading 4 bits carry a "servo function" code which activates the servo electronics appropriate to that code. The next 16 bits are four 1248 BCD characters (4 digits) which provide carriage, rotary table, and solenoid servo information for slab location and angle selection. The 1st, 2nd, 3rd, and 4th digit are thousands, hundreds, tens and units digits respectively. The last 4 bits carry a "start" code. When the "servo function" and "start" codes are present in their appropriate register locations, a command is sent to close the data input gate to the receiver. Therefore once a servo operation is underway, its termination prior to successful completion is prevented.

c) The purpose the multiplexer electronics (DD) is as follows:

   (1) alert "transmitter" and "receiver" electronics of compliance of servo systems with central computer commands.

   (2) provide "stop" and "sense" commands to both "carriage" and "rotary table" servo electronics.

(3) digitally compare voltages from "carriage" and "rotary table" servo potentiometers with desired programmed location commands stored in "receiver" memory.

(4) scan and actuate carriage, solenoid, rotary table, field detector, and klystron power output detector electronics.

Multiplexer operation:

Output voltages from the rotary table servo potentiometer and the ten carriage servo potentiometers are interfaced individually to a 16-bit four digit analog/digital converter via eleven analog gates.

An analog scanner selects the appropriate gate and applies its respective potentiometer voltage to the analog/digital converter via an operational amplifier. The operational amplifier has a high input impedance (20 meg Ohms typ.) and low output impedance (1 Ohm typ). It matches the 10K Ohm servo potentiometer outputs to the 10K Ohm analog/digital converter input. A pulse generator serves as a clock to drive the analog/digital converter.

The 16-bit four digit output from the analog/digital converter is in parallel BCD 1248 code. It is transformed to complementary BCD 1248 code, to be compatible with the 16-bit four digit number in complementary BCD 1248 code at the output of the receiver memory by a transistor circuit whose parallel 16-bit output is fed to the digital comparator input. The 16-bit parallel output of both the

transistor circuit and receiver memory are compared with respect to size and equality by a digital comparator circuit.

The output from the digital comparator circuit provides two kinds of commands to the carriage and rotary table servo electronic logic circuits i. e. a "sense" command and a "stop" command. When the 4 digit number received from the central computer and stored in memory is identical to the 4 digit output of the analog/digital converter, then the "stop" signal is present. When the 4 digit number stored in memory is greater than or equal to the 4 digit output of the analog/digital converter then a CCW signal is present; otherwise a CW signal is present.

If the "stop" output signal is present for more than 0.3 seconds then a pulse is generated which clears the "servo function" code from the memory; and triggers the transmitter output shift register to scan and transmit "?????". This code is recognized by the central computer as indicating successful completion of a programmed task, or compliance with a central computer command. The 0.3 second time delay insures that pulses, due to false commands such as noise or servo overshoots, are not generated which may instruct the central computer that a programmed instruction has been complied with. Clearing the "servo function" code from memory opens the input gate to the receiver allowing new instructions from the central computer to be admitted.

d) The purpose of the solenoid and picker motor servo electronics (GG) is as follows:

(1) select the total number and sequence of slabs comprising each configuration according to an arrangement programmed in the central computer.

(2) alert electronics system to instruct central computer of the successful completion of the above task.

Solenoid and picker servo operation:

The solenoid and picker motor servo electronics system controls the picker motors, on both sides of the longitudinal table. To prepare a configuration with the desired sequence and number of slabs, the central computer must originate the proper character sequence. This sequence when stored in the receiver memory consists of the 4-bit "solenoid-servo function" character, a 16-bit 4 digit code, representing those slabs chosen for the stack and a 4-bit "start" character. When the "solenoid servo function" character and "start" character are present in their appropriate memory register locations, voltages are applied to a gate circuit from a "function" comparator circuit and a "start" comparator circuit. These voltages, in addition to one applied on the gate circuit by an analog scanner circuit actuate a picker SCR (silicon controlled rectifier) circuit.

The state of a rotary solenoid (on/off) determines whether a slab will be in the configuration or excluded

from the configuration. Slabs excluded from the configuration lie lached by their respective rotary solenoids outside of the incident beam of radiation; and therefore, have no effect on the transmission of the configuration. The rotary solenoids, on both sides of the longitudinal table are controlled by SCR circuits. The SCR circuits drive the rotary solenoids to states stored in the receiver memory. A gate circuit interfaces the SCR circuits with the memory.

After the picker motor and solenoids have been operated, and the number and sequence of slabs in the slab configuration determined by the central computer has been realized, a micro-switch on the picker motor arm closes and generates a pulse. This pulse triggers a time delay circuit which in turn triggers a pulse forming circuit. The formed pulse triggers the transmitter output shift register to scan and transmit "?????" to the central computer. The time delay insures that transients have died away before further messages are sent to or from the central computer. This reduces any adverse effects that might result due to electrical noise. The "?????" is recognized by the central computer as permission to proceed.

e) The purpose of the carriage motor servo electronics (HH) is as follows:

(1) rectilinearly separate slabs (airspace) comprising

each configuration according to an arrangement programmed in the central computer.

(2) alert system electronics to instruct central computer of the successful completion of the above task.

Carriage servo operation:

The carriage servo electronics provide on/off, sense, and two-speed carriage motor control.

In order to drive a carriage to a programmed position, the central computer must originate the proper character sequence. This sequence when stored in the receiver memory consists of the 4-bit "carriage servo function" character, a 16-bit 4 digit analog voltage, representing the intended carriage location and a 4-bit "start" character. When the "carriage servo function" character and "start" character are present in their appropriate memory register locations, voltages are applied to a carriage gate circuit from a function comparator circuit and the start comparator circuit. These voltages, in addition to one applied on the carriage gate circuit by the analog scanner circuit actuate the appropriate carriage motor.

The carriage is driven to the location stored in the receiver memory, and stopped. After having stopped for 0.3 seconds a pulse is generated which clears the "carriage servo function" character from the receiver

memory and triggers the transmitter output shift register to scan and transmit "?????". This code is recognized by the central computer as evidence that the carriage (slab) has been successfully servoed to the location predetermined by the computer program. It is therefore an instruction to the computer to proceed.

f) The purpose of the rotary table servo electronics (GG) is as follows:

(1) angularly position all slabs comprising a configuration relative to the incident electromagnetic field, according to an arrangement programmed in the central computer.

(2) alert system electronics to instruct central computer of successful completion of the above task.

Rotary table servo operation:

To drive the rotary table to a programmed angular position, the central computer must originate the proper character sequence. This sequence when stored in the receiver memory consists of the 4-bit "rotary table servo function" character, a 16-bit 4 digit analog voltage, representing the intended angular position and a 4-bit "start" character. When the "rotary table servo function" character and "start" character are present in their appropriate memory register locations, voltages are applied to a stepper motor gate circuit from a function comparator circuit and the start comparator circuit.

These voltages, in addition to one applied on the gate circuit by the analog scanner circuit actuate a stepper motor slo-syn speed drive. The rotary table is driven by the stepper motor to the angular location stored in the receiver memory, and stopped. After having stopped for 0.3 seconds a pulse is generated which clears the "rotary table servo function" character from the receiver memory and triggers the transmitter output shift register to scan and transmit "?????". As in the case of the carriage servo and solenoid servo, this is an instruction to the central computer to proceed.

C. Description of the System Control Panel and Electronics

On the top of the rack panel (see Fig. 13) is the transmitter electronics card file (AA). Mounted just below this file is the Model 3440A Hewlett Packard Digital voltmeter (BB).

Beneath the DVM is the manual control panel (CC). In the upper left hand corner of the control panel is a digital thumbwheel switch. In the manual mode, this switch is set to any desired carriage location or rotary table angular position. Beside the thumbwheel switch is a light emitting diode "LED" digital display. Carriage locations and rotary table locations are read out on this 4-digit display. Next to the display, on the right, are the manual carriage push-button selector switches. Each carriage can be located individually by setting the thumbwheel switch to the desired location and by depressing its push-button. Below these switches are the manual solenoid push-button selector switches. Each slab can be put in or taken out of the microwave field by depressing its push-button. The state of each carriage or solenoid (on/off) can be read out on an indicator lamp located just above the push-button switches. The dual switches on the bottom right allow manual triggering of the solenoid servo cycle. The dual switches, on the bottom left, set the solenoid servo in the manual or automatic mode.

The card file just below the switch panel is the multiplexer (DD). The panel below the multiplexer (EE) serves a multi-purpose. The three toggle switches on the upper left set the servo systems in the manual or automatic mode. In the automatic mode the system is completely run by the central computer. Below are two power switches. These switches actuate relays which sequentially turn down the power in an order which avoids transient overloading. This permits aborting a servo operation while the experiment is in progress. Below are switches which select the semi-automatic or teletype mode. The system may be run completely by an operator seated at the keyboard of a teletype machine, also located in the lab.

In the upper right hand corner are switches which control the multiplexer analog scanner. The top three buttons, set, reset, and trigger the scanner. The two switches beneath set the transmitter scanner. Beneath these switches is the multiplexer and transmitter "LED" scanner display. The scanner indicates which servo is being operated. It also indicates when signals are being transmitted to the central computer from the transmitter.

Below this panel are the receiver file (FF), solenoid file (GG) and carriage file (HH).

D. Description of the Computer Program

The central computer (Xerox Sigma 7) is programmed in Fortran IV language. The program directs the performance of the following sequential operations in the experiment:

(1) randomly selects slabs which comprise the configuration.

(2) randomly positions slabs which comprise the configuration.

(3) samples the radiation intensity at the XTAL field detector.

(4) samples the radiation intensity at the klystron power output XTAL detector.

(5) computes the ratio of the field detector reading to the klystron detector reading.

(6) prints out this ratio on the teletypewriter.

The above sequence is then repeated.

E. Description of Repeatability Tests and Electro-Mechanical Systems Errors

Carriage position repeatability was measured using a dial micrometer indicator. The micrometer was mounted to the longitudinal table with its plunger pressed against a carriage. The carriage was automatically slewed repeatedly between two positions roughly 1 inch apart. This sequence was repeated again and again ten (10) times. The mean deviation in the end points is $\pm$0.006 inches or 1/40 wave. The accuracy of this measurement depends largely on the force that the plunger exerts on the carriage. Too stiff a plunger in the dial indicator was found to spring the carriage potentiometer anti-backlash gear thereby causing position errors. Several micrometers were tried until a suitable one was found.

Mean power transmission coefficient measurements for styrofoam configurations having ten (10) slabs was repeated both with randomly selected slab positions and numbers. The coefficient repeated within 0.4% (see Table 8). For comparison, the mean power transmission coefficients for single slabs of either styrofoam or polystyrene repeat within 0.2%.

The carriage potentiometer linearity is $\pm$.01%. This is equivalent to an error of $\pm$0.004" in carriage location. over the length of the longitudinal table. The anti-

backlash gears have ±0.001" play. The stainless steel reference racks contribute an error of ±0.004" (spacing error between racks, alignment error, plus rack tolerance) in carriage location over the length of the longitudinal table. The carriage potentiometer analog/digital converter and its matching operational amplifier contribute errors of ±0.005"(1 mv. noise) ±0.005" (±1 LSB), ±0.005" (1 mv. linearity). Errors due to temperature drift are negligible over the time it takes to set up a single slab configuration (index of refraction profile) e. g. three minutes.

3. EXPERIMENTAL MODELS

A. Choice of Material for the Slab Configurations

The Papanicolaou approximation[32] is derived for the case of dielectric media having a low index of refraction. The materials selected for this experiment therefore had to have low absorption characteristics at the frequencies used. Difficulty was encountered in finding literature on the index of refraction and loss tangents of modern commercially available materials at 60GHZ. Several materials were tested. Among those tested were commercial grade blue styrofoam (see Fig. 10) and high density white polystyrene (see Fig. 11). The styrofoam sheet is light in weight and therefore large thicknesses can be used e. g. 3" nom. thk. Since the average power transmission is inversely proportional to the length of the medium (see Appendix B), slabs having the greatest practical thickness were sought. Materials yielding configurations having low mean power transmission are desirable since a better comparison can be made between the prediction of the Papanicolaou approximation and the Born approximation.[33] The predictions of Born and Papanicolaou differ theoretically most markedly at low power transmission levels.

A large slab thickness also yields a medium with only small total air space. It is important to reduce the size of the regions unoccupied by slabs in order to approximate the "Random Binary Transmission Process."[34]

Also, the Papanicolaou approximation requires a small correlation length.[35] Therefore the slabs must be packed together as densely as possible. The low index of refraction of the styrofoam does not yield a mean power transmission less than 90% for ten slabs, even when they are manually configured for minimum transmission. This led to the choice of a higher index material i. e. polystyrene. The minimum thickness of polystyrene needed to prevent extensive warping is ½ inch. Even these thin sheets are very heavy. This makes them difficult to lift out of the microwave field. Twenty sheets were used to try to get the average power transmission down to approximately 60%. Because of their weight, the polystyrene slabs were cut to as small a size as practical without causing edge diffraction effects i. e. 13" X 17". Several other materials checked lacked machineability e. g. polyethelene. Others lacked resilience and had high absorbtion at 60GHZ e. g. pressed wallboard.

The surface of the styrofoam is not perfectly smooth. The manufacturer's name is stamped in some places. These blemishes are 0.020 inches deep and 0.125 inches wide in some places. Every effort was made to select and position these areas away from the optical axis. These blemish dimensions correspond approximately to 1/10 and 1/2 wave respectively. Because of the low index (near unity) of the material, effects due to these marks are small. Other-

wise, the material has a smooth skin with surface irregularities (dents) of the order of ±0.003 inches or less than 1/100 wave.

The surface quality of the polystyrene is excellent. It is smooth to better than ±0.001 inches or better than 1/200 wave and has no surface imperfections.

The interior of the styrofoam material has small imperfections (bubbles) of the order of 0.005 inches or 1/40 wave uniformly distributed throughout the body of the slab. Therefore, the styrofoam can be considered as being homogeneous.

The polystyrene is solid throughout; it may have small bubbles of immeasurable size. The polystyrene can be considered as being homogeneous also.

The thickness of the styrofoam was measured six (6) times around the edge of each slab with a vernier calliper and an average taken for the thickness on the optical axis. The maximum deviation from the average measured for any one slab was 0.028 inches or 1/7 wave.

The thickness of the polystyrene slabs was measured six (6) times around the edge of each slab with a micrometer and an average taken for the thickness on the optical axis. The maximum deviation from the average thickness measured for any one slab was 0.005 inches or 1/40 wave.

The parallelism of the faces of the styrofoam and polystyrene slabs was calculated using the maximum thickness deviation of the slab. The angles computed were 1/60 deg. and 1/20 deg. for the styrofoam and polystyrene respectively.

The sagitta of each slab was measured to determine if any warp was present. Most of the slabs were slightly warped. The maximum sagitta measured for either material was 0.050 inches for polystyrene. This is over the 17 inch width of the slab. This corresponds approximately to a sagitta of 0.001 inches or 1/200 wavelength over a 2 inch circle drawn on the optical axis e. g. the approximate horn opening dimension of the XTAL field detector.

B. Choice of Material for the Conducting Strip Configurations

On the basis of previous experimental results at 60GHZ[36] there is no evidence for the dependence of the angular diffraction pattern of a single or double strip on the conductivity of the strip material i. e. for common materials such as steel and aluminum having width dimensions of the order of a wavelength. It is desirable to keep the strip thickness as small as possible, compared to a wavelength, to approximate an infinitesimally thin strip.[37] In doing this the strip is likely to warp or take a permanent set unless the material is resilient. Steel is superior to aluminum in this respect. Steel

feeler gauge stock having a thickness of 0.020 inches and a width of 0.500 inches was chosen. Prior experimental work has been conducted in electromagnetic diffraction using similar strips.[38] The tolerance on both width and thickness are ±0.002 and ±0.0005 respectively. The 0.500 inch strip width was chosen because it is small compared to the size of the XTAL field detector horn opening i. e. 1.6" X 1.3". This insures that the horn does not lie completely in the diffraction shadow of the strip. The 0.500 inch strip width was chosen also because it is small compared to the size of the flat center portion i. e. ±5% amplitude variation, of the microwave beam (see Figs. A.1-A.4). Therefore, at least to first order, on the optical axis the edges of the strips are illuminated by plane waves.

A flat material was sought for supporting the strips as they are hanging in the microwave field. The three inch thick styrofoam slabs were chosen as the base material for supporting the strips. The strips were cemented to the slabs. Although the surface of the styrofoam is warped the sagitta is no greater than 0.001" over a 2" X 2" area. The index of refraction of the styrofoam is near unity (see Appendix E). Therefore, the effect of the slabs presence on the power transmission of the strips is minimized. In addition the mean power transmission of the strips mounted on the slabs can be compared with the mean power transmission of the styrofoam

slabs alone.

C. Mounting and Alignment of Slab and Strip Configurations

Each styrofoam slab was milled out to accommodate a plastic tab (m) which was cemented to the slab with Elmer's glue. Elmer's glue was used since it does not melt the styrofoam. Most other cements chemically attack styrofoam. The tab is used for attaching the slab to a carriage mounting block. Mounting holes are machined into the tab for this purpose. An insulating tab rather than a conducting one is used to prevent severe microwave reflections from the tabs. The polystyrene slabs were machined with tabs (q) as part of their basic structure.

For the styrofoam configuration, ten (10) slabs were mounted on their respective carriages as in Fig. 27. For the polystyrene configuration, twenty (20) polystyrene slabs were mounted on their respective carriages (two on a carriage) as in Fig. 28. The slabs were made plumb within $\pm\frac{1}{4}$ degree. The slabs were aligned parallel to each other to better than $\pm\frac{1}{2}$ degree. For the styrofoam slabs the radiation was normally incident 0° $\pm\frac{1}{2}$ deg. For the polystyrene slabs the radiation was incident at 2.2° $\pm\frac{1}{2}$ deg. The slab alignment was done using a vernier calliper, plumb line, and autocollimating telescope with a gauss eyepiece.

For the strip configuration, ten (10) slabs (with strips) were mounted on their respective carriages as in Fig. 27.

The strips are 25" long as compared to the 24" height of the styrofoam (see Fig. 10). At the top and bottom of each slab the strip exceeds the slab edge by ½". This ½" strip projection facilitates the edge-on alignment of the strips. Two (2) taut 0.016" nylon chords were set up as edge references. Both were arranged parallel to the longitudinal table. The plane of the chords was made plumb to within ±¼ deg. One was strung across the top of the ten slabs, and the other was strung across the bottom of the slabs. The edges of each of the ten strips, both at the top and at the bottom, were adjusted so that each one just touched the nylon reference chord $\begin{matrix}-0.016" \\ +0.000"\end{matrix}$. Therefore the strips were aligned edge-on to within ±0.008" of one another.

D. Geometry of the Slab Configurations

Ten (24" X 24") styrofoam slabs were mounted on the longitudinal table, one to a carriage (see Fig. 27). They were arranged initially to give near minimum transmission with ten (10) slabs in the field, i. e. 83%. The carriages were run in the manual mode until this condition was attained. The spacing between adjacent slabs (air space) was found to be approximately ¼". To gain a periodic arrangement, as in a crystal, and to more nearly simulate the "Random Binary Transmission Process" the spacing was made ¼ inch for all slabs with only a small resultant increase in the power transmission, i. e. 85%. The ¼"

spacing configuration was chosen rather than another configuration with larger airspace so as to keep the slabs as densely packed as possible. This was done to better approximate the "Random Binary Transmission Process," and reduce the correlation between the index of refraction of the airspaces. This configuration places limits on the range of motion that each slab can have rectilinearly. Each slab has a range of motion of 0.100 inches or 5/8 wave. This range allows the slabs and carriages to move rectilinearly without colliding with one another and also provides sufficient clearance without rubbing between adjacent slabs when they are rotated in and out of the field.

The ½ inch spacing between slabs (see Fig. 8, 10, 27) was maintained for the strip configurations so that a comparison of the mean power transmission coefficients for the styrofoam slabs holding the steel strips could be made with those found for the styrofoam slabs alone. For this purpose, the range is maintained the same.

The twenty polystyrene slabs were mounted on the longitudinal table two (2) to a carriage (see Fig. 1-4). The distance between each pair of slabs mounted on a carriage is nominally 3.250 inches. This is the width of the carriage mounting block. The block dimensions were chosen to give a high packing density for a wide range of slab

widths. The configuration for twenty polystyrene slabs (see Fig. 28) was chosen to both minimize the power transmission and maximize the packing density. Overlapping the slabs of adjacent carriages allowed achieving a high packing density.

The air separations were manually adjusted initially as follows. Starting with arbitrary locations for each slab, slab #1 was moved until minimum power transmission was reached. Then slab #2 was moved until another minimum was reached. The procedure was repeated sequentially down the line for each slab. A repetition of this procedure four (4) times was found to be adequate. For the case of the polystyrene the minimum power transmission was 11.5%.

E. Generation of Random Slab Configurations

The random selection of slab location and total number in a configuration is accomplished through the use of two (2) random number generator subroutines in the central computer program. They make available numbers uniformly distributed between the numerical limits -1 and +1. Each time the computer sets up an index of refraction profile, the carriages are selected sequentially and to each one is designated two (2) random numbers (one from each generator). The carriage locations are determined by the first random number generator. The carriage location is proportional to the number generated. The nominal carriage

position occurs when the first random number generated is zero. The number of slabs in the field is determined by the second random number generator. If the number generated is negative (-) then the slab for which it is generated is held out of the field. If the number generated is positive (+) then the slab is placed in the field.

The uniformity of the numbers generated was ascertained using the CHI SQUARE TEST (see Appendix D). The results of this test are shown in Fig. A.5. The calculated probability distribution of the generator compares well with the theoretical CHI SQUARE probability distribution.

4. MEASUREMENT OF THE MEAN POWER TRANSMISSION COEFFICIENT

A. Normalization of the Power Transmission Measurements

The purpose of having two (2) XTAL detectors is so that one XTAL can monitor the field power transmission and the other can monitor the klystron power output. By taking the ratio of the field detector reading to the klystron detector reading there is constant normalization of the transmission regardless of power level changes in the klystron's output. For convenience, the outputs from each XTAL are initially set equal to unity, with no slabs in the field. Since the noise of the klystron is typically $\pm\frac{1}{2}\%$, the error associated with the transmission normalization process is $\pm 1\%$. This is far less than the $\pm 10\%$ fluctuation in klystron power output over $1\frac{1}{2}$ hours i. e. the time for a typical experiment. The power level fluctuations in the klystron's output are due to the age of the tube, temperature changes of the tube (even though the tube is mounted in an oil bath), and sharp 115 vac. power line fluctuations. There is drift of $\pm 2\%$ typically between the klystron XTAL (N) (see Fig. 1) and the field XTAL (Y) (see Fig. 4). The crystals are mounted approximately 20 feet from each other. The drift is due to local temperature differences in the chamber and differences in power levels detected. The drift of each XTAL is roughly linear in time. That is, if the XTAL output is drifting downward near the beginning of an experiment, then it continues on the average to drift downward all through the experiment with small fluctuations of about $\pm\frac{1}{2}\%$. This has been determined by measuring the XTAL

outputs with no slabs in the field, for 1½ hour intervals. The effect of drift is eliminated by taking the average drift measured over the time for a complete experiment and by correcting the average power transmission coefficient by this amount.

The crystals used to detect the klystron power output and field intensity are square law devices. Deviations from the square law characteristic cause errors. The behavior of similar crystals e. g. ±1% as square law devices at power levels comparable to those in the present experiment has been demonstrated elsewhere.[38] A further check was done to determine the XTAL linearity. A thin metal mask was placed over the mouth of the field detector horn. First one-half of the horn was covered; then the other. The power transmission measurements made while the right half and the left half were covered were 0.507 and 0.504 respectively. The transmission is 0.992 with no mask in place. This shows that at 50% attenuation the XTAL linearity is better than 1%. The results also indirectly demonstrate the symmetry of the field around the optical axis.

Since the crystals (XTAL'S) are not matched i. e. difference in internal resistance, there may also be differences in their readings at corresponding power levels. During a typical experiment, the XTAL monitoring the

klystron power output and the XTAL monitoring the power transmitted by the random medium do not detect the same signal power levels e. g. the power transmission varies typically between 100% and 11%. To determine the size of this effect thin absorbers i. e. paper & plastic tape, were placed at the mouth of the klystron waveguide and the output of both XTAL'S was read. The greatest error observed was $\pm\frac{1}{2}\%$ for an attenuation of 80%.

The XTAL voltage is amplified (X100) by a Standing Wave Ratio (SWR) meter. The meter's linearity is $\pm\frac{1}{4}\%$. The amplified signal is then digitized by a digital voltmeter (DVM). The DVM analog to digital conversion is good to $\pm 1/10\%$ (linearity $\pm\frac{1}{2}$ LSB).

The digital signal is then coded for transmission to the computer. There is no loss of accuracy in this step.

The noise level of the XTAL, SWR meter, and DVM is $\pm 1/10\%$ measured with the klystron turned off. All cables linking the XTALS with the SWR meter and the DVM are of the coaxial type.

B. Measurement of Standing Wave Effects

Standing waves (see Appendix F) originate at several locations. Namely at the field detector, longitudinal table, klystron waveguide, and random medium.

Part of the radiation falling on the field detector (see Fig. 5) is reflected back to the klystron waveguide (d) (see Fig. 12). Reflections at the mouth of the field detector horn (R) and at the XTAL (Y) itself contribute to this effect. These reflections arise from a mismatch between the above components and their surroundings. A dielectric sheet (Q) was inserted at 45° at the mouth of the field detector horn. The purpose of this sheet is to attentuate any reflected radiation. An E-H tuner (S) is used to match the XTAL to the detector waveguide and thereby reduces reflections from the XTAL. Using this procedure, the effect of the standing waves on power transmission measurements is reduced from $\pm 5\%$ to less than $\pm 0.4\%$.

The random medium, composed of plane parallel dielectric slabs, reflects all radiation that is not transmitted, back to the klystron. This radiation is focused by the parabolic mirror onto the mouth of the klystron rectangular waveguide. For random media having high transmission e. g. ten 3" thick styrofoam slabs, the reflected radiation is small (10%); and therefore the re-reflected radiation from the klystron waveguide is very small (within

the noise level of the klystron) and is therefore undetectable. For the polystyrene ¼ inch sheets, however, the transmission is significantly lower. For example 20 sheets have an average transmission of approximately 62%. Therefore, the average reflected radiation is 38%. The angle of incidence of the polystyrene slack was made 2.2°. By doing this the radiation reflected by the stack and focused on the klystron waveguide was made less, since now the real image of the klystron waveguide falls 4.4° off of the waveguide. The effect of the standing waves on the transmission measurements is reduced from ±5% to ±1½%. The angle of incidence could not be made larger because the incident radiation would strike the edges of the slabs and cause diffraction effects. For the ten ½" wide strips mounted on the 3" thick styrofoam slabs, at normal incidence, the effect of these standing waves is ±1½%. Estimates of the standing wave effects above were made by measuring the change in the readings of the klystron power output XTAL when the random medium was changed i. e. by varying the number and spacing of slabs in the field. Theoretically, in the absence of any reflections from the medium, there would be no measurable changes. However, since there is radiation reflected from the medium back to the klystron, and re-reflected back into the field by the klystron waveguide, there are changes (apparent ones) in the

klystron power output. The output power level and frequency of the klystron both fluctuate with time. The klystron frequency changes by ±0.1 GHZ typically over a period of 1½ hours. These measurements were made with a frequency meter mounted onto the klystron power output detector. This corresponds to a wavelength change of ±0.01 mm. or 1/500 wave. The power output (noise) of the klystron fluctuates typically by ±½%.

Due to the size of the longitudianl table (5 ft. X 1 ft. X 1 ft.) and its proximity to the field e. g. the field passes 12" below the table, there is some scattering along the length of the table. To reduce this scattering, a system of baffles i. e. collimating apertures (M, A, C), were erected (see Fig. 1). The baffle material is Eccosorb type 72 absorber. It is pliable and comes in convenient ¼ inch thick sheets. The reflected power is less than ¼%. The transmission is negligible. These apertures insure that the incident radiation is restricted to a region around the optical axis and well below the longitudinal table. Radiation diffracted from the baffle edges and diffracted from the table to another baffle

edge can reach the field detector only by third order diffraction. Such effects, even for metallic edges are small.[39] By using these collimating apertures, these scattering effects were reduced from ±2% to negligible values. The longitudinal table scattering effects were determined by making power transmission measurements with no slabs in the field. The carriages were operated up and down the length of the table; the picker motor was also operated. No variation in transmission was detected. The collimating apertures were placed on the parabolic mirror (e), in front of the parabolic mirror (M), between parabolic mirror and longitudinal table (A), and between longitudinal table and field detector (C). All were aligned on the optical axis of the XTAL detector. Their sizes are 6" X 6", 6" X 6", 6" X 6", 4" X 4", respectively. The size of the collimating apertures was chosen in the following way. Aperture (C) was chosen so that an observer standing at the XTAL field detector, looking toward the klystron mirror could not see any of the edges of the slabs that are in or out of the field. Therefore, any radiation reaching the field detector from the edges of the slabs would have to do so by some indirect path, i. e. by secondary diffraction. The 6 inch X 6 inch apertures (M) & (A) between the longitudinal table and the klystron were chosen to prevent radiation from directly reaching the longitudinal table onto the XTAL field

detector. The size of the apertures were made as small as possible without producing large effects in the wavefront of the incident radiation (see Appendix A). To determine the presence of stray radiation at the field detector, aperture (C) was vignetted with a metal plate; the stray radiation was too small to be detected.

The klystron waveguide has a 4.775 X 2.388 mm. rectangular opening. A ferrite isolator is installed in the guide to prevent reflections from the klystron itself. Attempts to reduce reflections by covering the mouth of the klystron waveguide with absorbing material were unsuccessful. These attempts resulted both in increasing the reflections or seriously changing the radiation pattern of the waveguide so as to make the beam unusable.

C. Measurement of Diffraction Effects

The angular power distribution from the mouth of the open klystron rectangular waveguide is not uniform,[40] and the alignment of the waveguide with respect to the collimating parabolic mirror is critical.[41] Diffraction caused by the collimating apertures (e, M, A) can also alter the plane wave character of the field. To check the severity of these effects on the wavefront, the diffraction pattern of a single conducting strip was measured at three field locations. The results are compared with values predicted by Keller Diffraction Theory in Fig. A.3. The intensity of the field was also measured and plotted as a function of field location in Fig. A.4. In the central 2" of the field there is only a small fluctuation of the field intensity. The field intensity is normalized to 1.0. The field amplitude is very close to being constant i. e. $\pm 5\%$.

During a typical experiment, when slabs are rotated out of the field, they are held out by a distance sufficient to make diffraction from their edges a third order effect. Attempts to see these effects by completely removing slabs from their carriages after measurements had been made with the slabs rotated out of the field, and comparing readings before and after, proved these effects to be negligible. The effects are too small to measure. The slabs are deliberately made much larger than the

collimating apertures so that when the slabs are in the field edge diffraction is negligible.

D. Criteria for Convergence of the Power Transmission Measurements

The basic investigation has been to experimentally set up random configurations or index of refraction profiles for a prescribed number of slabs or length L of media,[42] and to measure the power transmission for each profile. The running mean power transmission coefficient for m profiles can be defined as

$$\langle |T(L)|^2 \rangle_M = \frac{1}{M} \sum_{i=1}^{M} T_i(L)$$

where $T_i(L)$ are the individual power transmission coefficient measurements resulting for each index of refraction profile for a particular length L. We can also define the mean power transmission coefficient as

$$\langle |T(L)|^2 \rangle = \lim_{M \to \infty} \frac{1}{M} \sum_{i=1}^{M} T_i(L)$$

The value of $\langle |T(L)|^2 \rangle$ can be estimated by measuring the $T_i(L)$'S and their corresponding running means until a sufficient number, say m=n is reached such that the fluctuations in the running mean are of the order of the limit on measuring accuracy of the experiment. A conservative estimate of this limit can be gotten by considering only the linearity of the crystals, i. e. 1%.

5. COMPARISON OF THEORIES

A. Papanicolaou Approximation

The propagation of scalar waves through a dielectric slab of random medium assumed to be plane stratified having an index of refraction with small fluctuations about a mean value has been considered by Papanicolaou et al.[43-44] The random refractive index can have, within certain limits, an arbitrary correlation function,[45] e. g. see Appendix E.1. An expression for the approximate value of the mean power transmission (referred to below as the "Papanicolaou approximation") characterizing the scattering properties of the medium is given by Papanicolaou[46] as (see Appendix B.1)

$$\langle |T(L)|^2 \rangle = \frac{4}{\sqrt{\pi}} e^{-\frac{\epsilon^2 L s}{4}} \int_0^\infty \frac{\chi^2 e^{-\chi^2} d\chi}{\cosh(\epsilon\sqrt{sL}\,\chi)}$$

The Papanicolaou approximation is derived for the specific case of normally incident radiation. The dielectric slab is assumed to be lossless, i. e. $|R(L)|^2 = 1 - |T(L)|^2$. The mean power transmission is equal to the mean of the square of the magnitude of the transmission coefficient T(L); R(L) is the reflection coefficient.[47]

A distinguishing feature of the Papanicolaou approximation is the appearance of the statistical parameter S (see

Appendix B.2, E.2) given as

$$S = \frac{k^2}{2} \int_0^\infty \rho(\tau) \cos 2k\tau \, d\tau$$

where S is a correlation function, k is the mean wave number, $\rho(\tau)$ is the autocorrelation of the real random process m(L), and L is the width of the random medium. 48-52 Unlike many other contemporary statistical methods which must assume a particular random process in order to effect a solution, the Papanicolaou approximation is completely general. Since S appears explicity in the solution as a variable, it permits the treatment of any plane stratified media so long as the random process m(L) characterizing that medium is known or can be assumed.

The autocorrelation of the random process m(L) is given in the derivation of the Papanicolaou approximation as only a function of the difference $|(L-L')|$.[66] That is,

$$\langle m(L)m(L')\rangle = \rho(|L-L'|)$$

This suggests that m(L) be at least stationary in the wide sense (or weakly stationary);[67] that is, the autocorrelation of m(L) is not a function of L alone, but of the magnitude of the difference L-L'. To realize this condition experimentally, the slabs must be arranged as closely to one another as possible. In order words, to reduce the correlation between the indices of refraction of adjacent as well as remote regions of the medium, we do not want to occupy these regions continuously with air alone. In addition, to reduce the correlation between regions inside the slabs themselves the slabs should be as thin as possible (compared to a wavelength). The length L of a medium meeting these conditions, for a finite number of slabs would be very small. The Papanicolaou theory predicts that even for such an idealized medium, the mean power transmission would be very large. A test of the theory at high mean power transmission levels would be inadequate because the non-linear nature of the theory only appears at low transmission levels. The difference between the predictions of linear theories, for example the Born approximation, and the Papanicolaou approximation grow as the mean power transmission of the medium decreases. Besides these experimental limitations the

Papanicolaou approximation was derived assuming small fluctuations in the index of refraction inside the medium. Again, for an experimental medium of practical size, a small index of refraction of the slabs would produce a correspondingly large transmission related to the square of the index fluctuations. Therefore, compromises in the experimental simulation of the assumed physical conditions used to derive the Papanicolaou approximation are necessary.

Although the Papanicolaou approximation was derived under the above assumptions, it was done so to simplify the mathematics.[68] The range of physical conditions the theory will actually predict is much broader. The experimental models investigated test the scope of its validity.

B. Born Approximation

When the index of refraction is very small the parameter E characterizing the size of the fluctuations of the wave number of the random medium is correspondingly very small (see Appendix E.3). Multiple scattering can then be neglected and the first Born approximation applied.[53] This is the case for which E^2LS approaches zero. Equation (3) i. e. the mean power transmission, is plotted in Figs. 16-20 as a function of E^2LS. When E^2LS equals zero the mean power transmission is unity and the slope of (3) is -1. This was determined numerically (see Appendix B). The slope of the Born approximation, therefore, is also -1 when the mean power transmission is unity. The Born approximation as a function of E^2LS is also plotted in the above figures. Clearly, the predictions of plane stratified random media differ markedly between the Papanicolaou and Born approximations as L increases.

C. Exact Theory

The problem of wave propagation through a non-random medium has been investigated thoroughly by many authors.[54-56] The medium is assumed to be divided into m plane - parallel layers, the first and m^{th} of which are semi-infinite. The electromagnetic properties of the m layers are unrestricted and dissimilar, and the thickness of the (m-2) finite layers are also different in general. A steady-state monochromatic wave, generated in the m^{th} layer, is assumed to be incident at any angle upon the $(m-1)^{th}$ layer. The exact solution of Maxwell' equations with appropriate boundary conditions leads to explicit expressions for finding the transmission coefficient. Two different computer programs were developed[57] following the equations of Brekhovskikh and Adams respectively. The results from these programs were cross-checked to eliminate the possibility of programming errors. The mean power transmission coefficient for an ensemble of profiles is calculated as the arithemetic mean of the individual coefficients. Since in practice the properties of most naturally occurring media are impossible to be measured accurately because they are subjected to random variations due to noise, humidity, wind velocity, thermal fluctuations, etc., the applicability of the exact approach is seriously limited.[58]

6. COMPARISON BETWEEN EXPERIMENT AND THEORY

A. Normalization Procedures

Normalization of the mean power transmission coefficients is accomplished using the fact that the quantity E^2S is a constant for each of the models, i. e. plane layered dielectric media, considered. A value of E^2S is sought such that the sum of the squares of the differences between the measured values of the mean power transmission coefficient and the corresponding values predicted by the Papanicolaou approximation for a particular model is minimized for the various L's considered.[59-60] The value of E^2S for which this occurs provides the "best fit" between the experimentally determined mean power transmission coefficients and the theoretical values. A program was developed which increases the constant E^2S incrementally and computes these sums. A similar program was developed using the Born approximation for comparison (see Tables 1-6 and Figures 16-18). The mean power transmission for both the styrofoam and polystyrene models was computed using "exact theory" and the results are listed in Tables 1-6 for comparison. These results were not plotted because there is no equivalent to the statistical parameter S in exact theory.

For the convenience of making future comparisons between experimental results and theoretical predictions we define

the quantity F as follows:

$$F = \sqrt{\frac{1}{n}\sum_{i=1}^{n}(R_i - M_i)^2}$$

where n is the total number of experimentally determined values of $\langle|T(L)|^2\rangle$, R_i is the experimental value of each $\langle|T(L)|^2\rangle$, and M_i is the corresponding theoretical value of $\langle|T(L)|^2\rangle$ for length of medium L_i. We note that the best fit occurs when F is minimized. F is a sort of standard deviation, taking the theoretical values as representing the mean.

In particular, for the plane stratified dielectric models considered, i. e. styrofoam and polystyrene, S is a constant. The statistics of the real random process m(L) remain invariant throughout the experiment, e. g. the autocorrelation of m(L). The mean wave number k (see Appendix E.4) is invarient because each model can be considered as being comprised of slabs having a constant uniform index of refraction; then E can also be taken as a constant. Therefore, the only variable in the product E^2SL is the L term, where E^2S is a constant.

The value of S is a constant for the model having ½" strips mounted on styrofoam slabs for the same reasons given above. However, since the Papanicolaou approximation was derived for dielectric slabs, the value of E for the strip case is undefined. Furthermore, the expression for the mean power transmission assumes normally incident plane waves. It also assumes that during propagation the wavefronts remain plane. The radiation scattered from the edge of each strip takes the form of cylindrical waves (see Appendix A).

Predictions on the mean power transmission of the random strip model e. i. ½" strips mounted on styrofoam slabs, are beyond the scope of the Papanicolaou theory, at least in so far as it has been presented. Furthermore, there is no "exact solution" to the strip model. Only the single strip problem can be solved exactly.[61] There is however the

possibility of solving the random strip problem approximately by applying geometrical diffraction theory.[62] This method has been applied to fixed arrays of two (2) $\frac{1}{2}$" strips with good results.[63]

In order to compare the mean power transmission measurements of the strip model with those of the styrofoam model, an equivalent value of E^2S is sought. The value of S occurring in both models is identical. The value of E for the styrofoam model is real (see Appendix E.3). The equivalent value of E for the strip model is likely to be complex because the strip is made from conducting material.[64] If an expression for the mean power transmission coefficient were derived using Papanicolaou theory for conducting media we can speculate that the E^2 term would be real i. e. E*E.

Values of the mean power transmission coefficients for each of three (3) models; the styrofoam model, polystyrene model, and the strip model, are listed in Tables 1-6. The experimental values were compared to the Papanicolaou approximation and a "best fit" was achieved. The experimental values and the corresponding Papanicolaou values representing the "best fit" condition are listed. In addition, the experimental values were compared to the Born approximation and a "best fit" was achieved. The Born values representing this "best fit" condition are listed. Also, the "exact" values were compared to the Papanicolaou approximation and a "best fit" was achieved. The "exact" values representing this "best fit" condition are listed. The index of refraction used for the computation of the "exact" values are 1.093 and 1.330 for styrofoam and polystyrene respectively. These are the first roots calculated using the "transmission method" (see Appendix E).

Exact calculations of the mean power transmission coefficients for each of the second roots for styrofoam and polystyrene respectively i.e. 1.12 and 1.683, were made. The results disagree with experiment by +4.2% and -25.2% for ensembles of ten (10) styrofoam and twenty (20) polystyrene slabs respectively. Due to the large disagreement with experiment they were discarded and the first two roots chosen. The disagreement between exact theory and experiment is $\frac{1}{2}$% and 2% respectively for the same ensembles cited above. Clearly, the first roots are the better choice.

B. Styrofoam Model

The experimental values for the mean power transmission coefficients are given in Tables 1 and 2 for fixed slab positions and for random slab positions respectively. In both cases the slabs in the microwave field are selected at random. The least squares best fit occurs when the constant E^2S is equal to 0.00090 and 0.00080 respectively. A small difference between the values of E^2S is expected because in the latter case the slab positions are random, the range of motion i. e. 0.100," being small compared to a wavelength. Therefore, S remains relatively unaltered, and since E is constant, the change in the product E^2S is small.

In Table 1, the value F is equal to 0.006 when the experimental values are compared to the Papanicolaou approximation. The value of F is equal to 0.006 also when the experimental values are compared to the Born approximation. For comparison, the value of F is equal to 0.006 when the "exact" values are compared to the Papanicolaou approximation. Therefore, the experimentally determined values agree approximately on the average with all the theoretical values to about ½%.

In Table 2, the value F is equal to 0.003 when the experimental values are compared to the Papanicolaou approximation. The value of F is equal to 0.003 also

when the experimental values are compared to the Born approximation. For comparison, the value of F is equal to 0.003 when the "exact" values are compared to the Papanicolaou approximation. Therefore the experimentally determined values agree approximately on the average with all the theoretical values to about 1/3%.

Therefore, for the styrofoam model, for both fixed slab positions and for random slab positions, agreement with theory is on the average approximately the same, i. e. ½%. Referring to Fig. 16 we expect that good agreement with the Born approximation implies good agreement with the Papanicolaou approximation, since the curves are so close. We note that the mean average value of the power transmission is never less than 92% for ten (10) slabs whether they have random or fixed positions. The minimum transmission measurement for a configuration of ten (10) slabs occurs when all ten slabs are in the field and is approximately 85% (see Fig. 21). The probability that all 10 slabs will be in the field simultaneously is equivalent to the probability of tossing a coin heads up ten times in a row, i. e. $(0.5)^{10}$. Therefore, although this event can occur, it is unlikely. Taking 0.935 as the mean, then, the maximum deviation is about 8%. Thus, after twenty-five profiles the fluctuations in the running mean are less than 1/3%, well below the criteria for convergence, i. e. 1% previously adopted (see Fig. 24).

For the styrofoam model the length of the medium is roughly proportional to the number of slabs comprising an ensemble. Noting the experimental linear character of the mean power transmission coefficients as a function of the length L of the medium (see Figure 16), an estimate of the mean power transmission coefficients can be made using the fact that the minimum power transmission of an ensemble comprised of ten (10) slabs is 85%; assuming that each slab comprising an ensemble enters the field in only 50% of the slab configurations (this follows from the fact that the random process m(L) has a zero mean value). As an example, for an ensemble of ten (10) slabs, the mean power transmission coefficient can be computed as $(\frac{1.00 + 0.85}{2})$ or 0.925. This is in good agreement with the experimental value of 0.925 for fixed slab positions (see Table 1).

Using the value $E^2S = 0.00090$ we may compute the mean power transmission of a single slab of styrofoam. The nominal thickness of a single slab is 3" or approximately 7.62 cm. Therefore $E^2SL = 0.0068$. From Fig. 16 we can plot this and find the corresponding value of the mean power transmission i. e. 99.3%. This implies a value of 98.6% for the transmission of a single slab. Comparing this value with the 99.2% measured value (see Appendix E), we see that they are in good agreement, i. e. within 0.6%.

The value of F in Tables 1 and 2 is equal to 0.87 and 0.5 respectively when comparing the experimental values to the exact values. Therefore, the experimentally determined values for the styrofoam model agree approximately on the average with the exact values to about 0.9%.

In order to determine the effect on the mean power transmission coefficients of randomizing the slab positions as opposed to maintaining the slabs fixed at nominal locations, data from similar sources is compared.

Comparing the experimental values with one another in Tables 1 and 2 for the styrofoam model, the maximum difference is 2%. The range of mean power transmission coefficients considered is from 0.970 to 0.925. The maximum difference occurs for an ensemble of seven (7) slabs.

Comparing the Papanicolaou values with one another in Tables 1 and 2, the maximum difference is 1% and occurs for an ensemble of seven (7) slabs.

Comparing the Born values with one another in Tables 1 and 2, the maximum difference is 1% and occurs for an ensemble of ten (10) slabs.

Comparing the "exact" values with one another in Tables 1 and 2, the maximum difference is 1½% and occurs for an ensemble of ten (10) slabs.

Therefore, the maximum effect of randomizing the slab positions in the styrofoam model is a change of 2% and this occurs between the experimental values. By comparison, the next largest difference occurs between the exact values and is 1½%. Therefore, the maximum effect of randomizing the slab positions is slightly greater for the experimental values i. e. by ½%. This indicates that the maximum rate of change of the difference in mean power transmission coefficients from randomizing the slab positions, is about

the same for experiment and theory and is about 1½%.

C. Polystyrene Model

The experimental values for the mean power transmission coefficients are given in Tables 3 and 4 for fixed slab positions and for random slab positions respectively. In both cases the slabs in the microwave field are selected at random. The least squares best fit occurs when the constant E^2S is equal to 0.0079 and 0.0073 respectively. A small difference between the values of E^2S is expected because in the latter case the slab positions are random, the range of motion, i. e. 0.100" being small compared to a wavelength. In Table 3, the value F is equal to 0.02 when the experimental values are compared to the Papanicolaou approximation. The value of F is equal to 0.04 when the experimental values are compared to the Born approximation. For comparison, the values of F is equal to 0.03 when the "exact" values are compared to the Papanicolaou approximation. Therefore, the experimental values agree approximately on the average with the Papanicolaou approximation to about 2%. Agreement on the average between the experimental values and the Born approximation is about 4%.

In Table 4, the value F is equal to 0.02 when the experimental values are compared to the Papanicolaou approximation. The value of F is equal to 0.03 when the experimental values are compared to the Born approximation. For

comparison, the value of F is equal to 0.03 when the "exact" values are compared to the Papanicolaou approximation. Therefore the experimentally determined values agree approximately on the average with the Papanicolaou approximation to about 2%, and with the Born approximation to about 3% (see Figs. 17-18).

Therefore, for the polystyrene model, for both fixed slab positions and for random slab positions, experimental agreement with the Papanicolaou theory is on the average approximately 2%. This is 1½% higher than for the styrofoam model. Agreement between the exact theory and the Papanicolaou approximation for the polystyrene is 3% compared with about ½% for the styrofoam model. This is 2½% higher. We note that agreement between experiment and the Papanicolaou approximation is better than between experiment and the Born approximation for both cases considered by about 1%.

The minimum transmission measurement for a configuration of twenty (20) polystyrene slabs occurs when all the slabs are in the field and is approximately 11.5%. Again, the probability of this occurring is $(0.5)^{10}$. Taking 0.62 as the mean, then the maximum deviation is about 51%. Thus after fifty profiles the fluctuations in the running mean are less than 1%, the criteria for convergence. Of course, since a power transmission of 11.5% is unlikely, the fluctuations in the running mean will be far less than 1%

(see Fig. 25).

The mean power transmission of ten (10) polystyrene slabs is 0.780 as compared to 0.935 for styrofoam (see Fig. 22). The mean power transmission of the polystyrene is significantly lower even though the length of the styrofoam medium is greater i. e. 83.65 cm. compared to 39.10 cm. because the index of refraction of the polystyrene is much higher i. e. 1.330 compared to 1.093. In the Papanicolaou Theory the power transmission is related indirectly to the square of the index of refraction. Therefore, the power transmission is very sensitive to changes in the index of refraction. The minimum power transmission measurement shown is 54%. Therefore, the maximum deviation is about 24%. Thus after twenty-five profiles the fluctuations in the running mean are less than 1%. The fluctuations are higher for the polystyrene model because of the higher index of refraction.

Using the value $E^2S = 0.0073$ we may compute the mean power transmission of a single slab of polystyrene. The nominal thickness of a single slab is $\frac{1}{4}$" or 0.635 cm. Therefore $E^2SL = 0.0044$. From Fig. 19 we can plot this and find the corresponding value of the mean power transmission i. e. 97%. This implies a value of 94% for the transmission of a single slab. Comparing this value with the 94.9% measured value (see Appendix E) we see that they

are in good agreement i. e. within 0.9%. We note for comparison that the agreement between the measured value and calculated value was within 0.6% for styrofoam.

The value of F in Tables 3 and 4 is equal to 3.27 and 2.8 respectively when comparing the experimental values to the exact values. Therefore, the experimentally determined values for the polystyrene model agree approximately on the average with the exact values to about 3.3%. Disagreement between the experimental values and exact values for the polystyrene model is therefore about 2.4% higher than for the styrofoam model.

For the polystyrene model the length of the medium is roughly proportional to the number of slabs comprising an ensemble. Noting the experimental linear character of the mean power transmission coefficients as a function of the length L of the medium (see Figures 17 and 18) an estimate of the mean power transmission coefficients can be made using the fact that the minimum power transmission of an ensemble comprised of twenty (20) slabs is 11.5%. As an example, for an ensemble of twenty (20) slabs, the mean power transmission coefficient can be computed as $(\frac{1.00 + 0.115}{2})$ or 0.557. The experimental value is 0.640 for fixed slab positions. The error in the estimate is therefore about 8%. Therefore the polystyrene model is only approximately linear.

Comparing the experimental values with one another in Tables 3 and 4 for the polystyrene model, the maximum difference is 4%. The range of mean power transmission coefficients considered is from 0.885 to 0.625. The maximum difference occurs for an ensemble of eight (8) slabs.

Comparing the Papanicolaou values with one another in Tables 3 and 4, the maximum difference is 2% and occurs for an ensemble of sixteen (16) slabs.

Comparing the Born values with one another in Tables 3 and 4, the maximum difference is 1% and occurs for an ensemble of (16) slabs.

Comparing the exact values with one another in Tables 3 and 4, the maximum difference is 2% and occurs for an ensemble of (16) slabs.

Therefore, the maximum effect of randomizing the slab positions in the polystyrene model is a change of 4% and this occurs also between the experimental values. By comparison, the next largest difference occurs between the exact values and is 2%; a difference of 2% also occurs between the Papanicolaou values. Therefore, the maximum effect of randomizing the slab positions is greater for the experimental values i. e. by 2%. This indicates that the maximum rate of change between mean power coefficients, which results from randomizing the slab positions, is about the same for experment and theory; assuming of course that we consider a 2% difference as small.

D. Strip Model

An approximate value for the magnitude of the equivalent index of refraction can be found for the strips using the fact that the parameter S is identical for both the styrofoam and strip models. From Appendix E we find S is approximately equal to 0.033 for the styrofoam model assuming a "Random Binary Transmission Process." We have from (see Appendix E.3)

$$\eta = \sqrt{\frac{1+\epsilon}{1-\epsilon}}$$

For example, (see Table 5) when L = 7.75 cm., then $E^2LS = 0.100$. Using the values of L and S given above we find the magnitude of the equivalent E as 0.62. Substituting this value of E in the equn. for n above we get n = 2.06. We note that this is far greater than the index of the styrofoam slabs alone i. e. 1.093. This result is consistent with the larger fluctuations in transmission measurements present in the strip model as compared to the styrofoam model (see Figs. 21 and 23).

The experimental values for the mean power transmission coefficients are given in Tables 5 and 6 for random slab positions and for fixed slab positions respectively. In both cases the slabs in the microwave field are selected at random. The least squares best fit occurs when the constant E^2S is equal to 0.012 and 0.013 respectively. A small difference between the values of E^2S is expected because in the latter case the slab positions are random, the range of motion i. e. 0.100", being small compared to a wavelength. Therefore, S remains relatively unaltered, and since the effective E is constant, the change in the product E^2S is small.

In Table 5, the value F is equal to 0.03 when the experimental values are compared to the Papanicolaou approximation. The value of F is equal to 0.02 when the experimental values are compared to the Born approximation.

In Table 6, the value F is equal to 0.04 when the experimental values are compared to the Papanicolaou approximation. The value of F is equal to 0.06 when the experimental values are compared to the Born approximation.

Therefore, the experimentally determined values agree for both random and fixed slab positions, approximately on the average with the Papanicolaou approximation to about 3½%, and with the Born approximation to about 4%. Comparing these values with those for the styrofoam and polystyrene models, we note that the value of F is increasing as the index of refraction increases (see Figs. 19-20).

The minimum power transmission for a configuration of ten (10) strips occurs when all the strips are in the field and is approximately 27%. As before, the probability of this occurring is very small. The power transmission for a single strip mounted on a styrofoam slab is about 75%. Taking 0.45 as the mean, then the maximum deviation from the mean is about 55%, with all of the slabs out of the field. Thus, as before, after fifty profiles the fluctuations in the running mean are less than 1% (see Figs. 23 and 26).

Comparing the size of the maximum deviations from the mean between the styrofoam and strip models when L = 83.65 cm. i. e. for an ensemble of ten slabs, we note that the maximum deviation for the strip model is about seven (7) times greater.

The large attentuation in power transmission for a single strip can be explained using geometrical theory i. e. for wavelength small compared to the strip width. The width of a strip and the XTAL field detector horn are 0.500" and 1.6" respectively. Geometrically, then, the strip shadow covers 31% of the area of the mouth of the horn. Assuming that the XTAL detects radiation uniformly across the mouth of the horn, then the power transmission should be 69%. Now since the strips are actually only about two (2) wavelengths wide, we would expect the power transmission to be higher. This is in agreement with the measurements, i. e. 75% compared to 69%.

An estimate of the mean power transmission of the strips can be made using the method applied to both the styrofoam and polystyrene models. The minimum power transmission of an ensemble comprised of ten (10) strips is 27%. The mean power transmission coefficients for an ensemble of ten (10) strips can be computed as $\left(\frac{0.75 + 0.27}{2}\right)$ or 0.51 (this time we have taken into consideration the effect of the geometrical strip shadow in attenuating the transmission). The experimental value is 0.455. The error is about 4%. Therefore the strip model is approximately linear.

Comparing the experimental values with one another in Tables 5 and 6 for the strip model the maximum difference is 9%. The range of mean power transmission coefficients considered is from 0.885 to 0.455. The maximum difference occurs for an ensemble of two (2) slabs. Agreement between the experimental values for random slab positions and fixed slab positions improves as the number of slabs increases.

Comparing the Papanicolaou values with one another in Tables 5 and 6, the maximum difference is 2% and occurs for an ensemble of seven (7) slabs.

Comparing the Born values with one another in Tables 5 and 6, the maximum difference is 2½% and occurs for an ensemble of ten (10) slabs.

Therefore, the maximum effect of randomizing the slab positions in the strip model is a change of 9% and this occurs between the experimental values. By comparison, the next largest difference occurs between the Born values and is 2½%. Therefore, the maximum effect of randomizing the slab positions is greater for the experimental values i. e. by 6½%. This indicates that the maximum rate of change between mean power transmission coefficients, which results from randomizing the slab positions, is much larger than predicted by statistical theory; the styrofoam model gave results which were consistent with theory. Therefore, the Papanicolaou approximation predicts the behavior of dielectric media, i. e. the media for which it was intended, better than it does media having conductors.

Comparing the size of typical fluctuations in power transmission for the polystyrene and the strip models, e. g. see Figures 22 and 23, they are similar in magnitude. This implies that the magnitude of the effective index of refraction of the strip model is of the same magnitude as that of the polystyrene model. Now the mean power transmission coefficient of the ensemble of ten (10) strips is 0.455 compared to that of the ensemble of ten (10) polystyrene slabs which is 0.780. In both cases the positions of the slabs are random. Now the difference between the mean values is 0.325 or 32.5%. This is in close agreement with the geometrically derived attenuation due to the strip shadow on the XTAL detector horn i. e. 31%. Thus, the magnitude of the effective index of refraction of the strip model is likely to be close to that of the polystyrene i. e. 1.330. The difference between this value and that calculated before i. e. 2.06, can be accounted for by the presence of the geometrical strip shadow on the horn. This shadow has the effect of shifting the mean power transmission coefficients of the strip model downward, and therefore seemingly giving the strip model a high effective index of refraction.

7. DISCUSSION

A. Limits of Accuracy

For the polystyrene model, agreement between the exact theory and the Papanicolaou theory is about 3%, as compared to the styrofoam model where agreement is about ½%. The values of the mean power transmission coefficient calculated by the exact method depend significantly on the correct evaluation of the index of refraction.

To determine the magnitude of the effect that a change in the index of refraction has on the evaluation of the "exact" value of the mean power transmission coefficients, it was assumed for purposes of an illustrative example, that the power transmission of a single slab of polystyrene was measured in error by -0.2%. This hypothetical error is deliberately chosen to be small i. e. one-half the noise level of the klystron. Now since the measured value was 0.949, then the perturbed value is 0.947 (see Appendix E.). Using this perturbed value for the slab power transmission, the perturbed index is calculated to be 1.332 (compared to the original value of 1.330). We can now compute the perturbed mean power coefficients. As an example, for an ensemble of twenty (20) slabs having random positions, the perturbed value is 0.596 as compared to 0.605 previously (see Table 4). Therefore an error of only -0.2% in the measurement of the transmission can produce an error of -0.9% in the calculation of the exact mean power trans-

mission of an ensemble of twenty (20) polystyrene slabs. Use of the exact method therefore stresses the need to know the index of refraction of the material to more than 4 significant figures. We can speculate that the index of refraction of cast or rolled plastics i. e. styrofoam, polystyrene and others, may not be this uniform from sheet to sheet. The index may indeed vary at random about the manufacturer's quality control mean value. In effect, the transmission difference between two (2) slabs of polystyrene, each having an index of refraction differing in the third decimal-place would be beyond the capability of our instruments to detect considering the noise limitations of the klystron alone.

For comparison, an error of -0.001" made in measuring the thickness of the polystyrene slab, produces a perturbed index of refraction of 1.328. We can now compute the perturbed mean power coefficients. As an example, as before, for an ensemble of twenty (20) slabs, the perturbed value is 0.619 as compared to 0.605 previously. Therefore, an error in thickness of only minus one-thousanth of an inch produces an error of +1.4% in the calculation of the "exact" mean power transmission. Since the maximum deviation from the average thickness measured for any one slab was 0.005 inches, it is likely that this is a source of error.

Sources of error affecting the accurate positioning of each carriage are listed in Table 9a. The standard error of the random sources is the same for each model i. e. 0.004" or 1/50 wavelength. This is in good agreement with the results of carriage repeatability tests i. e. ±0.006".

Now considering the systematic errors due to system non-linearity, the worst case occurs if they are all added arithemetically, i. e. 0.016" or 1/12 wavelength. The power transmission of a slab configuration is a periodic function of the spacing between the slabs. The period is one-half wavelength.[65] The amplitude of the power transmission variation with spacing is dependent on the index of refraction of the slabs and their thicknesses. Therefore, the change in power transmission can be considerable for a carriage positioning error of 1/12 wave. For a slab ensemble, since these errors are constant, there will be an average effect on the experimentally determined mean power transmission coefficients. Now, since the nominal slab configuration for each model is set up manually, the effects of system non-linearity do not enter. Also, since the range of carriage motion is small i. e. 0.100", compared to the total length of travel on the longitudinal table i. e. about 40", it is certain that the effects of system non-linearity are very small. It is assumed of course that the potentiometer, amplifier and A/D converter non-linearities are slowly varying functions over their useful range. Furthermore, it is unlikely that all the systematic errors will add, given for example any

arbitrary carriage location.

The manual spacing of slabs for a nominal model configuration (see Figures 27 and 28) is accomplished by taking four (4) measurements, one at each corner, between two adjacent slabs and computing the air wedge angle between slabs. Then the air spacing on the optical axis is calculated. The worst case occurs for polystyrene when two adjacent slabs having two oppositely warped surfaces face each other. Then the error in measuring their spacing is the sum of their sagitta distances. For slabs having a sagitta of 0.050" maximum, the error in spacing is 0.100" or $\frac{1}{2}$ wavelength. Of course, this extreme condition is unlikely. Such an error is likely to produce a large difference between the experimental values and those calculated exactly. The exact values are calculated using the nominal slab locations as input data, as well as the measured index of refraction of the material. The largest difference that occurs between experiment and the exact theory is 5.5% for an ensemble of six (6) polystyrene slabs (see Table 3). Since the index of refraction of the styrofoam is far less than that of polystyrene the effect of spacing errors is less.

The effect that an error in measurement of -0.003 in the index of refraction has on the "exact" value of the mean power transmission coefficients was computed for the styrofoam model. The perturbed index of the styrofoam is 1.090 as compared to its original value of 1.093. As an example, for an ensemble of ten (10) slabs having random positions the perturbed mean power transmission coefficient is 0.929 as compared to the original value of 0.940 (see Table 2). Therefore an error of only -0.003 in the measurement of the index of styrofoam can produce an error of -1.1% in the calculation of the exact mean power transmission of an ensemble of ten (10) slabs. Therefore, the sensitivity of the "exact" method to the calculation of the mean power transmission coefficients is similar for both the styrofoam and polystyrene models.

The effect that a change in the angle of incidence from 0.0 deg. to 2.2 deg. has on the mean power transmission coefficient of the polystyrene model was calculated using "exact" theory. As an illustrative example, the mean power transmission for an ensemble of twenty (20) slabs with an angle of incidence of 2.2 deg. is 0.609 as compared to 0.605 for 0.0 deg. (see Table 4). Therefore, the effect of changing the angle of incidence by 2.2 deg., on the "exact" value of the mean power transmission coefficient of polystyrene is +0.4%. This is the order of magnitude of the klystron noise. It is likely that since the index of refraction of the

styrofoam is far smaller than that of the polystyrene, that the effect will be even smaller. Furthermore, then, we can conclude that the tolerances on plumb, angle of incidence, and wedge angle i. e. $\pm\frac{1}{4}^{o}$, $\pm\frac{1}{2}^{o}$, $1/20^{o}$ respectively, for the polystyrene and styrofoam models considered will produce no significant errors in the measurement of the mean power transmission coefficients.

Both the blemishes and sagitta are small compared to a wavelength i. e. 1/70 and 1/200 wavelength respectively. Therefore, errors they may produce are insignificant.

An estimate of the order of magnitude of the effect that strip misalignment may have on the measurement of the mean power transmission coefficient can be made using geometrical theory. A 0.016" error in the in-line location of a strip relative to another strip, increases the width of the strip shadow on the XTAL field detector horn. The corresponding decrease in power transmission is $\frac{1}{2}\%$.

Sources of error affecting the accurate measurement of the power transmission coefficients of each slab configuration are listed in Table 9b. The worst condition occurs for both the polystyrene and strip models because of standing wave effects. The standard error of the random sources is 0.94%. This is in good agreement with the differences between experiment and the Papanicolaou values for the styrofoam model i. e. F = 0.006 (see Tables 1 and 2). Now considering the systematic errors due to system non-linearity, the worst case occurs if they are all added arithemetically, i. e. 1 3/4%. Combining the random and systematic errors arithemetically we get about 2 3/4% maximum. This is in good agreement with the value F for the polystyrene model i. e. F = 0.02, gotten when the experimental values were compared to the Papanicolaou values.

The values of F obtained for the strip model, when experimental values were compared to the Papanicolaou values, are higher i. e. 0.03 and 0.04. The Papanicolaou theory does not predict the mean power transmission of the strip model as well as it does the styrofoam and polystyrene models.

B. Conclusions

The design and fabrication of equipment to implement the simulation of spacially discrete fluctuations of index of refraction in a one dimensional random medium was completed. This equipment was used to investigate the mean power transmission coefficients of two different one dimensional plane stratified dielectric models having approximately the same length but varying in slab width and index of refraction; and a random conducting medium. The experiment was performed for both fixed and random slab positions.

The experimentally determined mean power transmission coefficients were compared with values predicted by both contemporary and classical theory, i. e. the Papanicolaou approximation, Born approximation and the exact solution of Maxwell's equations. Disagreement between the exact theory and both the Papanicolaou and experimental values arise principally because of limits on the accuracy in the determination of the index of refraction of the slabs comprising the respective models.

The experimental values for the low index styrofoam model compare with both statistical theories within ½%, and with the exact theory within 0.9%. The experimental values for the high index polystyrene model compare with the Papanicolaou approximation within 2%, the Born

approximation within 4%, and the exact theory within 3.3%.

The good agreement between the Papanicolaou and experimental values demonstrates that, despite the difference in statistics between the experimental models and those assumed for the derivation of the statistical theory the predictions of the Papanicolaou theory are still accurate. This is evidence of the broad scope of the theory beyond the assumptions maintained for its mathematical derivation. Furthermore, it shows that although it is an approximate theory, its ability to predict the mean power transmission coefficients of a layered dielectric random medium is within say 1% i. e. the difference between the Papanicolaou theory and experiment (2%) and the measuring accuracy (standard error) of (0.94%). This serves to underline the correctness of the assumptions and approximations with which it was derived. In addition, the Papanicolaou approximation is in better agreement with experiment than the Born approximation for the dielectric models considered.

The experimental values for the conducting random medium compare with the Papanicolaou approximation to within 3% and 4% for random and fixed strip positions respectively. Since the theory was derived for dielectric media alone, this serves as further evidence of the broad scope of the theory, and its possible general applicability to media beyond dielectrics for which it was originally intended.

The non-linear predictions of the Papanicolaou theory are most distinguishable from those of the linear theories, for example the Born approximation, at low mean power transmission levels. Realization of slab ensembles with accompanying low mean power transmission depends largely on the utilization of slab materials having a high index of refraction at 60 GHZ. The principle limitation is in obtaining low cost, rigid, lightweight, uniform materials having a high index of refraction with accompanying low absorbtion.

APPENDIX. A.

Measurement of the relative field intensity - Single Strip Diffraction

A proof is given, using the Keller Geometrical Theory of Diffraction[16] to show that a detector viewing a long perfectly conducting strip, edge on, measures only radiation diffracted from the near edge of the strip. Referring to the adjacent figure -

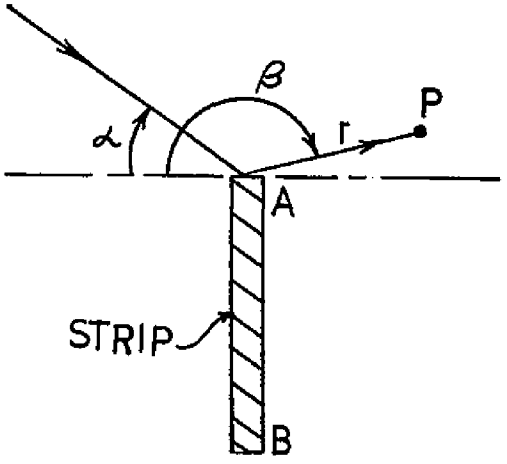

we have for the field at P, due only to strip edge A

$$U = \frac{V\, e^{i\left(\frac{\pi}{4} + kr\right)}}{2(2\pi kr)^{1/2}} \left\{ \sec\left[(\beta-\alpha)/2\right] + \csc\left[(\beta+\alpha)/2\right] \right\} \qquad A.1$$

where the incident radiation is normal to edge A and polarized with the E field parallel to the edge.

For the case of plane wave radiation incident on the strip, and edge on observation at P

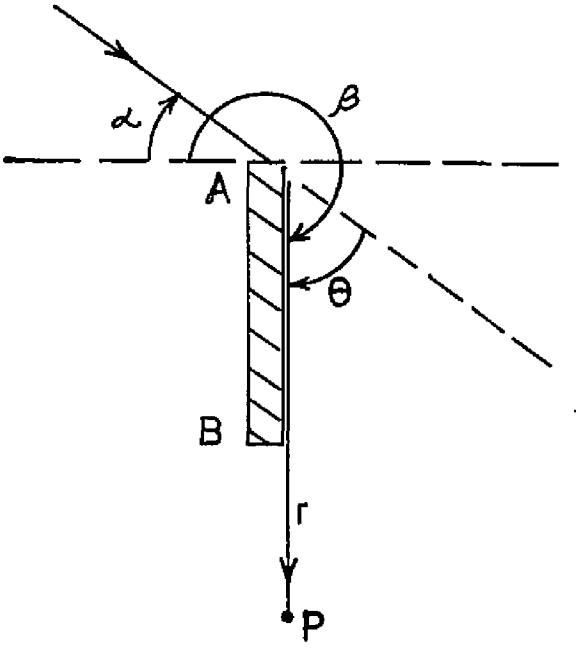

the angular part of the field at point P due only to the distant edge A becomes.

$$\left\{ \sec\left[(-\pi/2-\alpha)/2\right] + \csc\left[(-\pi/2+\alpha)\right] \right\} = 0$$

Therefore the distant edge of the strip does not contribute to the field measured at P, independent of the distance r. A detector at P will measure only the field diffracted by the closer edge B. This conclusion is implied by the boundary conditions on a perfect conductor, i. e. $E_{||} = 0$. Since the strip surface is between the observation point P and the edge A, any field diffracted by A toward P must pass over the surface of the strip. But $E_{||}$ cannot exist on the surface of the strip therefore $E_{||}$ diffracted in the direction of P must be zero. For normally incident radiation, the edge cannot depolarize the field, therefore $E_{\perp}$ is also zero.

APPENDIX. B.

Papanicolaou approximation - Numerical integration

The equation for the approximate mean power transmission can be found in [17] i. e.

$$\langle |T(L)|^2 \rangle = \frac{4}{\sqrt{\pi}} e^{-\frac{\epsilon^2 SL}{4}} \int_0^\infty \frac{\chi^2 e^{-\chi^2} d\chi}{\cosh(\epsilon\sqrt{SL^3}\chi)} \qquad \text{B.1}$$

where E is a small dimensionless parameter characterizing the size of the fluctuations of the wave number of the random medium, S is a statistical parameter, and L is the length of the random medium.

$$S \equiv \frac{k^2}{2} \int_0^\infty f(\tau) \cos 2k\tau \, d\tau \qquad \text{B.2}$$

Where $\tau = |L-L'|$, $f(\tau) = \langle m(L)\, m(L') \rangle$
$m(\chi) = m(x,\alpha)$ is a real random process with zero mean.

Also, for our experiment m(x) is zero in the region $L < x$. Therefore $f(\tau) = 0$. The same conclusion may be reached by assuming that any random process which occurs in the region $L < x$ is uncorrelated with processes occurring inside the region $0 < x < L$.

The second integral in (B.2) can be solved by noting that

$$\int_0^L \chi^2 e^{-\chi^2} d\chi + \int_L^\infty \chi^2 e^{-\chi^2} d\chi = \int_0^\infty \chi^2 e^{-\chi^2} d\chi = \frac{1}{2}\Gamma(3/2) = 0.4431$$

Thus

$$\int_L^\infty \chi^2 e^{-\chi^2} d\chi = 0.4431 - \int_0^L \chi^2 e^{-\chi^2} d\chi$$

We can evaluate this numerically, that is -

$$\int_L^\infty \chi^2 e^{-\chi^2} d\chi \longrightarrow 0.4431 - \frac{L}{1000} \sum_{\chi = L/1000}^{L} \chi^2 e^{-\chi^2} \qquad \text{B.5}$$

Combining (B.4) and (B.5) we get

$$\langle |T(L)|^2 \rangle = \frac{4}{\sqrt{\pi}} e^{-\frac{\epsilon^2 SL}{4}} \left\{ 0.4431 + \frac{L}{1000} \sum_{\chi = L/1000}^{L} \chi^2 e^{-\chi^2} \left(\frac{1}{\cosh\left(\epsilon\sqrt{SL}\chi\right)} - 1 \right) \right\}$$

B.6

This expression was evaluated on the computer and the results plotted in Figs. 16 - 20 by a Hewlett Packard 7200A Digital Plotter.

APPENDIX. C.

Absorption Measurements - Styrofoam, Polystyrene

Single slabs of each material were individually positioned in the field such that their transmission was a maximum. This occurs at Brewster's angle[18] with the incident electric field vector polarized in the plane of incidence. The measured transmission was 100% for both styrofoam and polystyrene. The absorption is too small to be measured.

APPENDIX. D.

Random Number Generator - Statistical Testing

There is a very useful measure for the discrepency between observed and expected frequencies which is called X^2 (CHI SQUARE). This test involves calculation of the mean square error between the actual and desired distribution. The quantity X^2 [19-20] is given as

$$\chi^2 = \sum_{r=1}^{n} \frac{(V_r - NP_r)^2}{NP_r} \qquad \text{D.1}$$

where n = number of cells in the distribution

V_r = observed frequency in each cell

N = total number of samples

P_r = hypothetical probability of falling in the r^{th} cell.

As $N \to \infty$, the probability distribution of X^2 tends toward:

$$P(\chi^2) = \frac{1}{2^{(n-1)/2}\,\Gamma[(n-1)/2]}\,\chi^{(n-3)/2}\,e^{-\chi/2} \qquad \text{D.2}$$

The computer random number generator provides numbers between -1 and +1. We divided this interval by one-hundred (n = 100 cells). Then 100 groups of 10,000 random numbers each were generated. X^2 was computed for each group. A histogram for X^2 was then plotted in Fig. A.6. For a rectangular distribution P_r is uniform, i. e. $P_r = 0.01$. Equation (D.2) is also plotted for comparison. The random number distribution is plotted in Fig. A.5.

Now for large N [21-22]

$$\sigma = \sqrt{\frac{P_r(1-P_r)}{n}} \qquad D.3$$

$$= \sqrt{\frac{0.01(1-0.01)}{100}}$$

$$\approx 0.01$$

The $\pm\sigma$ limits are shown and 27 cells (27% in this case) fall outside, which is well within the expected 32% value. The

value of X^2 is close to the mean value expected. Therefore, one can conclude that these numbers are in all probability statistically satisfactory.[23]

APPENDIX. E.

Index of Refraction - Measurements

1. Wedge Method

A solid wedge of styrofoam, 12" X 12" with an angle of $15.5^{\circ} \pm 0.5^{\circ}$ was fabricated.

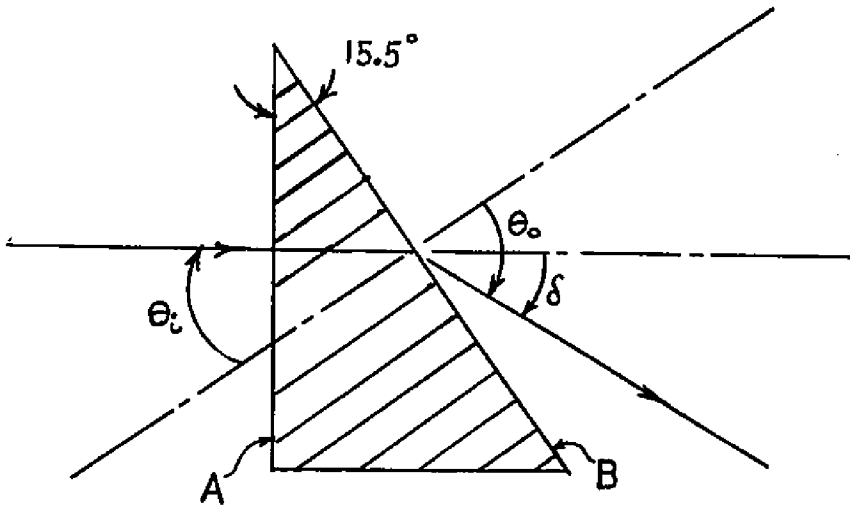

Surface A is flat to ±1/100 wave. This is the surface irregularity of the styrofoam sheet from which it was cut. Surface B is flat to ±1/20 wave. Surface B is not as flat as surface A since it was cut with a heat knife. The wedge was placed in the field of the incident radiation and the angular deviation of the refracted beam was measured using the microwave spectrometer.[24] The angular deviation was found to be $0.3^{\circ} \pm 0.2^{\circ}$ (very small)! The reading error is due to the tolerance on the spectrometer angular readout and the resolution of the detector.

Applying Snell's law we can calculate the index of

refraction of the styrofoam.

$$n = \frac{\sin \theta_o}{\sin \theta_i}$$

$$= \frac{\sin (15.5^\circ \pm 0.5^\circ + 0.3^\circ \pm 0.2^\circ)}{\sin (15.5^\circ \pm 0.5^\circ)}$$

$$= \begin{cases} 1.09 & \text{max} \\ 1.00 & \text{min} \end{cases}$$

The spectrometer detector (parabolic dish, horn and XTAL) reflects some radiation back toward the klystron source. The klystron (open ended waveguide) reflects a part of the radiation back toward the spectrometer detector. Therefore standing waves are set up. The effect of the standing waves on transmission measurements made using the spectrometer was found to be ±15%. The effect on the evaluation of the index of refraction was found later to be small after comparison with the index of refraction of styrofoam measured by a "transmission" method i. e. n = 1.09 max. for wedge method compared with 1.093 for "transmission" method.

Wedges could not be made from the polystyrene because the sheets were too thin i. e. ¼", therefore the wedge method could not be applied to the polystyrene.

2. Transmission Method

The materials measured were 3" nom. thk. styrofoam and ¼"

nom. thk. polystyrene. The power transmission of a slab of material was measured for normal incidence ($\theta = 0^{o} \pm 0.2$). Twenty-five measurements were made of the same slab and the results were averaged to reduce uncertainties from sources of non-systematic errors such as klystron noise. The mean power transmission of the styrofoam and polystyrene slabs measured were 0.992 and 0.949 respectively. The mean power transmission and thickness of each slab were used as input data to a program which computes the index of refraction of the material. The equations used in the program are those of Brekhovskikh.[25] Each index of refraction root which satisfied the boundary conditions was printed out. For styrofoam, the first two roots are n = 1.094 and 1.12 respectively. For polystyrene, the first two roots are n = 1.330 and 1.683 respectively.

3. Statistical Method

An estimate of the index of refraction of the styrofoam may be made using the value of E^2S gotten by the least squares best fit of the experimental power transmission values with the Papanicolaou approximation[26]; i. e. $E^2S = 0.00090$ (two significant figures). The "Random Binary Transmission Process"[27] approximates the styrofoam experiment for fixed slab positions and random numbers of slabs. For this process the autocorrelation of m(L) is given by[28]

$$\rho(\tau) = \langle m(L)\, m(L') \rangle = \begin{cases} 0 & \tau > T \\ 1 - \frac{\tau}{T} & \tau < T \end{cases} \qquad \text{E.1}$$

where $\tau = |L - L'|$

T = single styrofoam slab thickness (3" nom.)

$m(L)$ = real random function with zero mean having values of plus or minus one.

This is an approximation because there is actually a $\frac{1}{4}$" air space between the slabs in our model. This is not taken into account in the "Random Binary Transmission Process." Also, for simplicity, we assume that the slabs are uniformly thick.

Now substituting $\rho(\tau)$ into the expression for the parameter S we get

$$S = \frac{k^2}{2} \int_0^\infty \rho(\tau) \cos 2k\tau \, d\tau$$

$$= \frac{k^2}{2} \int_0^T \left(1 - \frac{\tau}{T}\right) \cos 2k\tau \, d\tau$$

$$= \frac{1}{8T} \left[1 - \cos 2kT \right] \qquad \text{E.2}$$

We see that S depends in part on a prior knowledge of the wave number k. K can be expressed in terms of the wave number k_s inside the styrofoam and k_o in air. Using the definition[29] of k, and the fact that m(x) has values of plus or minus one, we see that

$$k_o^2 = [1 - \epsilon] k^2$$

$$k_s^2 = [1 + \epsilon] k^2$$

Now since

$$\frac{k_o^2}{k_s^2} = \frac{n_o^2}{n_s^2} = \frac{1}{n_s^2}$$

where n_s is the index of refraction of the styrofoam. We can determine E as -

$$\epsilon = \frac{n_s^2 - 1}{n_s^2 + 1} \quad \text{or} \quad \frac{k_s^2 - k_o^2}{k_s^2 + k_o^2} \qquad \text{E.3}$$

The value of k follows as -

$$k = k_o \sqrt{\frac{n_s^2 + 1}{2}} \qquad \text{E.4}$$

Therefore, S depends on a prior knowledge of the index of refraction of the styrofoam, the quantity that we wish to find.

Now, since we know, from the transmission method, that n_s is approximately 1.09 (2 significant figures) we can assume this value to be correct and check the self-consistency of the present method (at least to an order of magnitude). Substituting $n_s = 1.09$ into (E.4) we get $k = 12.6$. Then substituting this value of k into (E.2) we get $S = 0.033$. Using the value $E^2S = 0.00090$ mentioned above we can solve for E

$$E^2(0.033) = 0.00090$$

$$E = 0.16$$

Then from (E.3) $n = 1.17$ (2 significant figures)

Comparing this value with the value of n_s assumed we see that they differ by 6.8%. The agreement is good considering the approximations made and the limited accuracy of the numbers used in the computation.

There is no statistical analytic approach to the polystyrene experiment because of the thin slabs, wide airspaces and overlapped slabs.

APPENDEX. F.

Standing Waves-Measurement

1. Traveling probe method[30] (see Fig. 5)

The XTAL field detector (Y) is mounted on a micrometer slide (T). This permits rectilinear motion of the detector toward or away from the klystron source along the optical axis. The effect of this motion on the power transmission measurements was ±0.4%, giving a VSWR[31] of

$$VSWR = \sqrt{\frac{P_{max}}{P_{min}}} = \sqrt{\frac{1.004}{0.996}} \qquad F.1$$

$$= 1.008$$

By comparison we evaluated the effectiveness of the E-H tunner (S) and the 45° dielectric sheet (Q) as elements in reducing the standing waves. In their absence, the power transmission varies by ±5.5% when the XTAL detector was moved, giving a VSWR of 1.057.

2. Phase Method

A sheet of dielectric material, preferably one having a high index of refraction, e. g. ¼" thk. polystyrene, was placed between the klystron and the field detector with the electric field vector in the plane of incidence. The sheet is rotated to vary the angle of incidence. That percentage

of radiation reflected from the XTAL field detector to the klystron, and back again to the XTAL field detector, passes through the sheet twice. That percentage of radiation absorbed and detected by the XTAL on the first pass travels through the sheet only once. Therefore, as the angle of incidence is varied so is the optical path difference and phase between these two components of the radiation incident on the XTAL. The result is either constructive or destructive interference depending on the angle of incidence, index of refraction, and thickness of the sheet. Tests for standing waves using this method yield results in agreement with those of the traveling probe method.

APPENDIX G

Derivation of the Papanicolaou Approximation*

Consider the propagation of scalar waves through a slab of random medium. Assume the slab to be plane stratified occupying the interval $0<x<L$. Assume k to be the wave number in the regions $-\infty<x<0$ and $L<x<\infty$. The index of refraction of the slab is taken to be a random function with small fluctuations about a mean value. Therefore, the wave number within the region occupied by the slab is a random function and can be written as $k\sqrt{1+Em(x)}$, where E is a small dimensionless parameter characterizing the size of the fluctuations, $m = m(x) = m(x,\omega)$ is a real random function with zero mean, $\omega \in \Omega$ and the triple (Ω, U, P) is a probability space; Ω is an abstract space[69-70], U is a Borel field consisting of subsets (events) of Ω, and P is the probability of these events.

Let v(x) be the time harmonic wave field at location x with the time factor term e^{-iwt} omitted. Then v(x) satisfys the equations.

$$v_{xx} + k^2 v = 0 \qquad -\infty<x<0\ ,\ L<x<\infty \qquad \text{G.1}$$

---

* A summary of the derivation of the Papanicolaou approximation is presented here for completeness. Unless otherwise specified, information on the details of the derivation are from G.C. Papanicolaou, "Wave Propagation in a One-Dimensional Random Medium," SIAM. J. Appl. Math. pp. 13-18, (1971).

$$v_{xx} + k^2(1 + Em(x))v=0 \qquad 0 < x < L \qquad G.2$$

where the field v and its derivatives v_x are continuous at x = 0 and x = L. Clearly $v(x) = v(x,\alpha)$ is also a random function. In what follows we suppress the dependence on α as is customary.[71]

Let Ae^{-ikx} represent a wave incident on the slab from the right in the region $L < x < \infty$; and Be^{ikx} the reflected wave in the same space interval. We may assume that the wave transmitted into the region $-\infty < x < 0$ is of the form e^{-ikx}. By definition, the reflection coefficient R(L) is B/A.

Let us consider L variable, and therefore $R(L) = R(L,\alpha)$ a random function. A stochastic equation satisfied by R(L) is now derived.

At x = L we have, using the continuity of v and v_x

$$v(L) = Ae^{-ikL} + Be^{ikL}$$

$$\frac{v(L)}{A} = e^{-ikL} + R(L)\, e^{ikL} \qquad G.3$$

and

$$v_x(L) = -ikAe^{-ikL} + ikBe^{ikL}$$

$$\frac{v_x(L)}{A} = -ike^{-ikL} + ikR(L)e^{ikL} \qquad G.4$$

Dividing G.4 by G.3 we get

$$\frac{v_x(L)}{v(L)} = \frac{ik\left[R(L)e^{ikL} - e^{-ikL}\right]}{R(L)e^{ikL} + e^{ikL}} \qquad G.5$$

Solving G.5 for R(L) we get

$$R(L) = e^{-2ikL}\left[\frac{ikv(L) + v_x(L)}{ikv(L) - v_x(L)}\right] \qquad G.6$$

where the length L is zero or positive i. e. $L \geqslant 0$.

Differentiate G.6 and eliminate v(L) and its derivatives from the resulting expression using G.2 and G.5. Then we obtain

$$\frac{dR(L)}{dL} = E\ \frac{ikm(L)}{2}\left[e^{ikL}\,R(L) + e^{-ikL}\right]^2 \qquad G.7$$

This is the desired stochastic differential equation for the stochastic process R(L).

Assume the process $m(x,\alpha)$ to be stationary, then for $x' = x+\tau$

$$< m(x)m(x') > = <m(L)m(L')> = \rho(|L-L'|)\,. \qquad G.8$$

Using a recent theorem of Hashminskii's,[75] R(L) satisfys the conditions for weak convergence to a Markov process[76] for E small; then the transition probability density P(L, R(L)) of R(L), given R(0) = 0, is obtained as a solution of the relevant backward Kolmogorov (Fokker-Planck) equation.[77-81]

To facilitate the solution of this equation, two new dependent variables u & ϕ are defined by

$$R = \sqrt{\frac{u-1}{u+1}}\, e^{i\phi}, \qquad u \geq 1,\ u(0)=1,\ 0 \leq \phi \leq 2\pi \tag{G.9}$$

The transition probability density is then found to be

$$P(L,u(L)) = \frac{e^{-\frac{\epsilon^2 sL}{4}}}{2\sqrt{2\pi}(\epsilon^2 Ls)^{3/2}} \int_u^\infty \frac{\chi e^{-\chi^2/4\epsilon^2 sL}}{\sqrt{\cosh\chi - \cosh u}}\, d\chi \tag{G.10}$$

The solution for the mean of the square of the magnitude of the reflection coefficient R(L) in G.7 follows as

$$\langle |R(L)|^2 \rangle = \int_0^1 |R(L)|^2 \, P(L, R(L)) \, dR$$

$$= \int_1^\infty \left(\frac{u-1}{u+1}\right) P(L, U(L)) \, du, \qquad \text{G.11}$$

where $P(L,U(L)) \neq P(L,R(L))$

This reduces to

$$\langle |R(L)|^2 \rangle = 1 - \frac{4}{\sqrt{\pi}} e^{-\frac{\epsilon^2 SL}{4}} \int_0^\infty \frac{x^2 e^{-x^2} dx}{\cosh(\epsilon\sqrt{SL}\, x)} + O(\epsilon^2) \qquad \text{G.12}$$

Consequently, using the relation

$$|R(L)|^2 = 1 - |T(L)|^2$$

or

$$\langle |R(L)|^2 \rangle = 1 - \langle |T(L)|^2 \rangle \qquad \text{G.13}$$

we obtain the mean of the square of the magnitude of the transmission coefficient T(L) as

$$\langle |T(L)|^2 \rangle = \frac{4}{\sqrt{\pi}} e^{-\frac{\epsilon^2 SL}{4}} \int_0^\infty \frac{x^2 e^{-x^2}}{\cosh(\epsilon\sqrt{SL}\, x)} dx + O(\epsilon^2) \qquad \text{G.14}$$

The parameter s is defined as

$$S \equiv \frac{k^2}{2}\int_0^\infty \rho(\tau)\cos 2k\tau \, d\tau \qquad G.15$$

where

$$\rho(\tau) = \rho(|L-L'|) = \langle m(L)\, m(L')\rangle \qquad G.16$$

Therefore s is proportional to the real part of the Fourier transform of the autocorrelation function $\rho(\tau)$.[82]

By using entirely different methods[72-73] the same results hold even when m(L) is not Markovian but merely stationary. Thus to $0(E^2)$ certain statistics of the solution are insensitive to the detailed description of the fluctuations in the refractive index.[74]

The expression $0(E^2)$ represents additional terms having multiplicative constants of order E^2 and higher. As an illustration, for styrofoam, $n_s = 1.09$ (see Appendix E). Therefore using E.3, $E^2 = 0.008$, or about 1%.

# Slabs	E^2LS (cm.)	L (cm.)	Experimental Value	Papanicolaou Approx.	Born Approx.	Exact Theory
5	0.040	41.50	0.970	0.960	0.965	0.970
7	0.060	58.35	0.935	0.945	0.950	0.950
10	0.080	83.65	0.925	0.925	0.925	0.925

Table 1. Experimental mean power transmission coefficient as a function of the length of the styrofoam random medium, for an angle of incidence = 0^{o}; and for fixed slab positions and randomly selected slabs.

# Slabs	Difference in % mean power transmission between Experimental & Papanicolaou Values--% F=0.006	Experimental & Born Values--% F=0.006	Exact & Papanicolaou Values--% F=0.006
5	+1.0	+0.5	+1.0
7	-1.0	-1.5	+0.5
10	0.0	0.0	0.0

Table 1. continued

# Slabs	E^2LS (cm.)	L (cm.)	Experimental Value	Papanicolaou Approx.	Born Approx.	Exact Theory
5	0.035	41.50	0.965	0.965	0.965	0.970
7	0.045	58.35	0.955	0.955	0.955	0.955
10	0.070	83.65	0.935	0.935	0.935	0.940

Table 2. Mean power transmission coefficient as a function of the length of the styrofoam random medium, for an angle of incidence $= 0^{\circ}$; and for random slab positions and randomly selected slabs.

# Slabs	Difference in % mean power transmission between Experimental & Papanicolaou Values--% F=0.003	Experimental & Born Values--% F=0.003	Exact & Papanicolaou Values--% F=0.003
5	0.0	0.0	+0.5
7	0.0	0.0	0.0
10	0.0	0.0	+0.5

Table 2. continued

# Slabs	E^2LS (cm.)	L (cm.)	Experimental Value	Papanicolaou Approx.	Born Approx.	Exact Theory
4	0.135	17.20	0.880	0.880	0.910	0.915
6	0.190	24.30	0.815	0.840	0.870	0.870
8	0.245	31.80	0.790	0.800	0.830	0.800
10	0.310	39.10	0.755	0.760	0.790	0.790
12	0.360	46.30	0.715	0.730	0.750	0.740
16	0.485	61.90	0.665	0.665	0.665	0.690
20	0.580	76.60	0.640	0.620	0.585	0.590

Table 3. Experimental mean power transmission coefficient for polystyrene as a function of the length of the polystyrene random medium, for an angle of incidence = 2.2°; and for fixed slab positions and randomly selected slabs.

# Slabs	Difference in % mean power transmission between Experimental & Papanicolaou Values--% F=0.02	Experimental & Born Values--% F=0.04	Exact & Papanicolaou Values--% F=0.03
4	0.0	-3.0	+3.5
6	-2.5	-5.0	+3.0
8	-1.0	-4.0	0.0
10	-0.5	-3.5	+3.0
12	-1.5	-3.5	+1.0
16	0.0	0.0	+2.5
20	+2.0	+5.5	-3.0

Table 3. continued

# Slabs	E^2LS (cm.)	L (cm.)	Experimental Value	Papanicolaou Approx.	Born Approx.	Exact Theory
4	0.125	17.20	0.885	0.890	0.910	0.915
6	0.175	24.30	0.835	0.850	0.870	0.875
8	0.230	31.80	0.830	0.810	0.830	0.795
10	0.285	39.10	0.780	0.775	0.795	0.790
12	0.335	46.30	0.715	0.745	0.755	0.740
14	0.385	21.30	0.760	0.715	0.715	0.720
16	0.445	61.90	0.690	0.685	0.675	0.710
20	0.570	76.60	0.625	0.625	0.595	0.605

Table 4. Experimental mean power transmission coefficient as a function of the length of the polystyrene random medium, for an angle of incidence = 2.2^{o}; and for random slab positions and randomly selected slabs.

# Slabs	Difference in % mean power transmission between Experimental & Papanicolaou Values--% F=0.02	Experimental & Born Values--% F=0.03	Exact & Papanicolaou Values--% F=0.03
4	-0.5	-2.5	+2.5
6	-1.5	-3.5	+2.5
8	+2.0	0.0	-1.5
10	+0.5	-1.5	+1.5
12	-3.0	-4.0	-0.5
14	+4.5	+4.5	+0.5
16	+0.5	+1.5	+2.5
20	0.0	+3.0	-2.0

Table 4. continued

# Slabs	E^2LS (cm.)	L (cm.)	Experimental Value	Papanicolaou Approx.	Born Approx.
1	0.100	7.75	0.885	0.910	0.945
2	0.200	16.25	0.745	0.830	0.880
3	0.310	24.70	0.770	0.760	0.820
4	0.415	33.15	0.730	0.700	0.760
5	0.525	41.50	0.670	0.645	0.695
6	0.625	50.00	0.545	0.600	0.635
7	0.725	58.35	0.535	0.560	0.575
8	0.835	66.80	0.530	0.520	0.515
9	0.940	75.25	0.420	0.485	0.450
10	1.050	83.65	0.455	0.455	0.390

Table 5. Experimental mean power transmission coefficient as a function of the length of the styrofoam and conducting strip random medium, for an angle of incidence = 0^o; and for random slab positions and randomly selected slabs.

# Slabs	Difference in % mean power transmission between Experimental & Papanicolaou Values--% F=0.03	Experimental & Born Values--% F=0.02
1	-2.5	-6.0
2	-8.5	-13.5
3	+1.0	--5.0
4	+3.0	-3.0
5	+2.5	-2.5
6	-5.5	-9.0
7	-2.5	-4.0
8	+1.0	+1.5
9	-6.5	-3.0
10	0.0	+5.5

Table 5. continued

# Slabs	E^2LS (cm.)	L (cm.)	Experimental Value	Papanicolaou Approx.	Born Approx.
1	0.105	7.75	0.885	0.905	0.940
2	0.215	16.25	0.835	0.820	0.875
3	0.325	24.70	0.815	0.750	0.815
4	0.445	33.15	0.670	0.685	0.750
5	0.555	41.50	0.655	0.630	0.685
6	0.665	50.00	0.600	0.585	0.620
7	0.780	58.35	0.540	0.540	0.555
8	0.895	66.80	0.520	0.505	0.495
9	1.010	75.25	0.445	0.470	0.430
10	1.120	83.65	0.495	0.440	0.365

Table 6. Experimental mean power transmission coefficient as a function of the length of the styrofoam and conducting strip random medium, for an angle of incidence = 0°; and for fixed slab positions and randomly selected slabs.

# Slabs	Difference in % mean power transmission between Experimental & Papanicolaou Values--% F=0.04	Experimental & Born Values--% F=0.06
1	-2.0	-5.5
2	+1.5	-4.0
3	+6.5	0.0
4	-1.5	-8.0
5	+2.5	-3.0
6	+1.5	-2.0
7	0.0	-1.5
8	+1.5	+2.5
9	-2.5	+1.5
10	+5.5	+13.0

Table 6. continued

AIRSPACE	DIMENSION (IN.) NOM.
d_{12}	2.77
d_{23}	0.24
d_{34}	2.32
d_{45}	0.20
d_{56}	2.13
d_{67}	0.43
d_{78}	2.03
d_{89}	0.30
d_{9-10}	2.02
d_{10-11}	0.44
d_{11-12}	2.06
d_{12-13}	0.26
d_{14-15}	2.12
d_{15-16}	0.39
d_{16-17}	2.18
d_{17-18}	0.19
d_{18-19}	2.12
d_{19-20}	0.45
	2.56

TABLE 7. Nominal airspace dimensions for polystyrene slab configuration (See Fig. 28).

Slab Configuration	Power Transmission Measurement		Deviation T_2-T_1
	T_1(Run #1)	T_2(Run #2)	
1	0.961	0.966	+0.006
2	0.931	0.933	+0.003
3	0.966	0.970	+0.004
4	0.930	0.942	+0.012
5	0.889	0.893	+0.004
6	0.912	0.911	-0.001
7	0.944	0.955	+0.011
8	0.956	0.956	0.000
9	0.923	0.918	-0.005

Table 8. Experimental power transmission measurements as a function of slab configuration, for a medium consisting of ten (10) randomly selected and randomly positioned styrofoam slabs, are repeated for comparison.

a. Carriage (slab) position errors.

Type	Source	Error Classification	Model: Styrofoam	Model: Polystyrene	Model: Styrofoam with Strips
noise	A/D converter	random	±0.005"	±0.005"	±0.005"
1LSB	A/D converter	random	±0.005"	±0.005"	±0.005"
play	gear	random	±0.001"	±0.001"	±0.001"
linearity	carr. pot.	systematic	±0.004"	±0.004"	±0.004"
linearity	op. amp.	systematic	±0.004"	±0.004"	±0.004"
linearity	A/D converter	systematic	±0.004"	±0.004"	±0.004"

Table 9. Summary of Sources of Error.

b. Power Transmission Coefficient Measurement Errors

Type	Source	Error Classification	Model: Styrofoam	Model: Polystyrene	Model: Styrofoam with Strips
standing waves	medium	random	negligible	±1½%	±1½%
standing waves	field detector	random	±0.4%	±0.4%	±0.4%
noise	klystron	random	±½%	±½%	±½%
wavelength change	klystron	random*	small	small	small
±0.01 mm. mismatch	XTAL'S	systematic	±½%	±½%	±½%
linearity	XTAL	systematic	±1%	±1%	±1%
linearity	SWR	systematic	±¼%	±¼%	±¼%
linearity	DVM	systematic	±0.01%	±0.01%	±0.01%
±5% ampl. variation	beam	systematic*	small	small	small
phase variation	beam	systematic*	small	small	small

Table 9. Summary of Sources of Error.

c. Deviation from the Theoretical Model

Type	Source	Deviation Classification	Model: Styrofoam	Model: Polystyrene	Model: Styrofoam with Strips
blemish	dents	systematic	0.003"	none	0.003"
parallelism	wedge angle	systematic	1/60 deg.	1/20 deg.	1/60 deg.
sagitta	warp	systematic	1/200 wave	1/200 wave	1/200 wave
angle of incidence	alignment	systematic	$0 \pm \frac{1}{2}$ deg.	$2.2 \pm \frac{1}{2}$ deg.	$0 \pm \frac{1}{2}$ deg.
plumb	alignment	systematic	$\pm \frac{1}{4}^{o}$	$\pm \frac{1}{4}^{o}$	$\pm \frac{1}{4}^{o}$
in-line symmetry	strip alignment	systematic	—	—	±0.008"

* The effect on the measurement of the mean power transmission coefficient was not experimentally determined.

Table 9. Summary of Sources of Error.

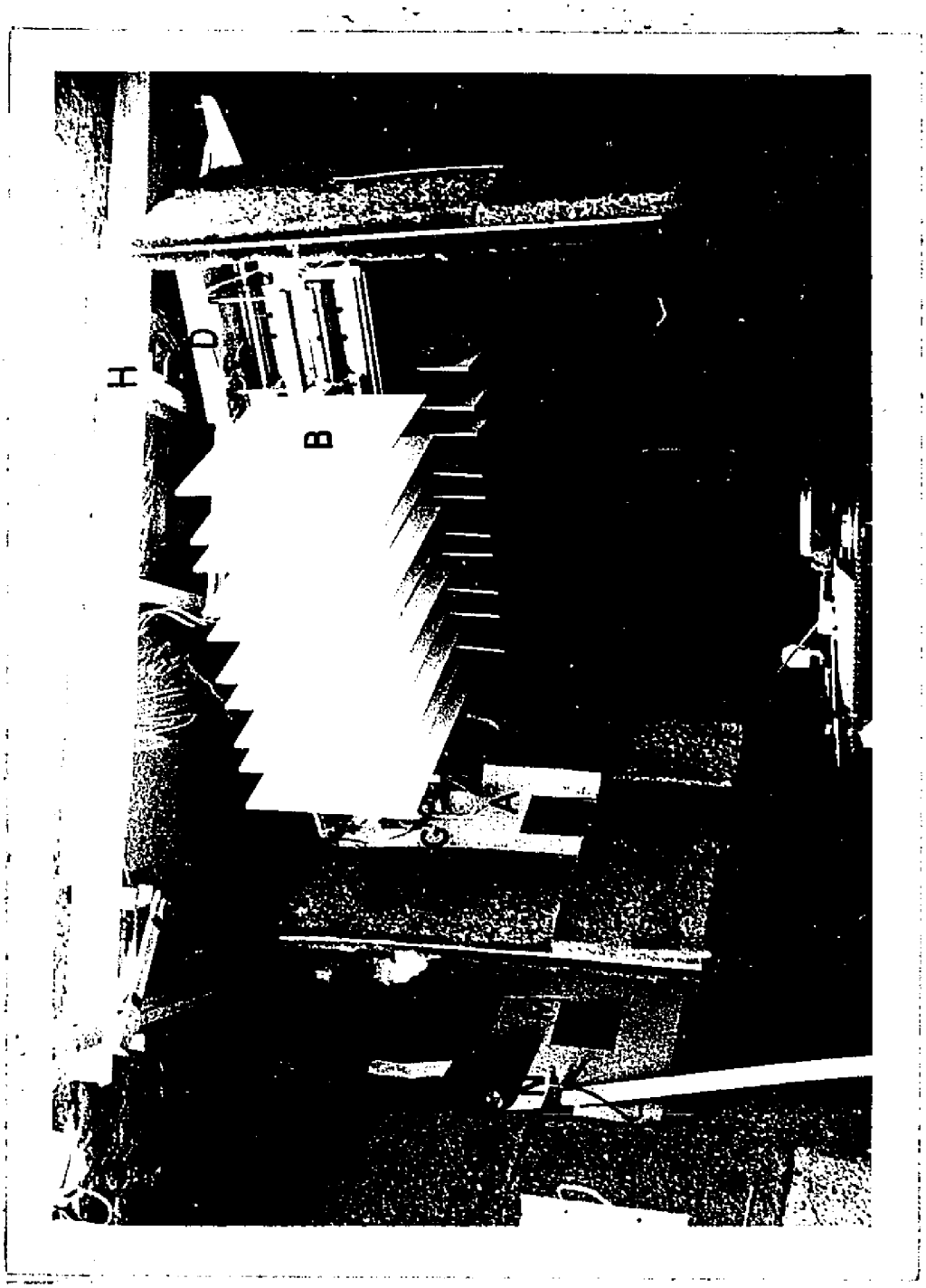

Figure 1. Longitudinal Table (side view). Shown are collimating apertures, twenty (20) polystyrene slabs held out of the microwave beam, klystron power output detector, overhead supporting structure, and the rotary table.

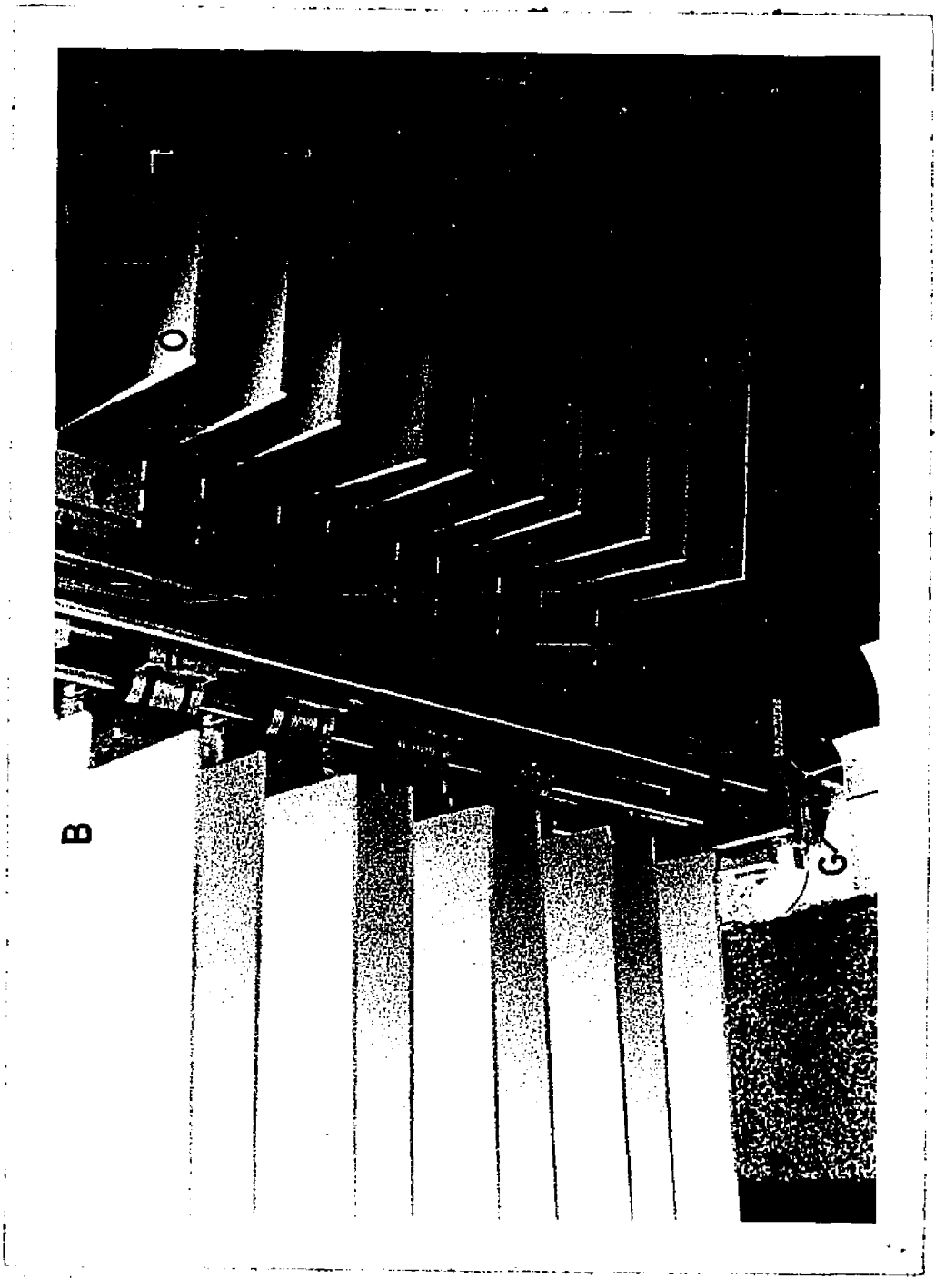

Figure 2. Longitudinal Table (bottom view). Shown are twenty (20) polystyrene slabs held out of the microwave beam.

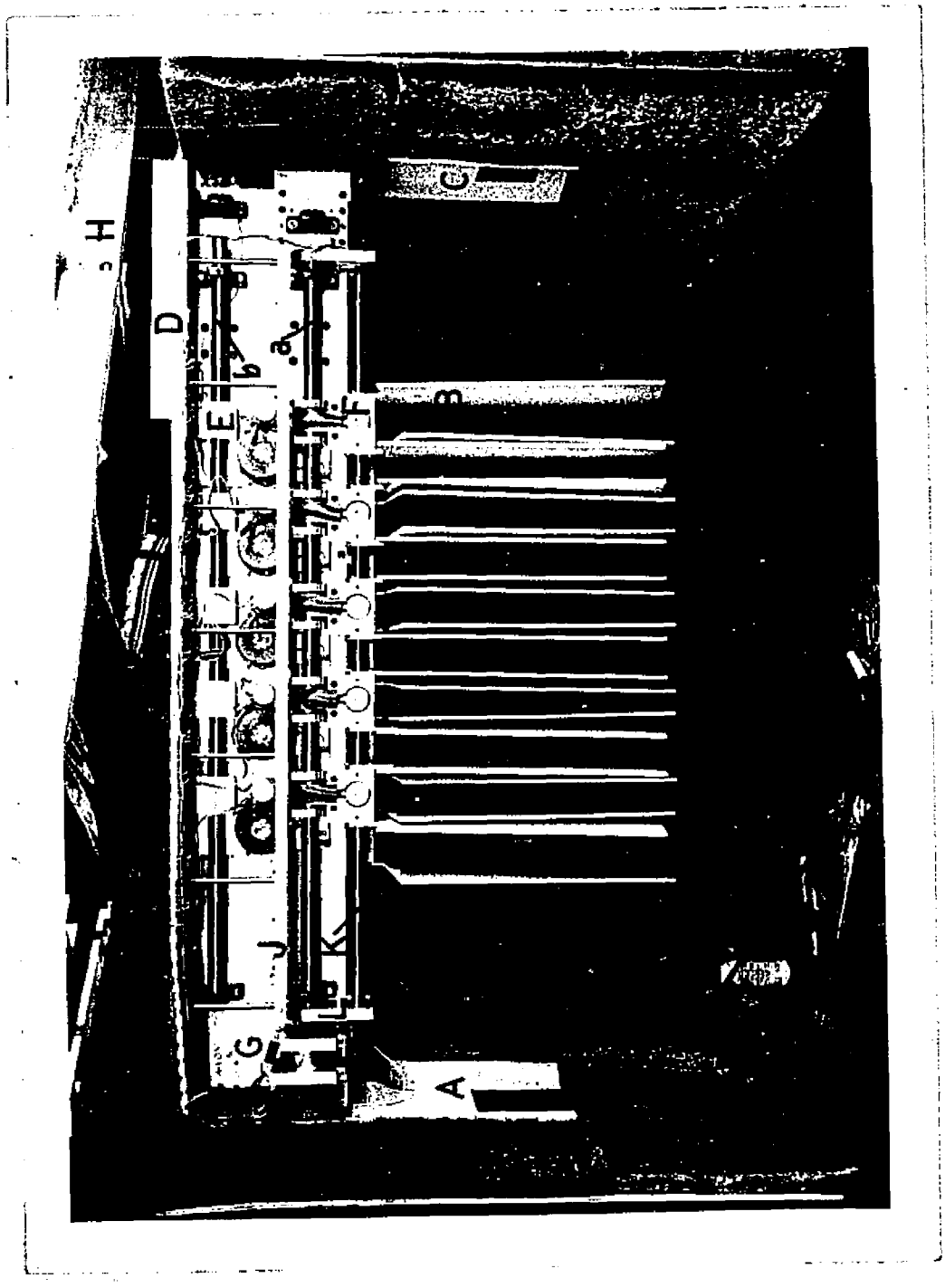

Figure 3. Longitudinal Table (side view). Shown are collimating apertures, twenty (20) polystyrene slabs placed in the microwave beam, rotary table, and the overhead supporting structure.

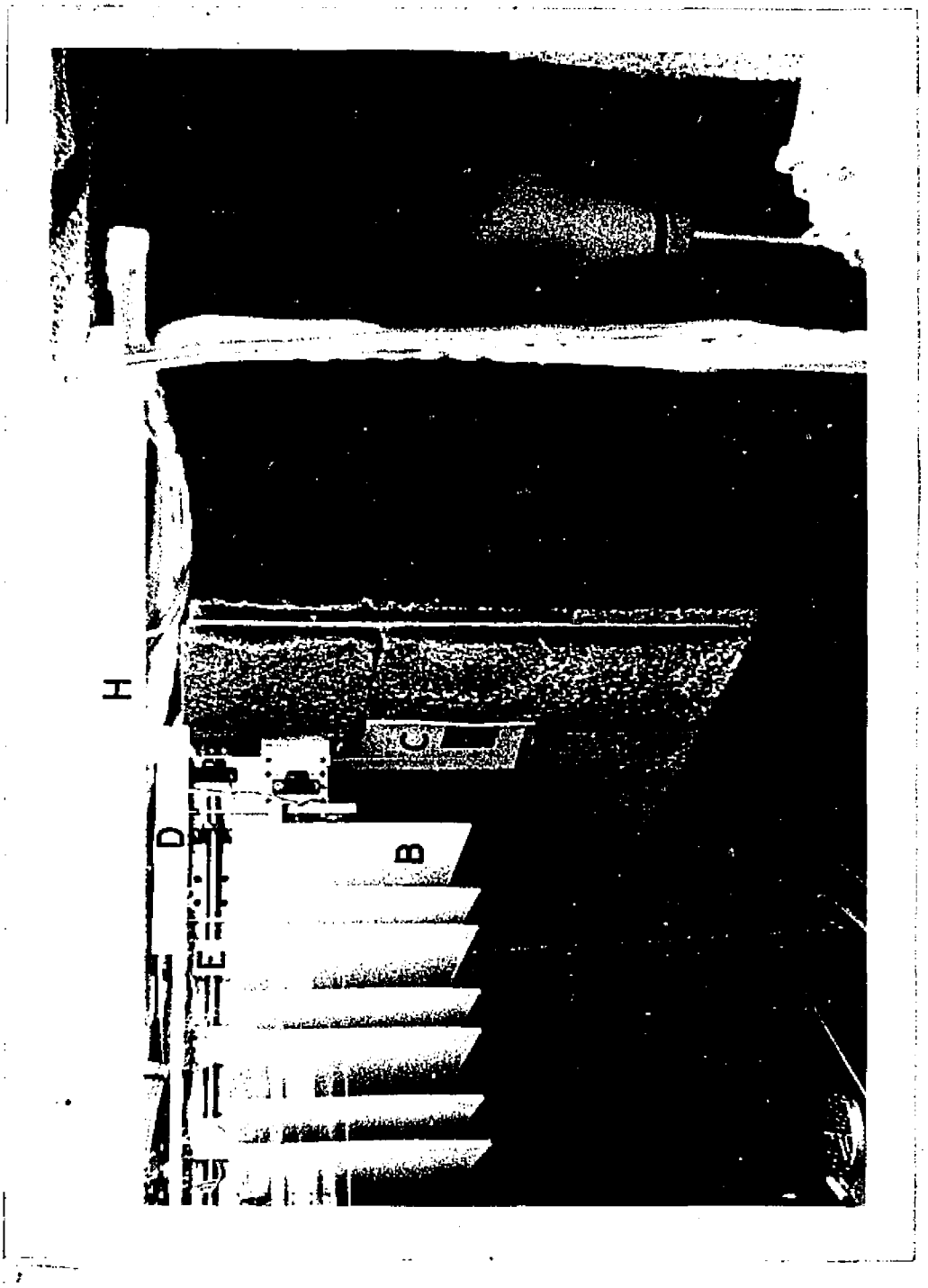

Figure 4. Longitudinal Table (side view). Shown are collimating apertures, and the field detector.

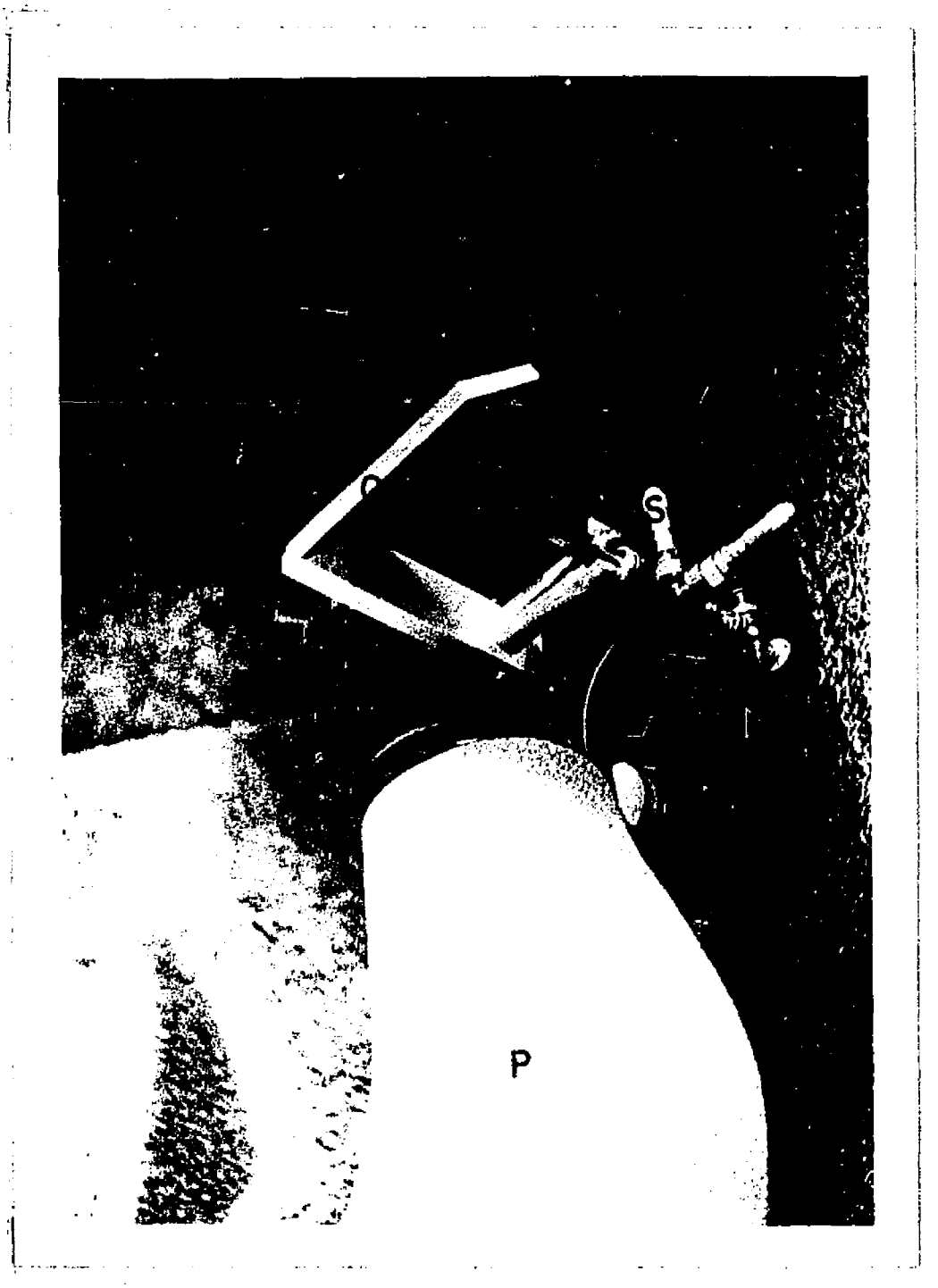

Figure 5. Field detector (bottom view). Shown are 45° dielectric sheet attenuator, horn, E-H tunner, XTAL, and pedestal mount.

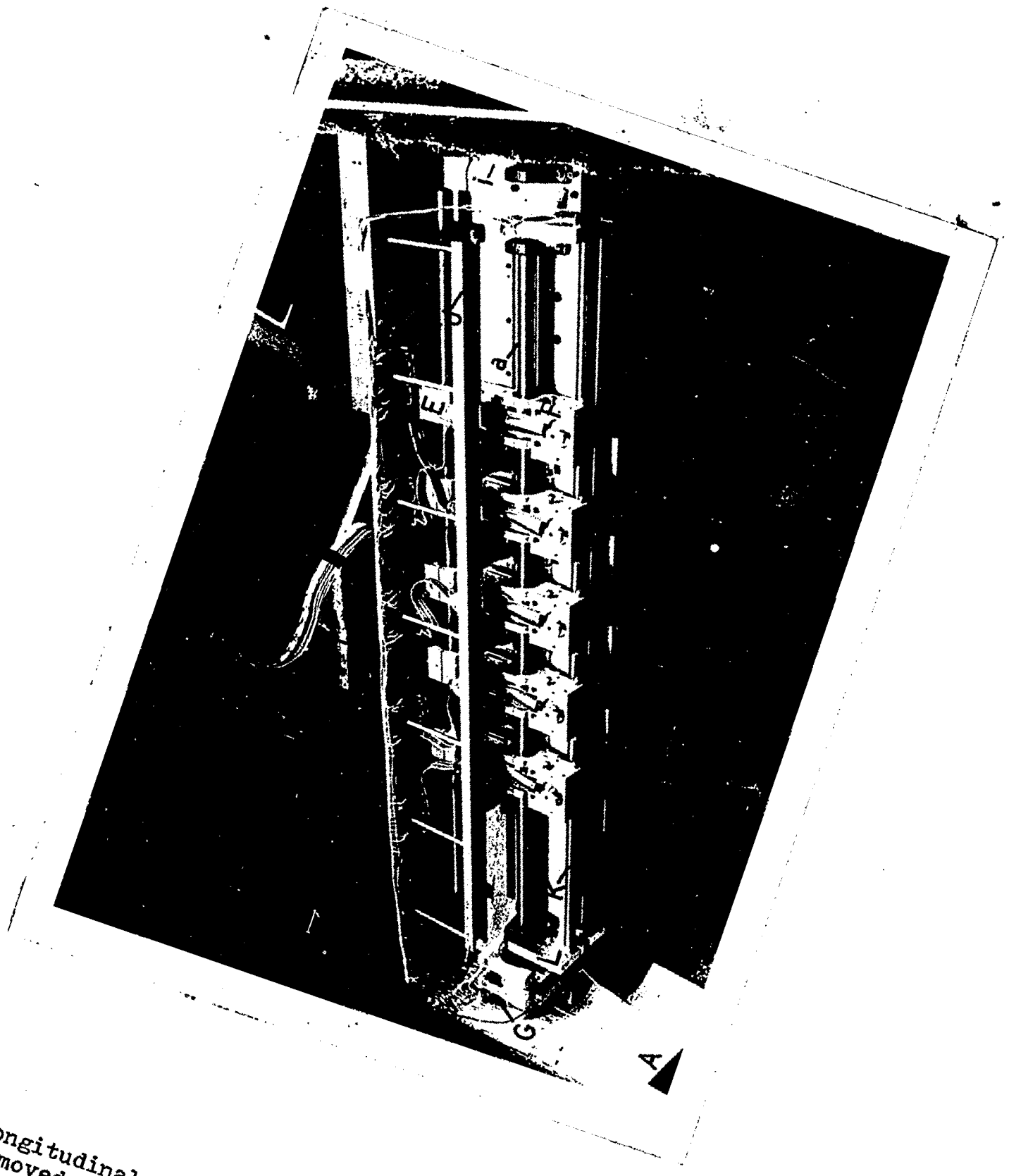

Figure 6. Longitudinal Table (3/4 bottom view). Slabs removed.

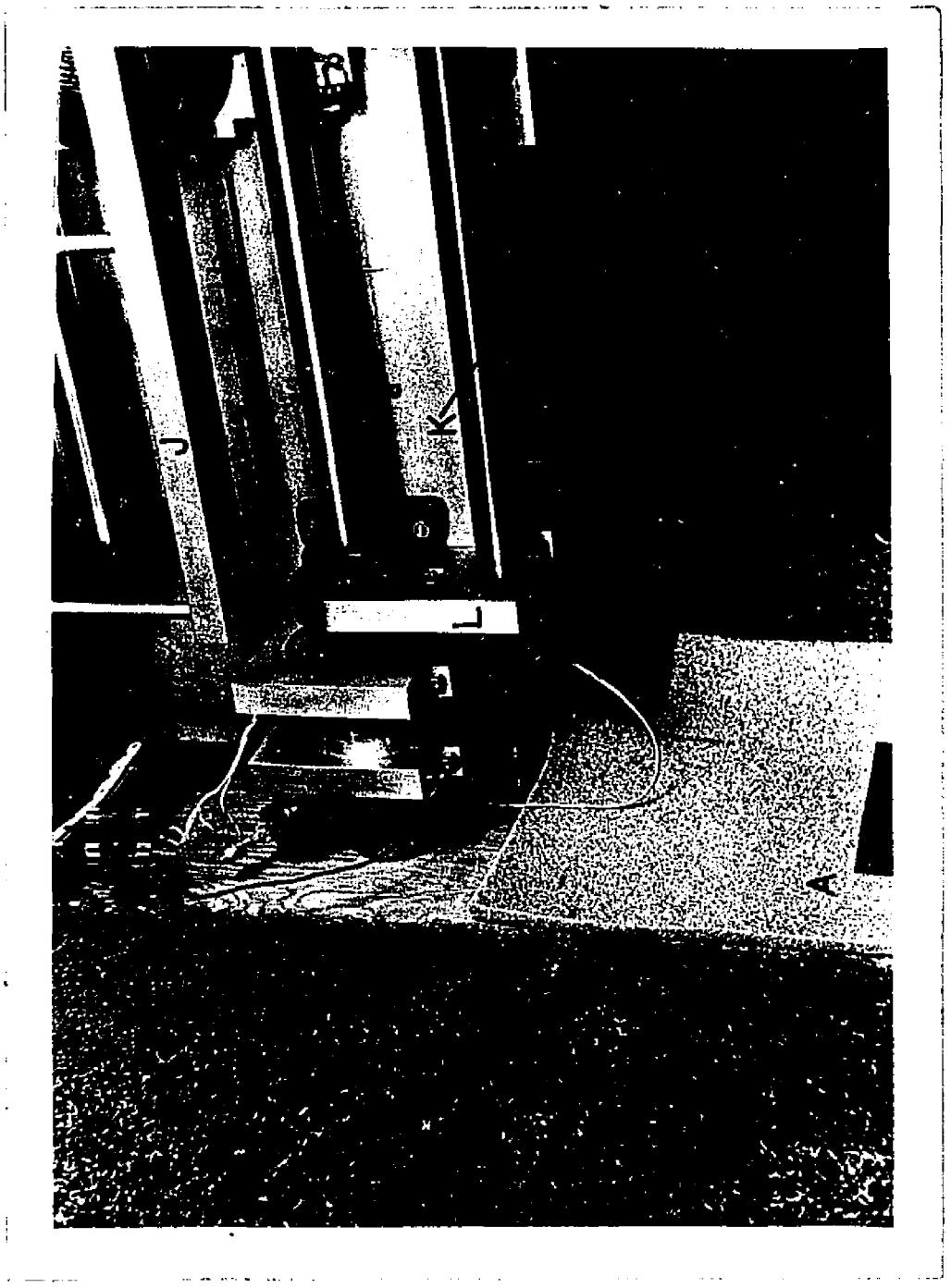

Figure 7. Longitudinal Table (side view, close-up). Shown are picker motor, picker arm, precision rack, picker channel, stainless steel carriage shafts.

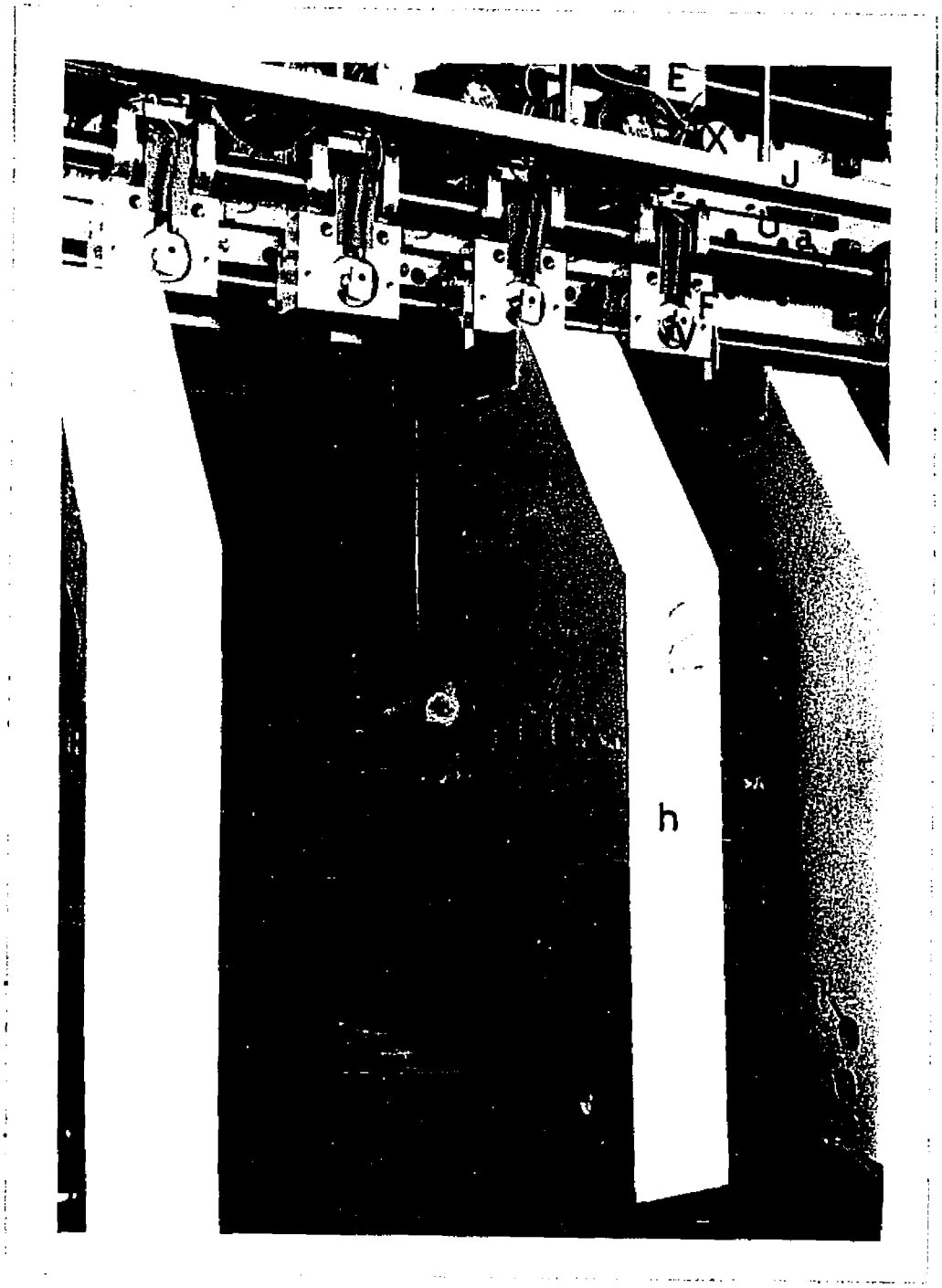

Figure 8. Longitudinal Table (side view). Shown are styrofoam slabs, with strips, placed in the microwave beam.

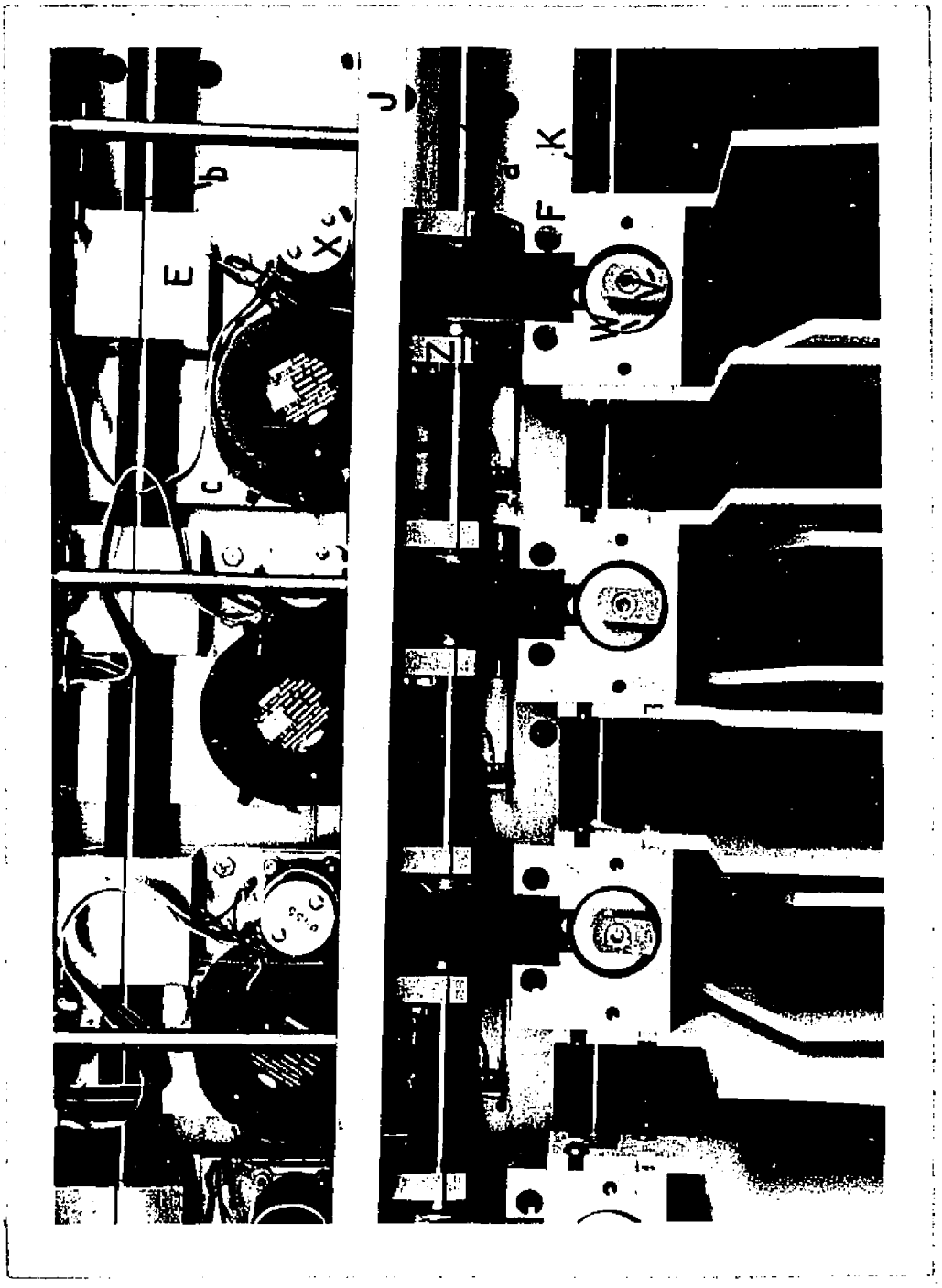

Figure 9. Longitudinal Table (side view). Close-up of carriage assemblies. Shown are the carriage potentiometer, drive motor, solenoid arm, solenoid and picker channel. Also shown are polystyrene slabs mounted on their respective carriage blocks.

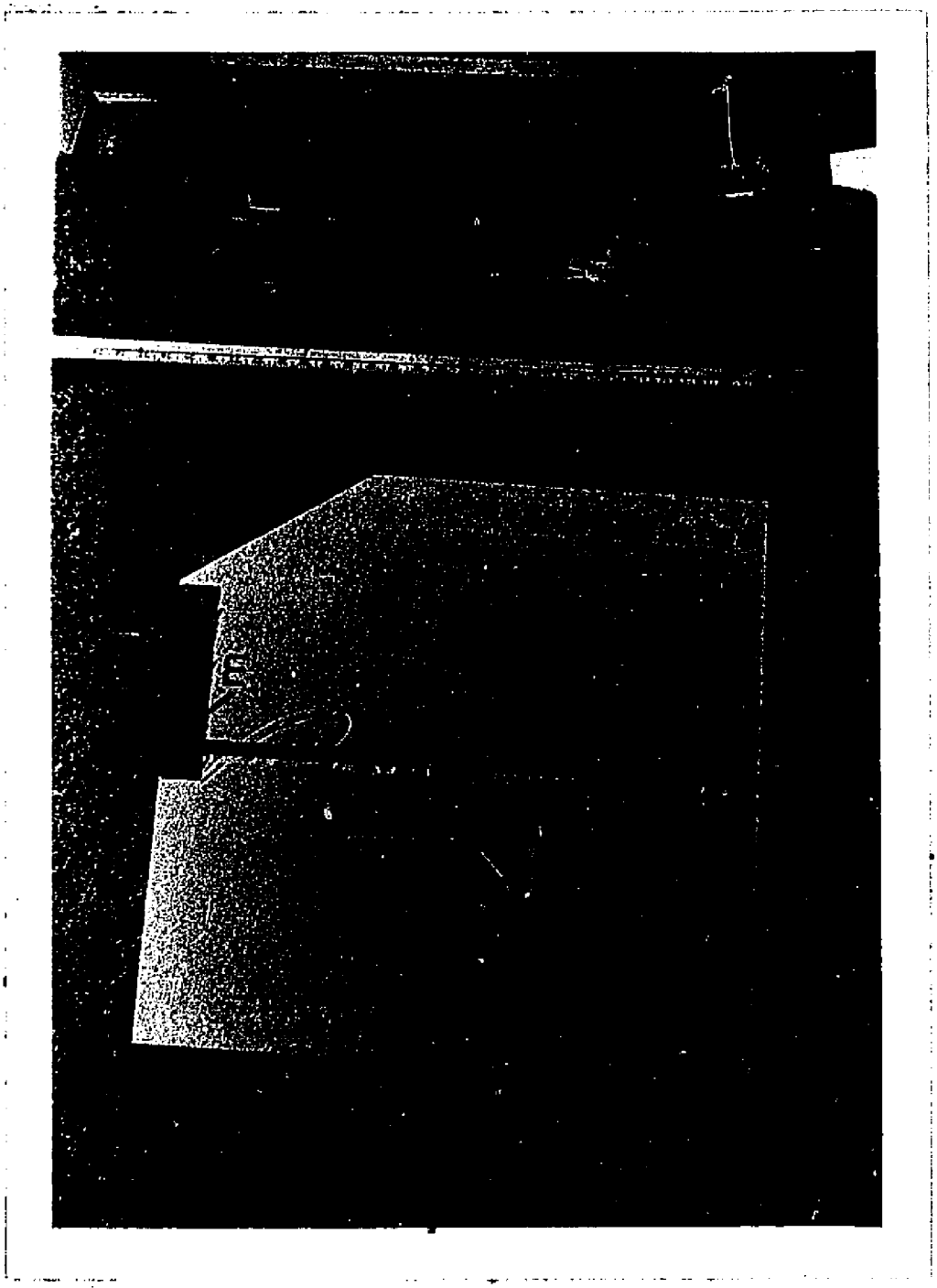

Figure 10. Styrofoam slab, with $\frac{1}{2}$" wide metal strip.

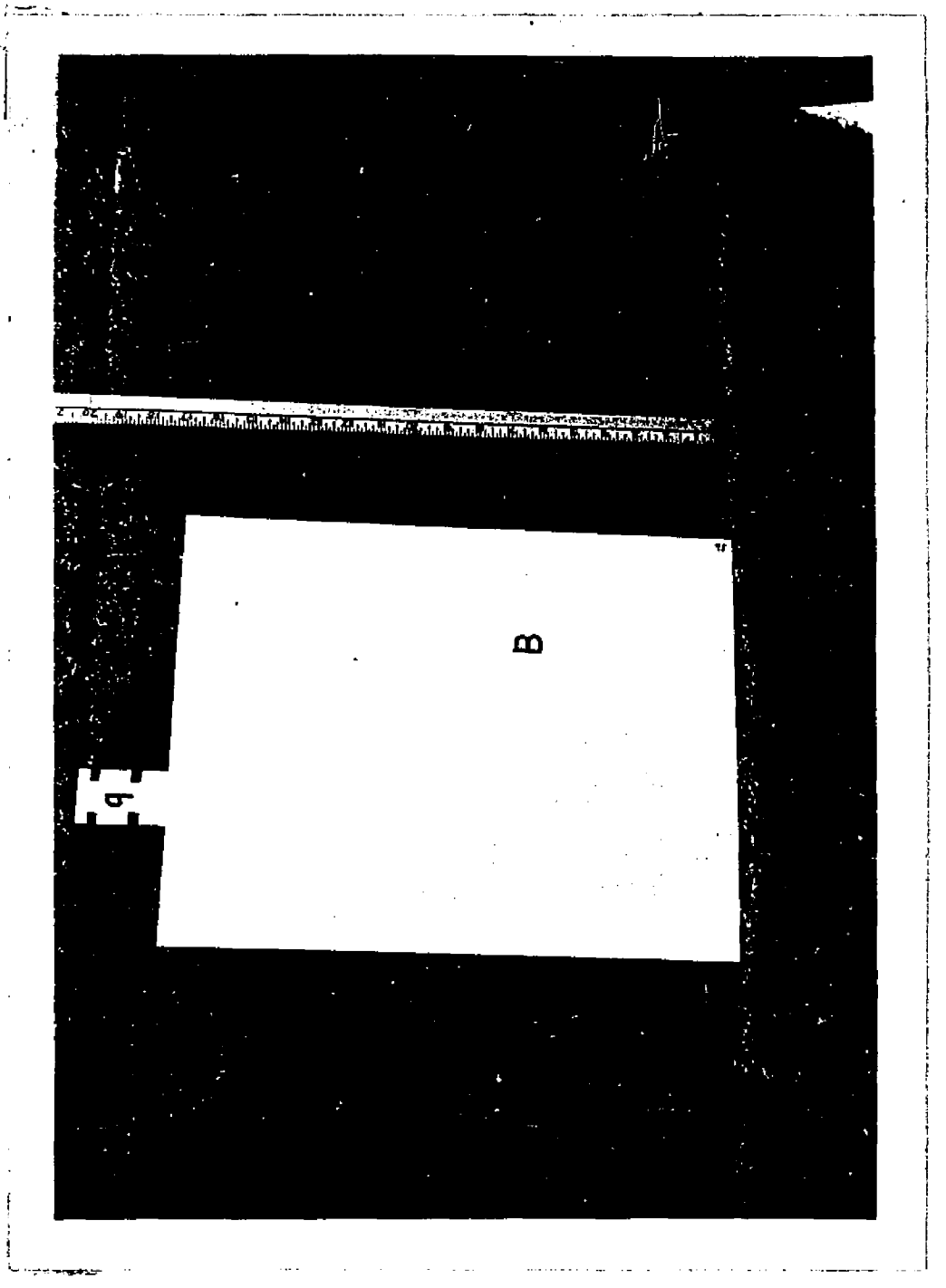

Figure 11. Polystyrene slab, with machined mouting tab.

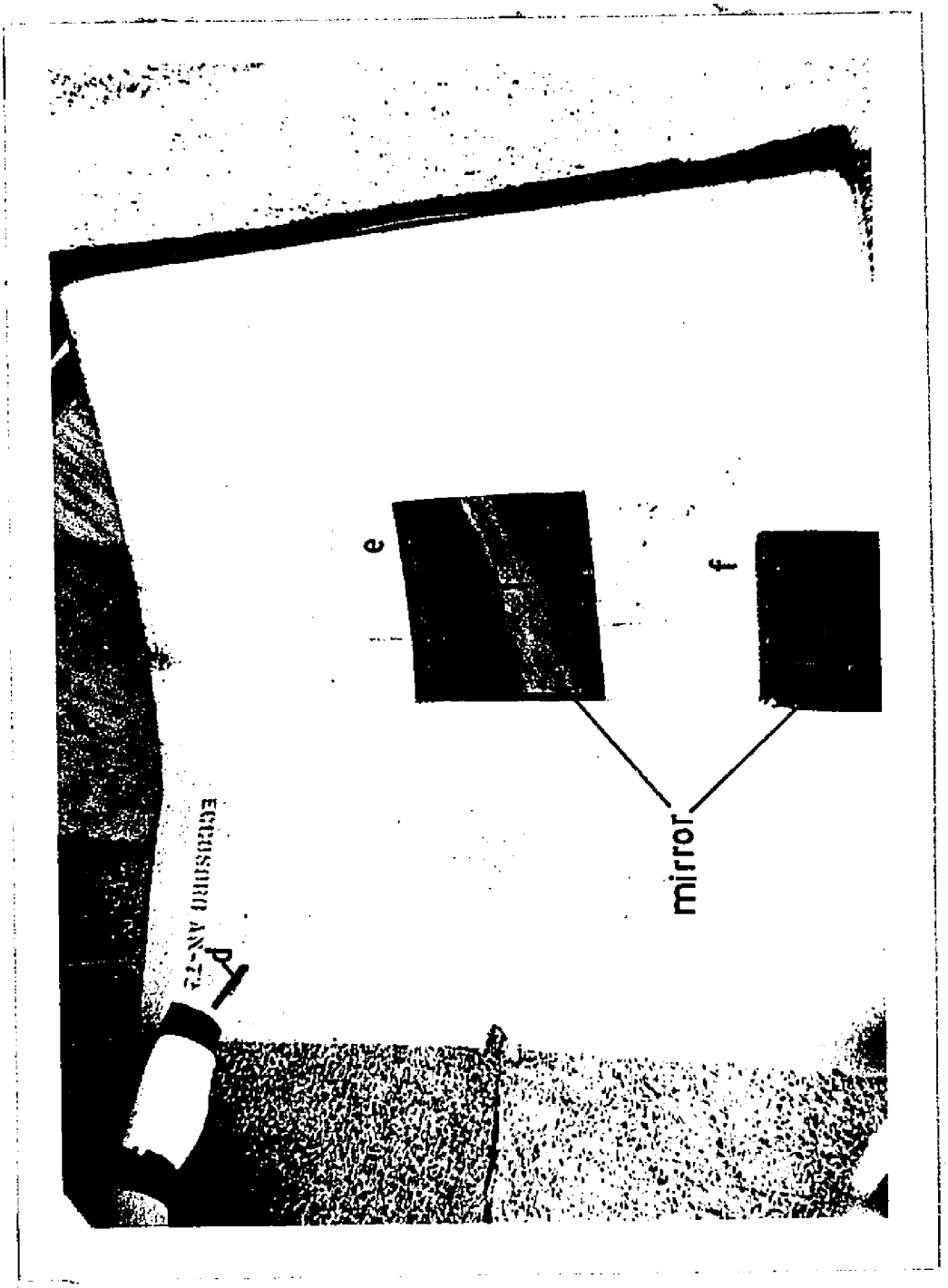

Figure 12. Klystron source (top view). Shown are klystron waveguide, collimating apertures and parabolic mirror.

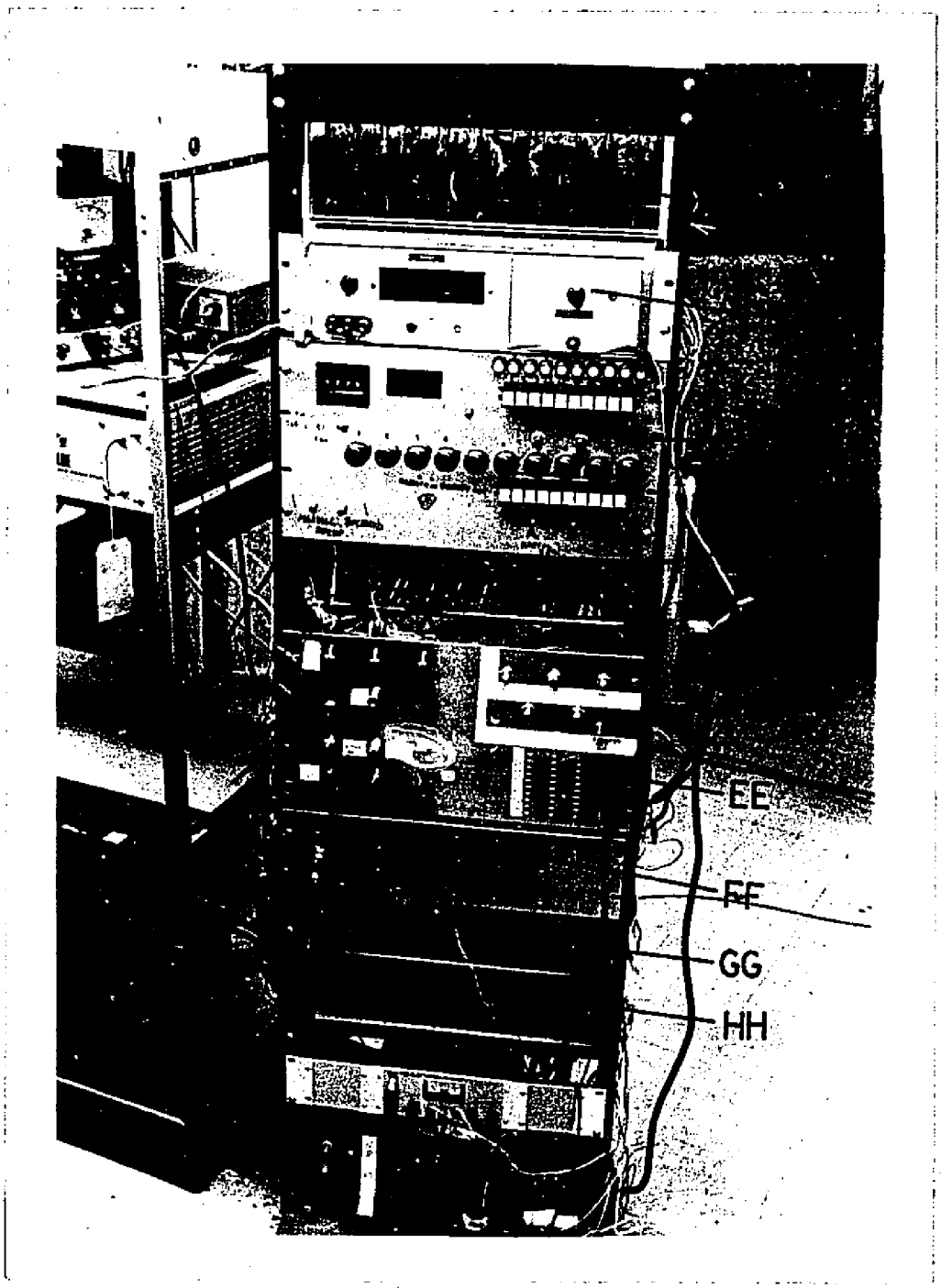

Figure 13. Control panel and electronics (front view). Shown are transmitter, DVM, manual and automatic controls, receiver, displays, multiplexer, solenoid, and carriage servo electronics.

Figure 14. Transmitter electronics (top view). Close-up of transmitter integrated circuit electronics.

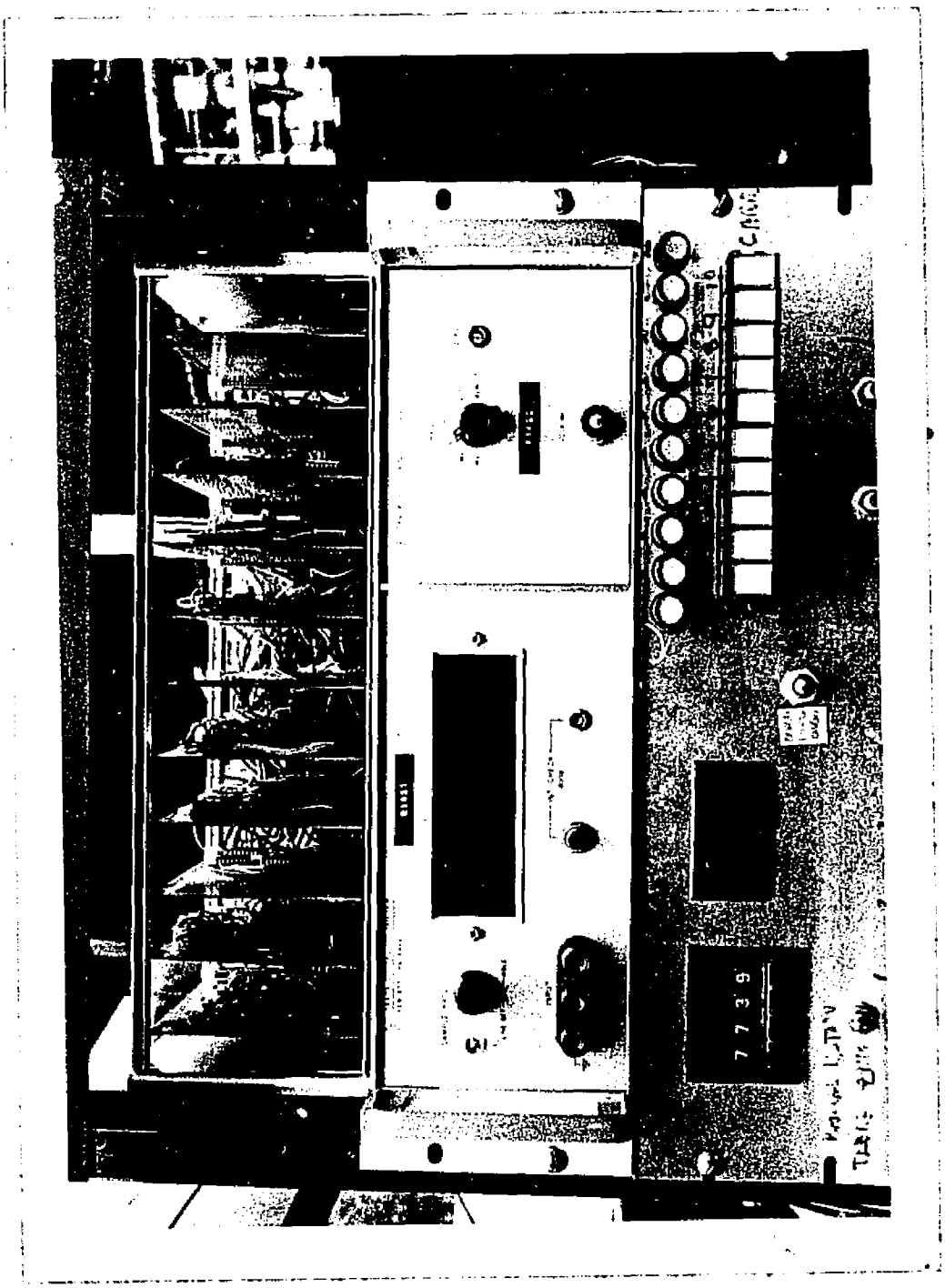

Figure 15. Transmitter electronics (front view). Close-up of transmitter integrated circuit electronics.

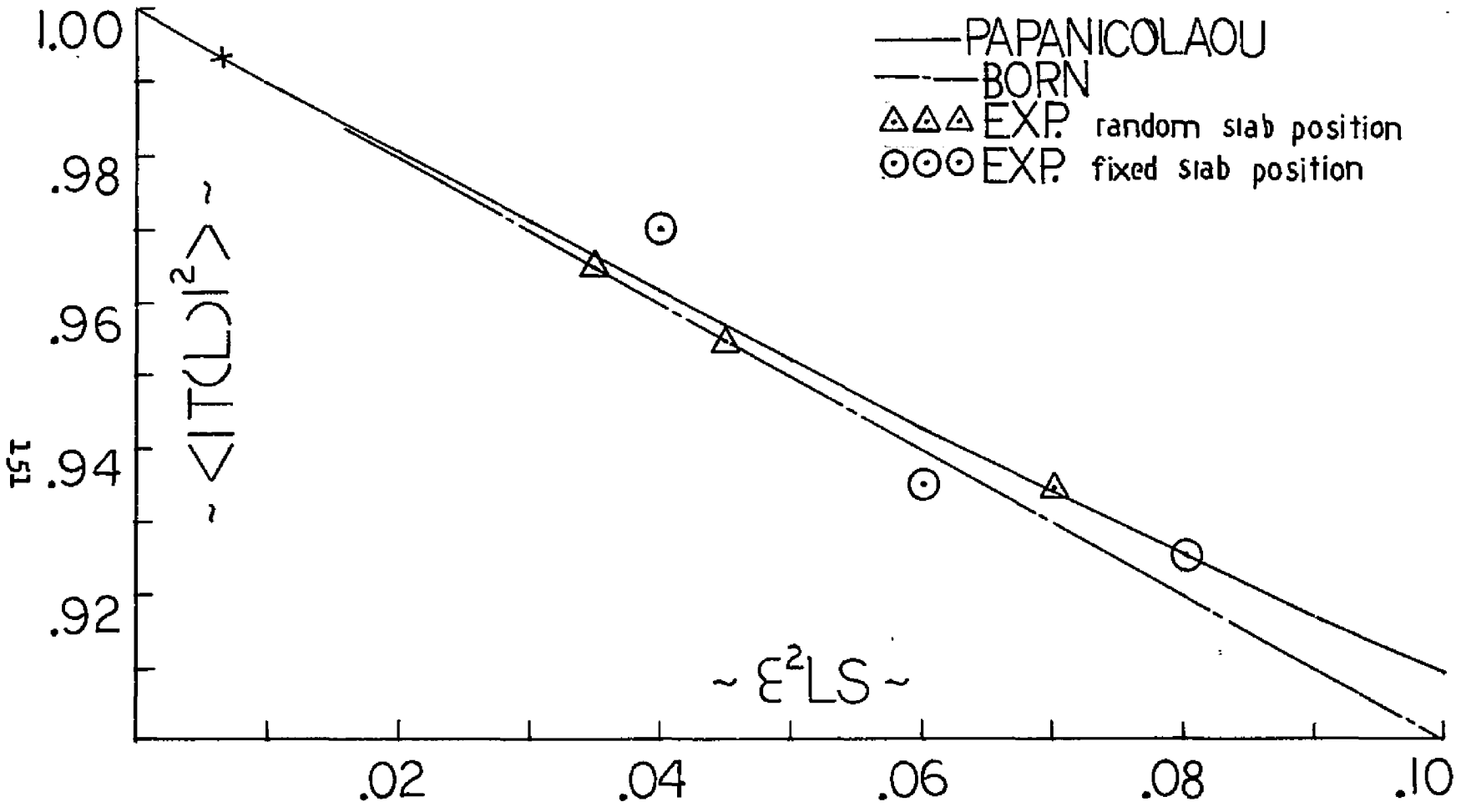

Figure 16. Plot of the experimental and theoretical mean power transmission coefficient as a function of the parameter E^2LS for a plane stratified medium consisting of randomly selected styrofoam slabs with both fixed and random positions.

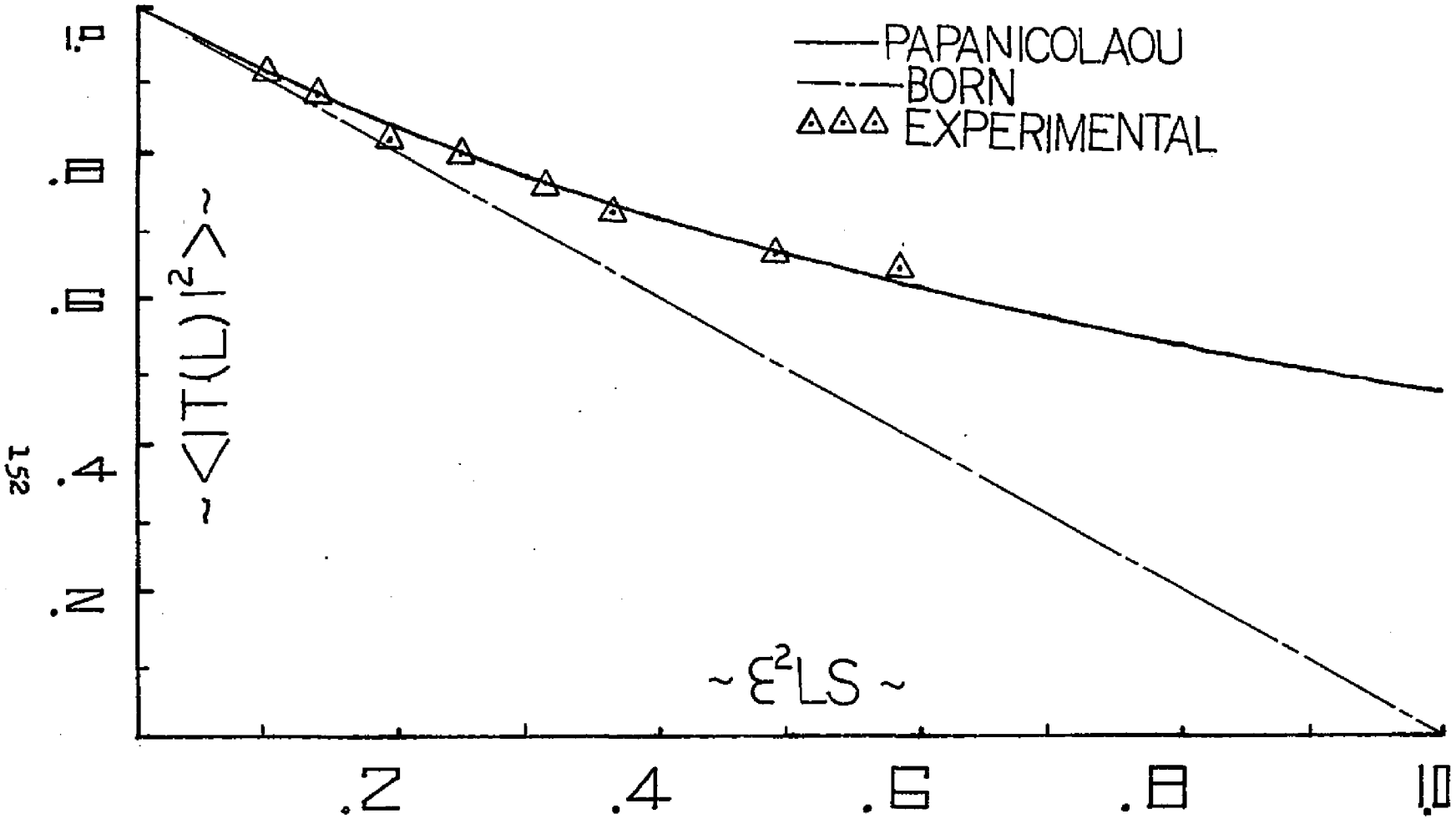

Figure 17. Plot of the experimental and theoretical mean power transmission coefficient as a function of the parameter. E^2LS for a plane stratified random medium consisting of randomly selected polystyrene slabs with fixed positions.

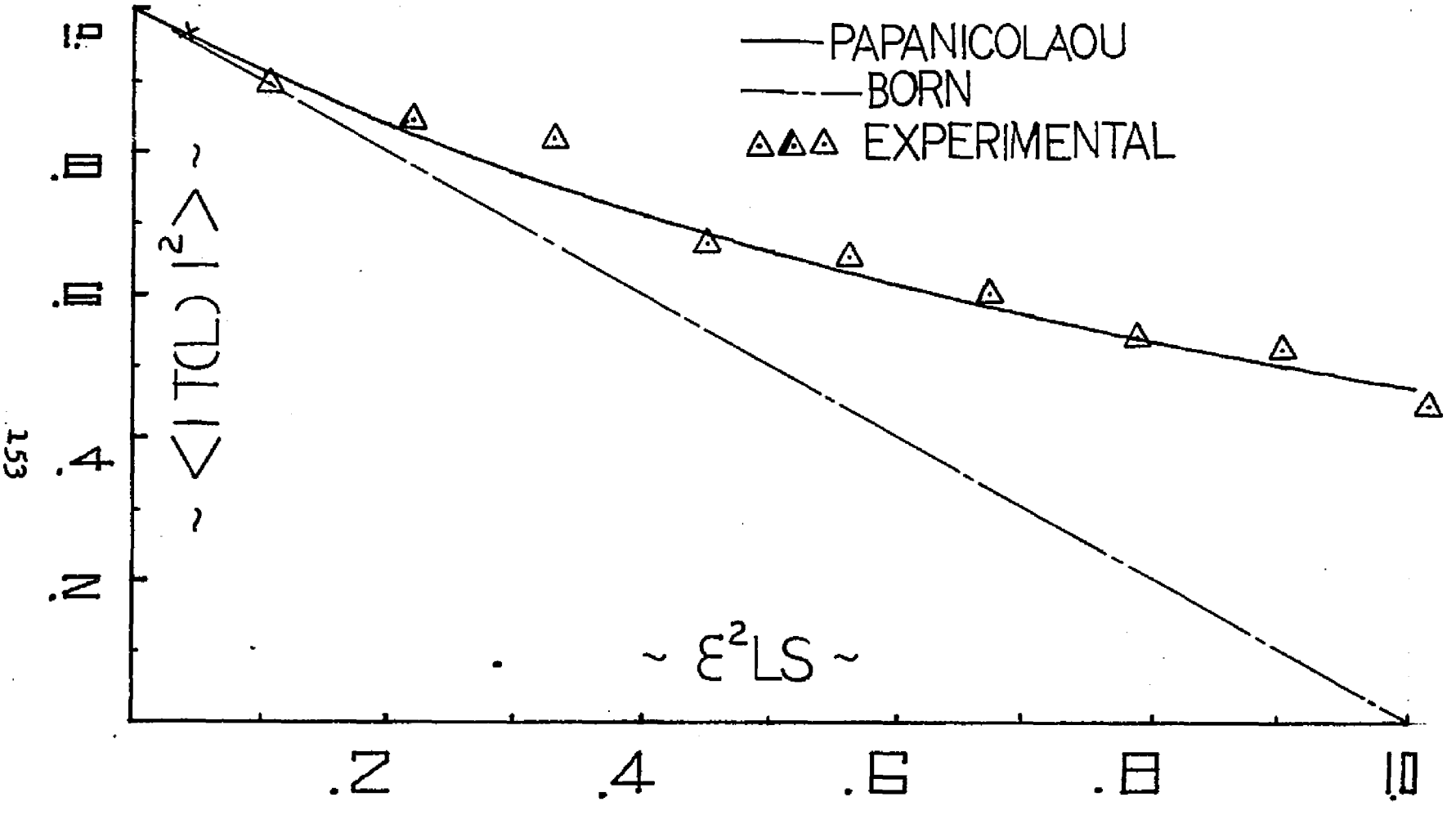

Figure 19. Plot of the experimental and theoretical mean power transmission coefficient as a function of the parameter E^2LS for a medium consisting of fixed positioned randomly selected conducting styrofoam slabs with strips.

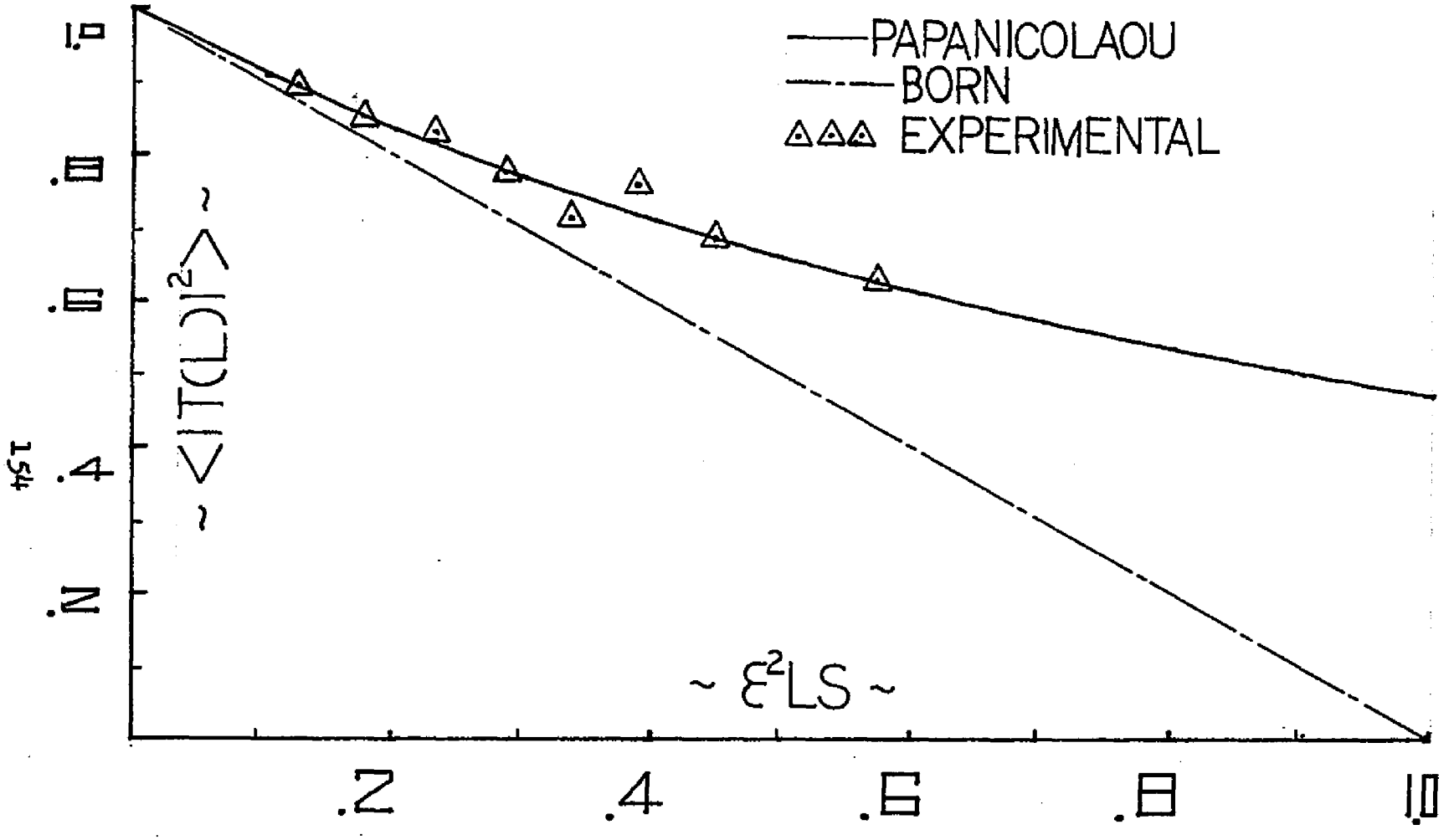

Figure 18. Plot of the experimental and theoretical mean power transmission coefficient as a function of the parameter E^2LS for a plane stratified medium consisting of randomly selected polystyrene slabs with random positions.

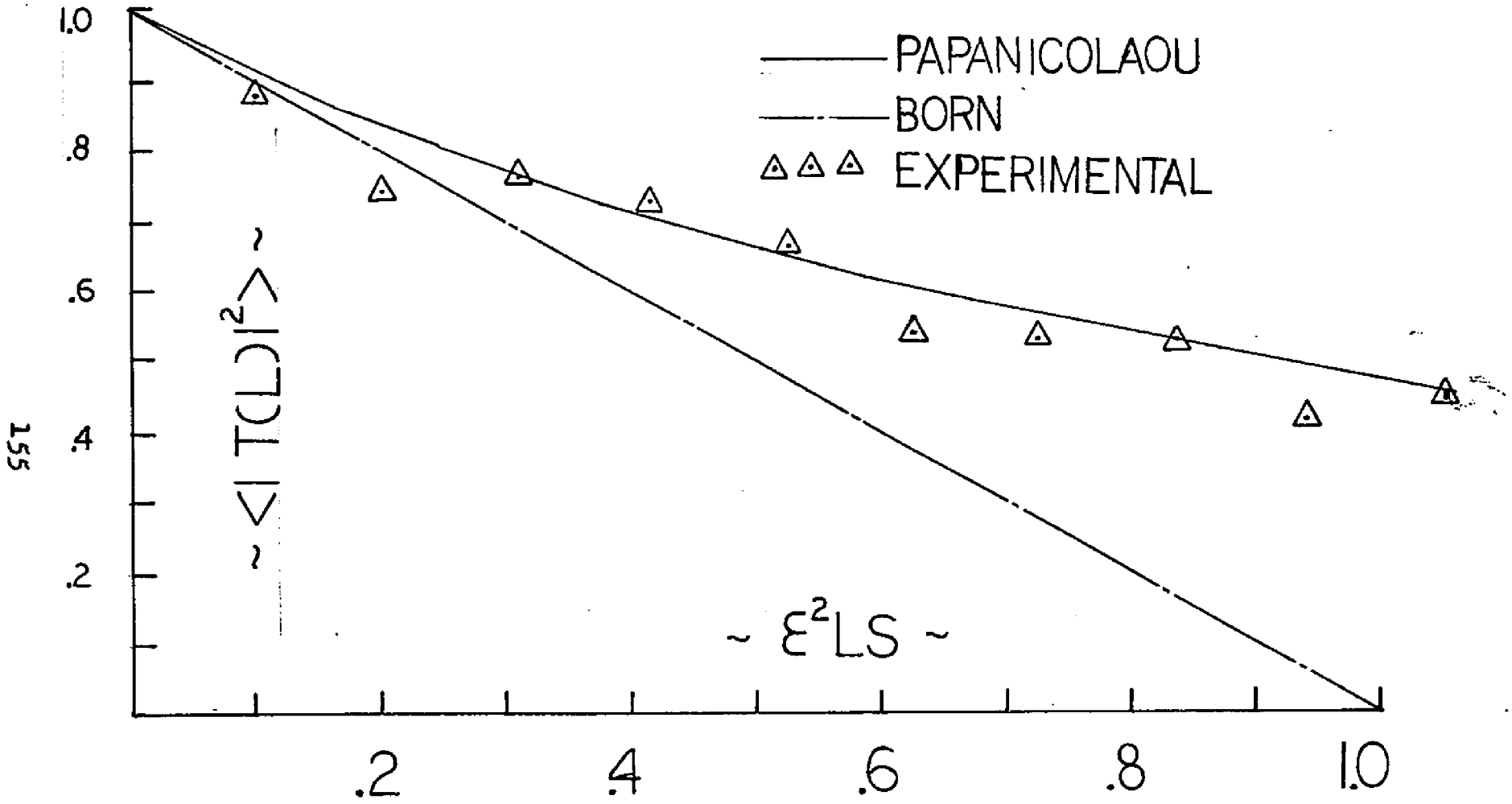

Figure 20. Plot of the experimental and theoretical mean power transmission coefficient as a function of the parameter E^2LS for a medium consisting of randomly selected and randomly positioned styrofoam slabs with conducting strips.

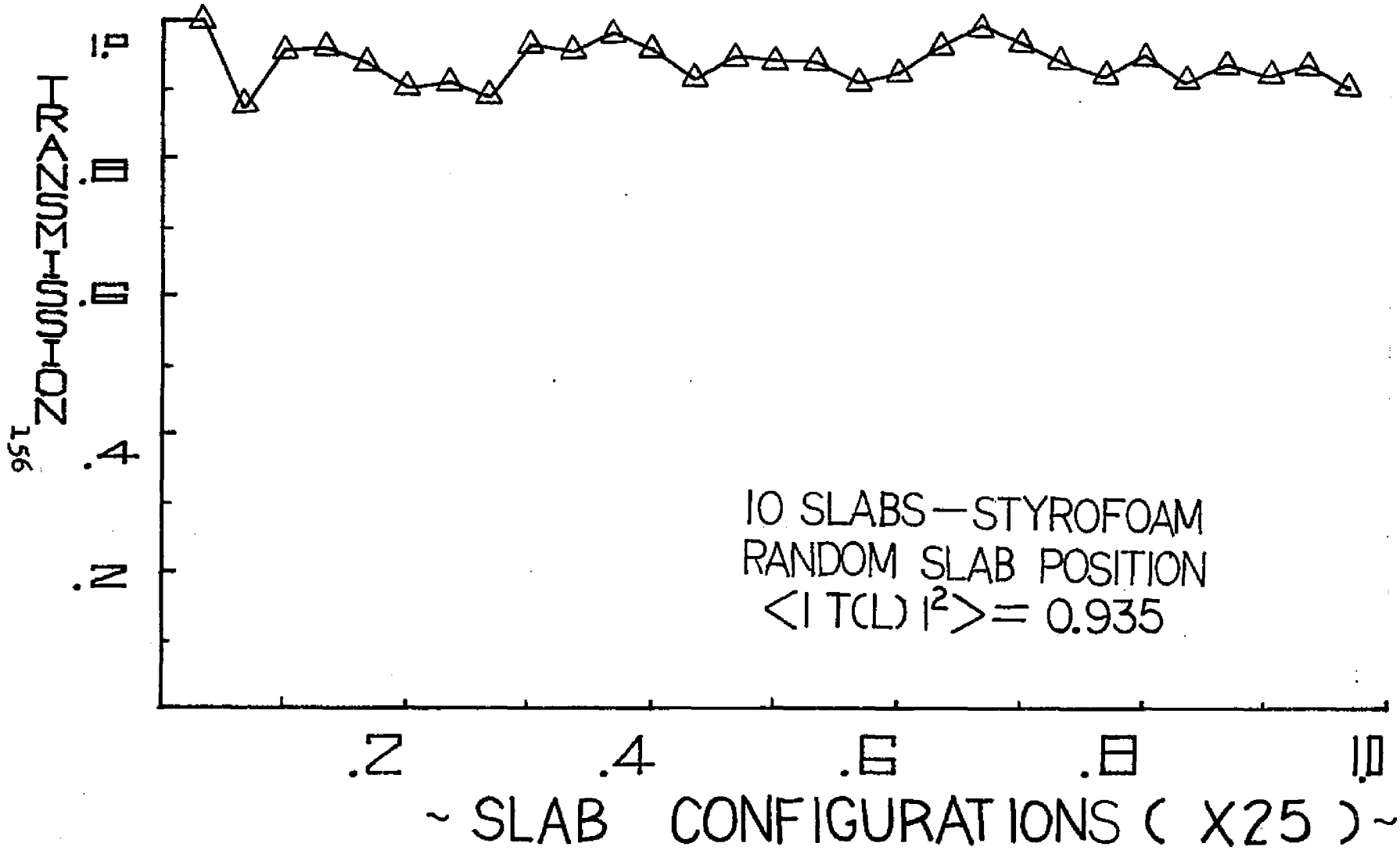

Figure 21. Plot of the experimental power transmission coefficient as a function of slab configuration for a medium consisting of ten (10) randomly selected and randomly positioned styrofoam slabs.

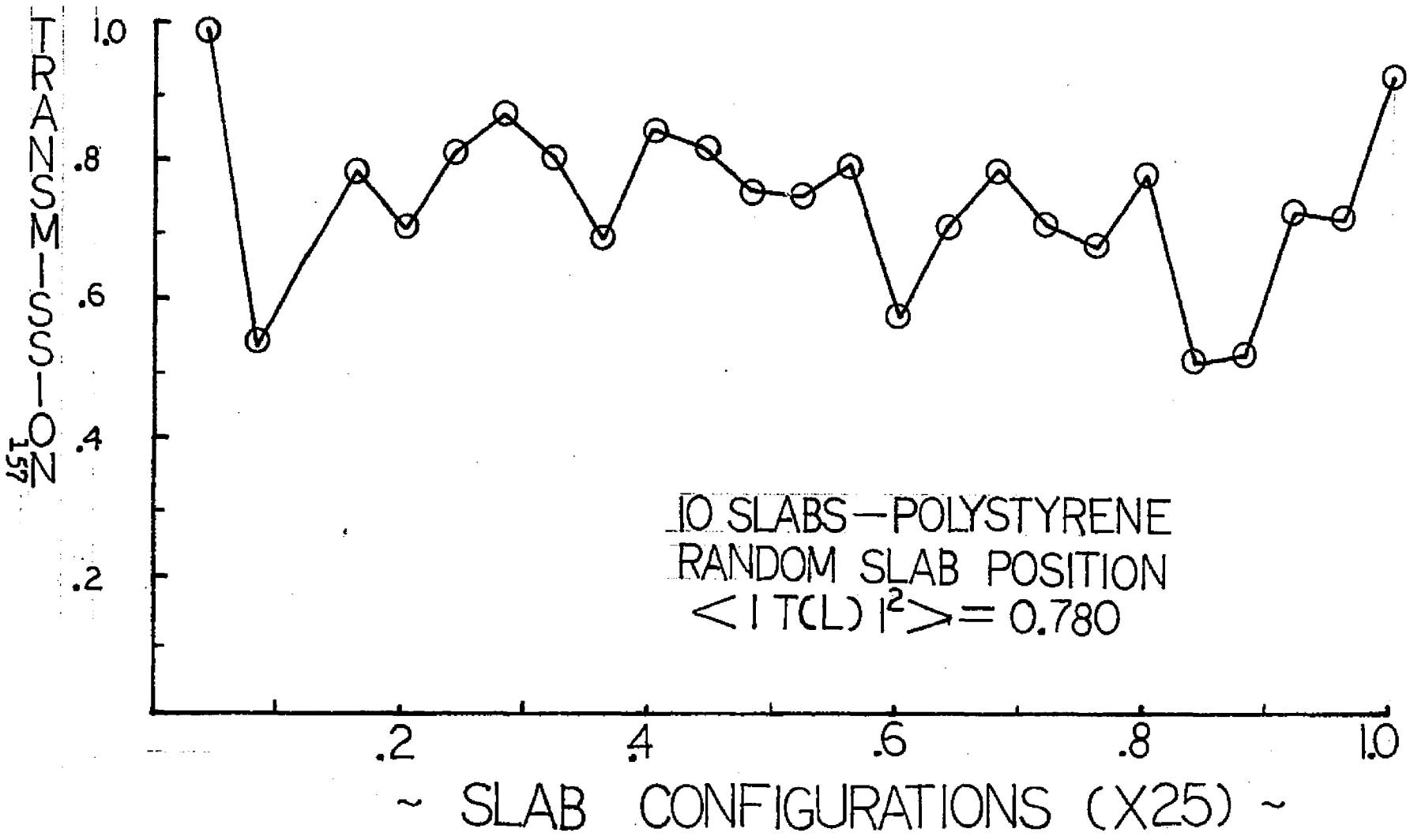

Figure 22. Plot of the experimental power transmission coefficient as a function of slab configuration for a medium consisting of ten (10) randomly selected and randomly positioned polystyrene slabs.

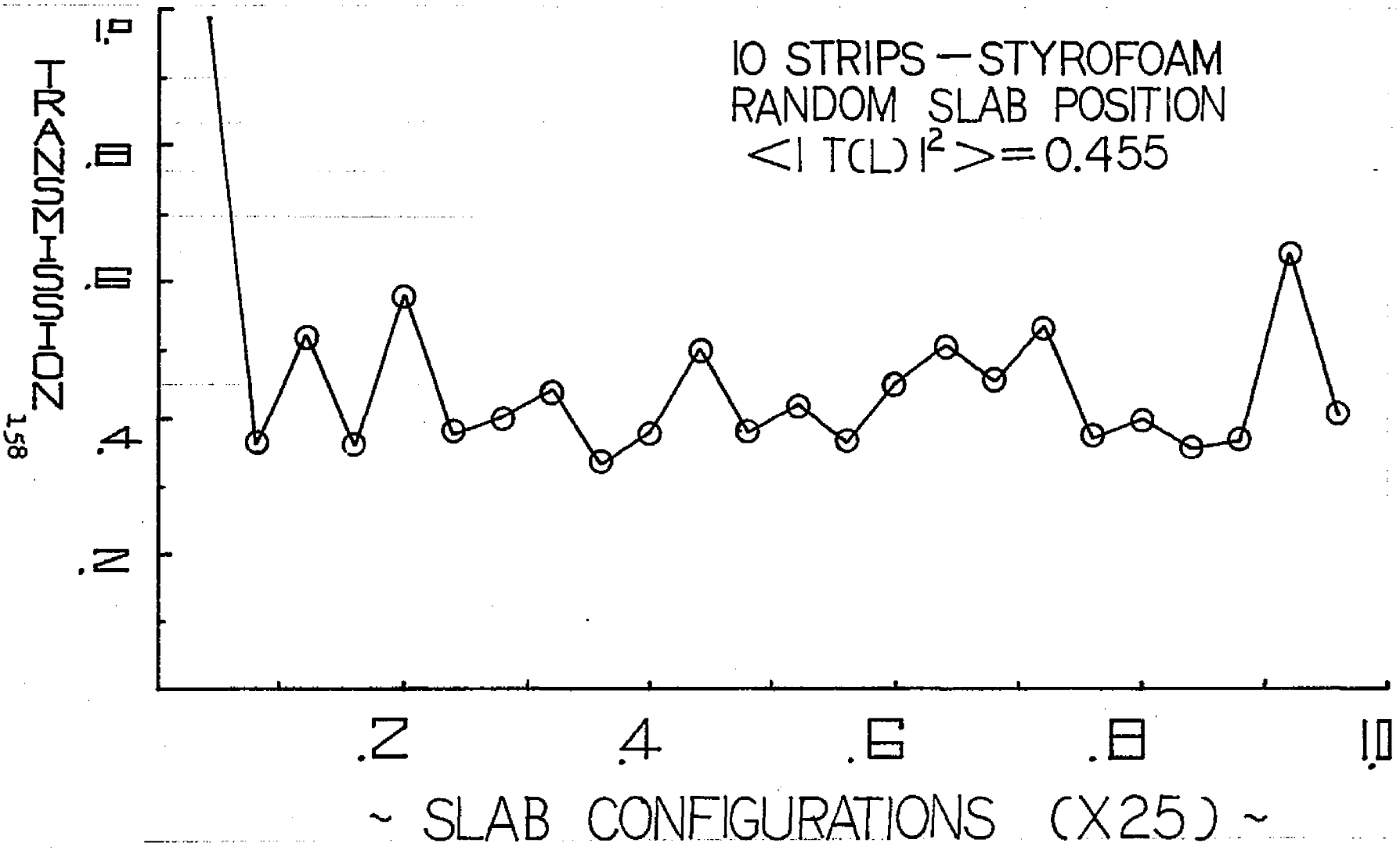

Figure 23. Plot of the experimental power transmission coefficient as a function of slab configuration for a medium consisting of ten (10) randomly selected and randomly positioned styrofoam slabs with conducted strips.

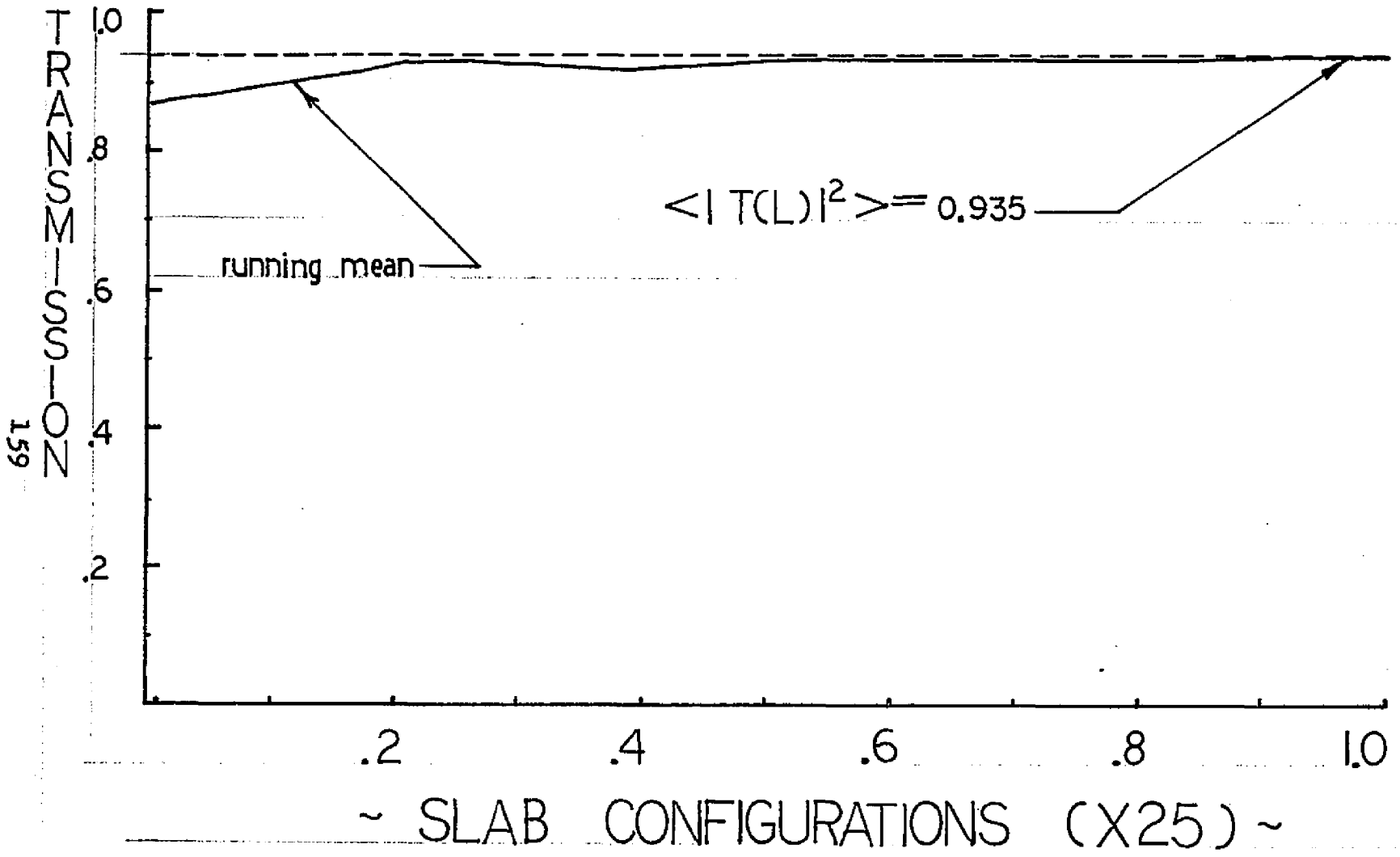

Figure 24. Plot of the running mean power transmission coefficient as a function of slab configuration for a medium consisting of ten (10) randomly selected and randomly positioned styrofoam slabs.

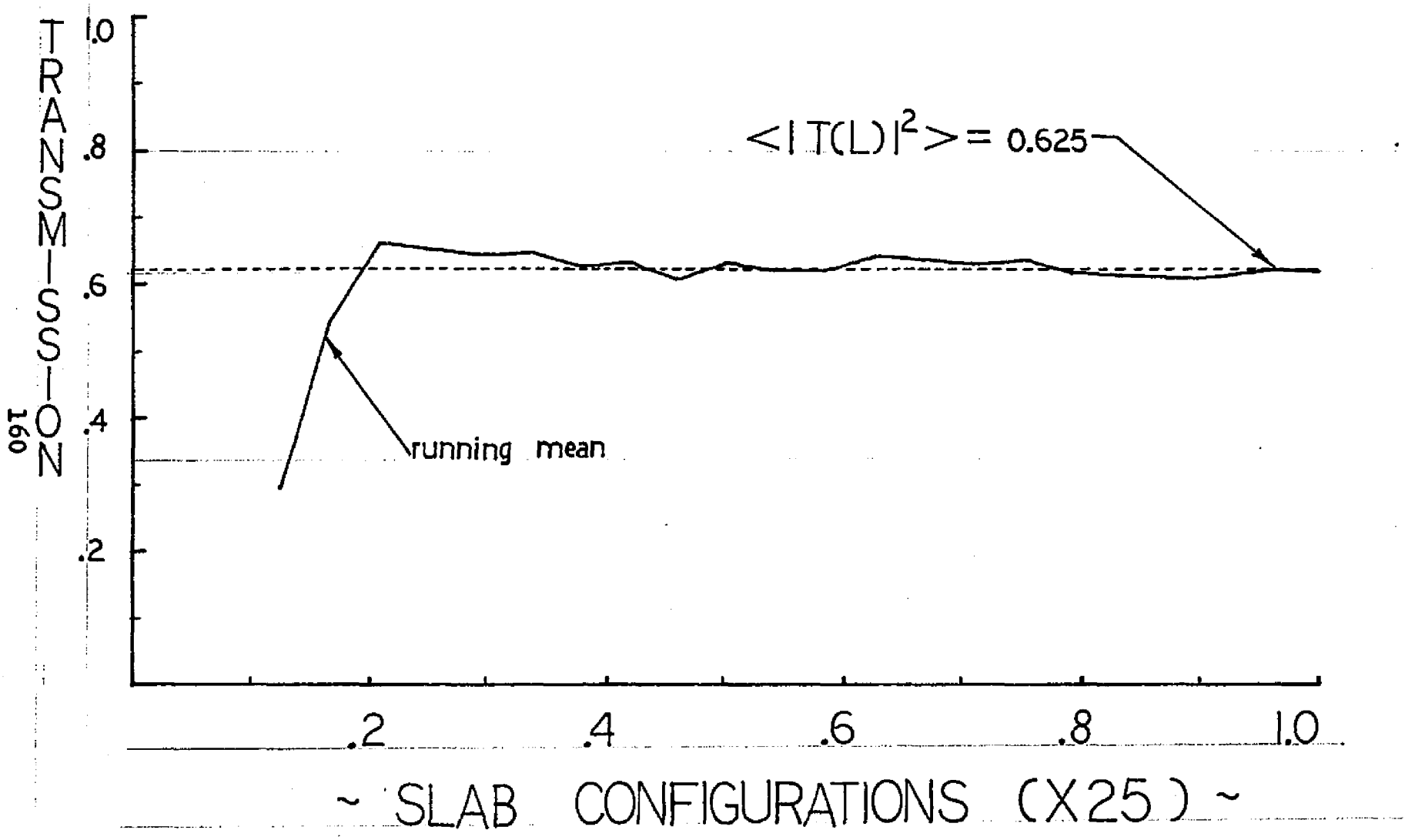

Figure 25. Plot of the running mean power transmission coefficient as a function of slab configuration for a medium consisting of twenty (20) randomly selected and randomly positioned polystyrene slabs.

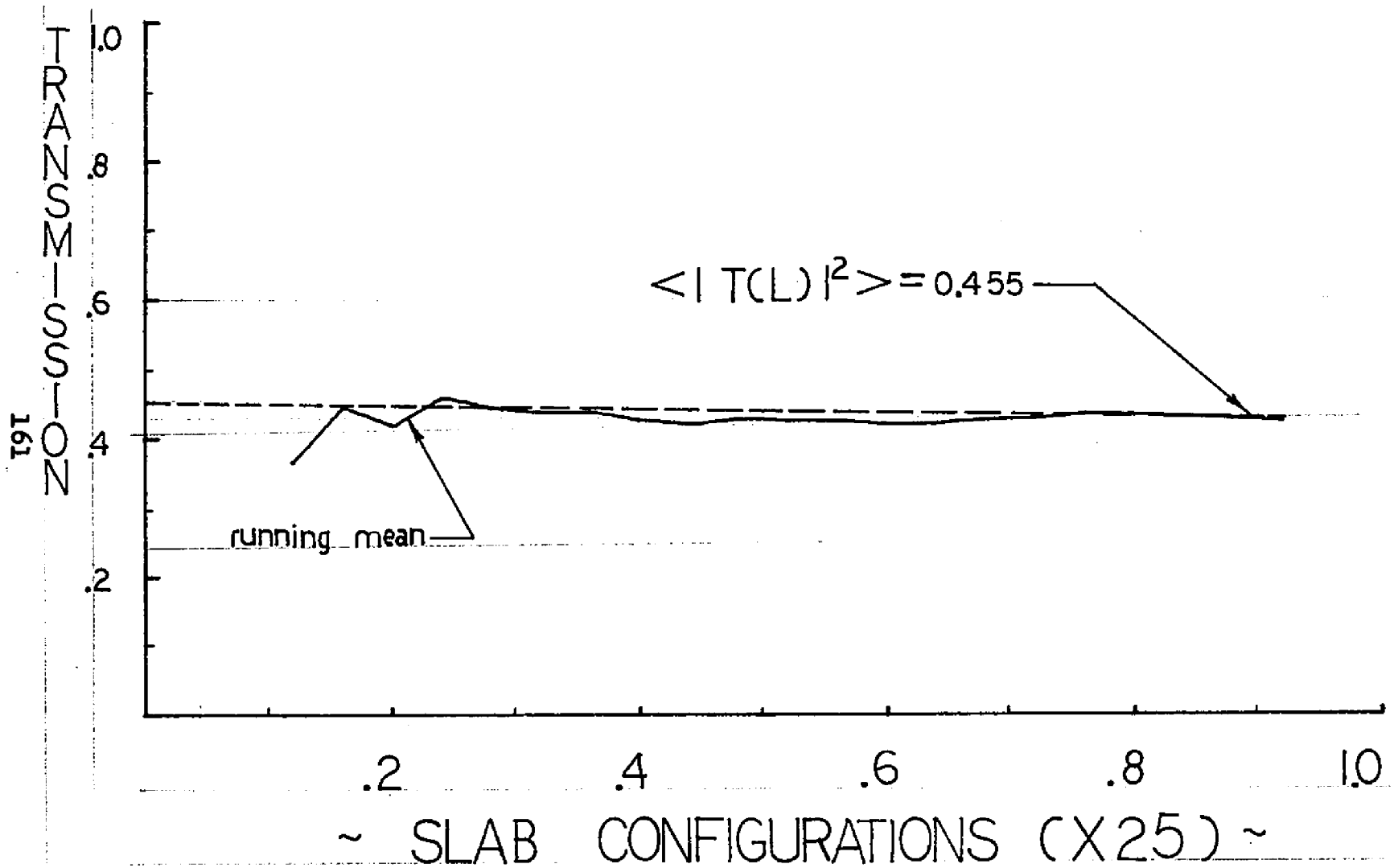

Figure 26. Plot of the running mean power transmission coefficient as a function of slab configuration for a medium consisting of ten (10) randomly selected and randomly positioned styrofoam slabs with conducted strips.

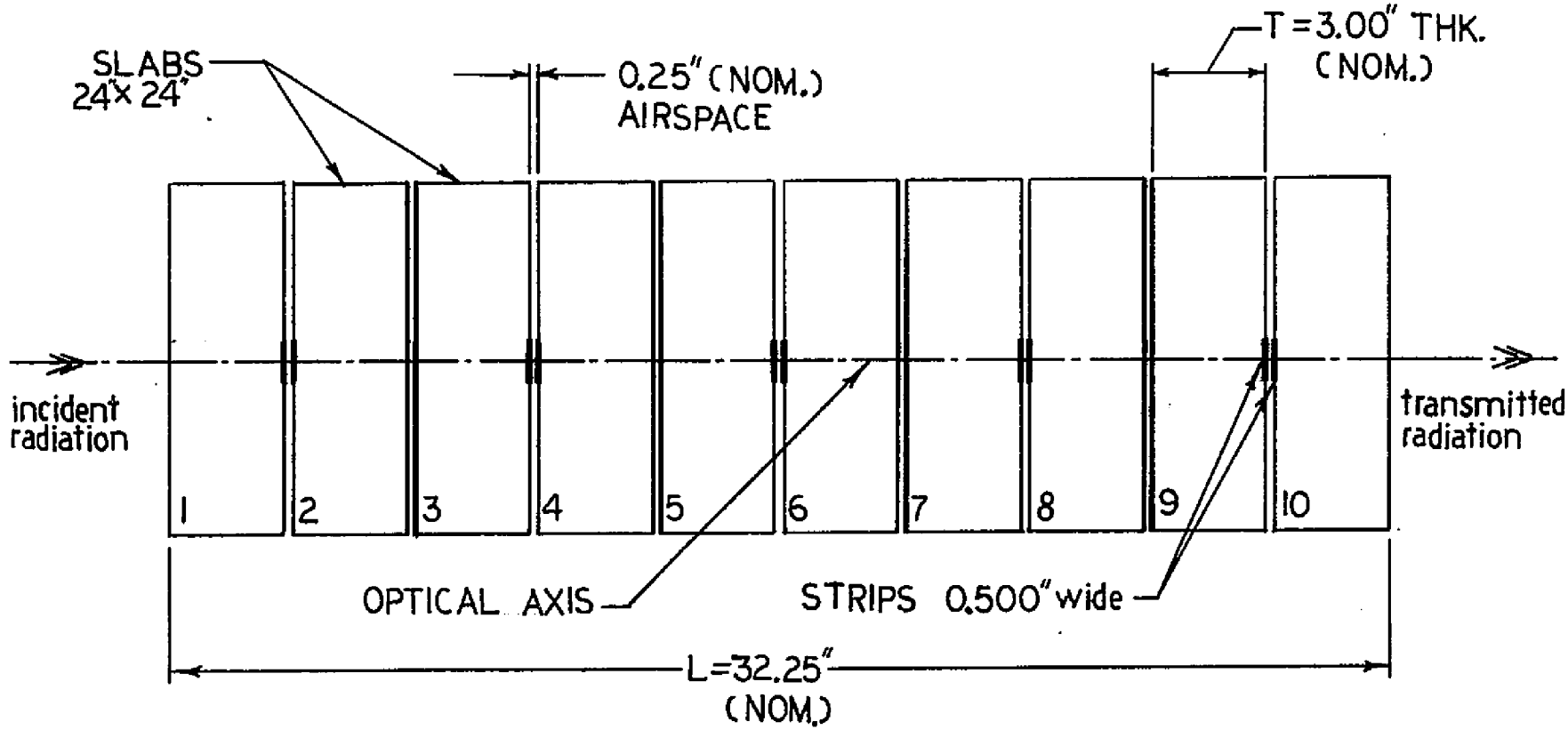

Figure 27. Schematic diagram of a styrofoam slab configuration with conducting strips.

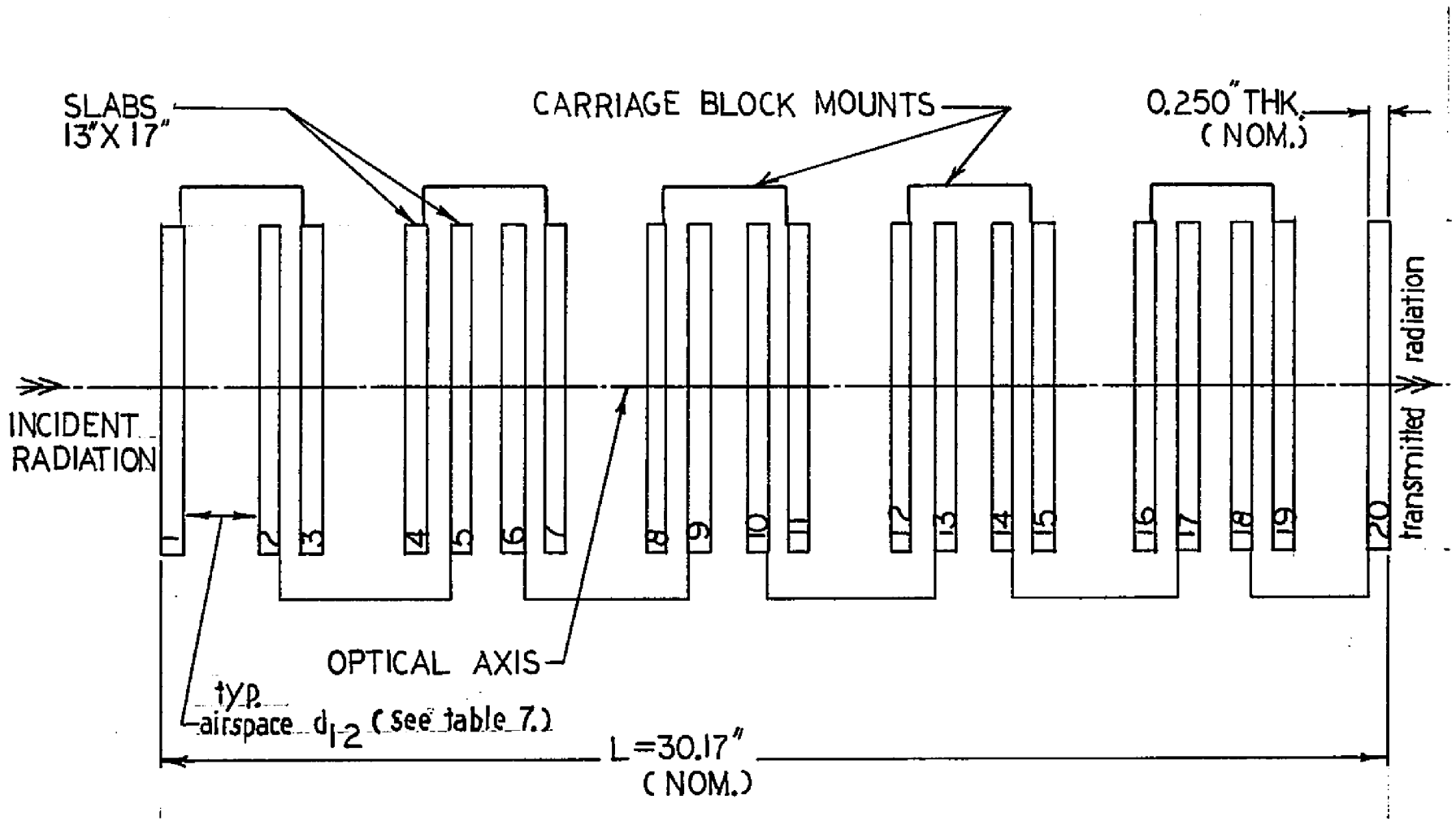

Figure 28. Schematic diagram of a polystyrene slab configuration.

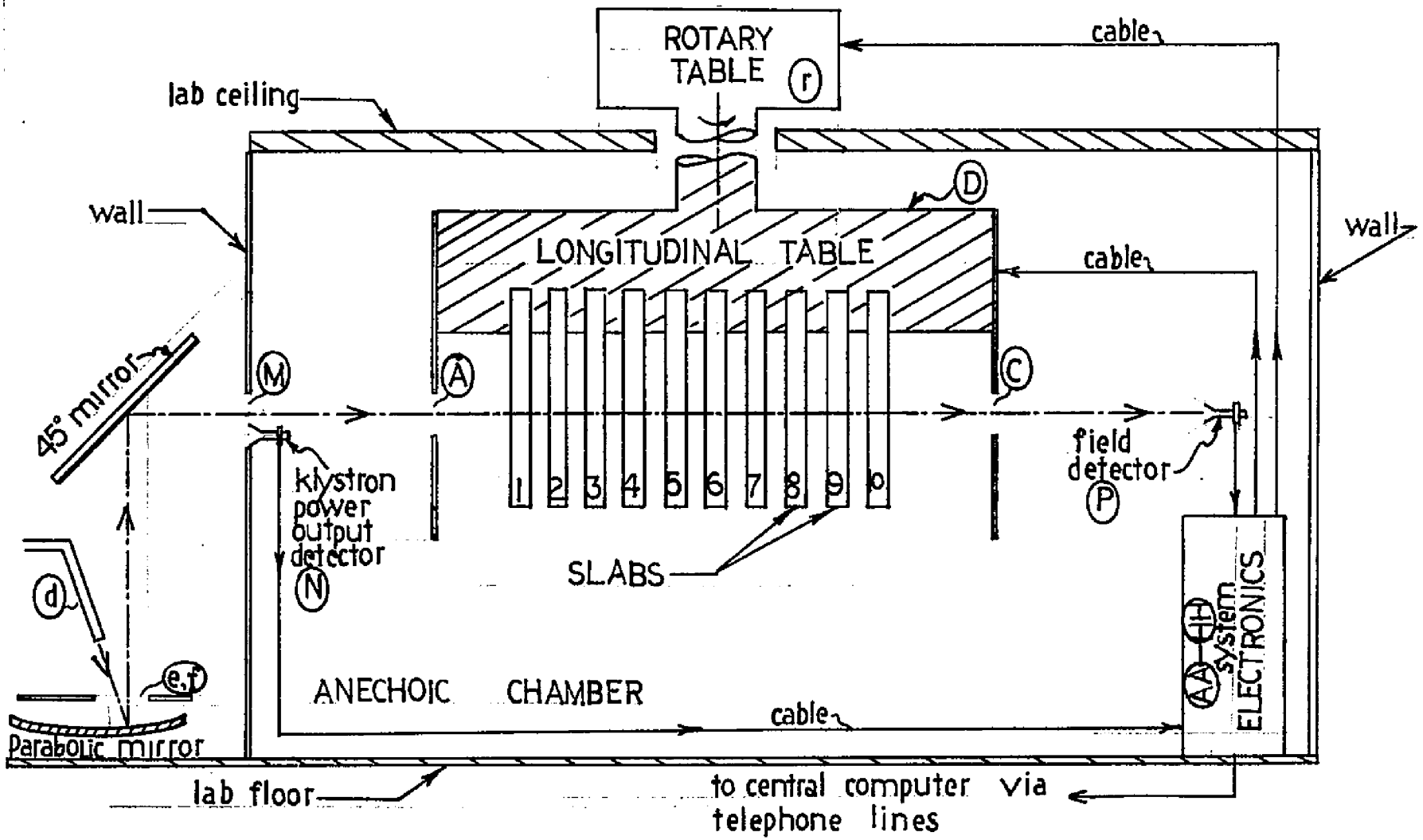

Figure 29.a Schematic system diagram.

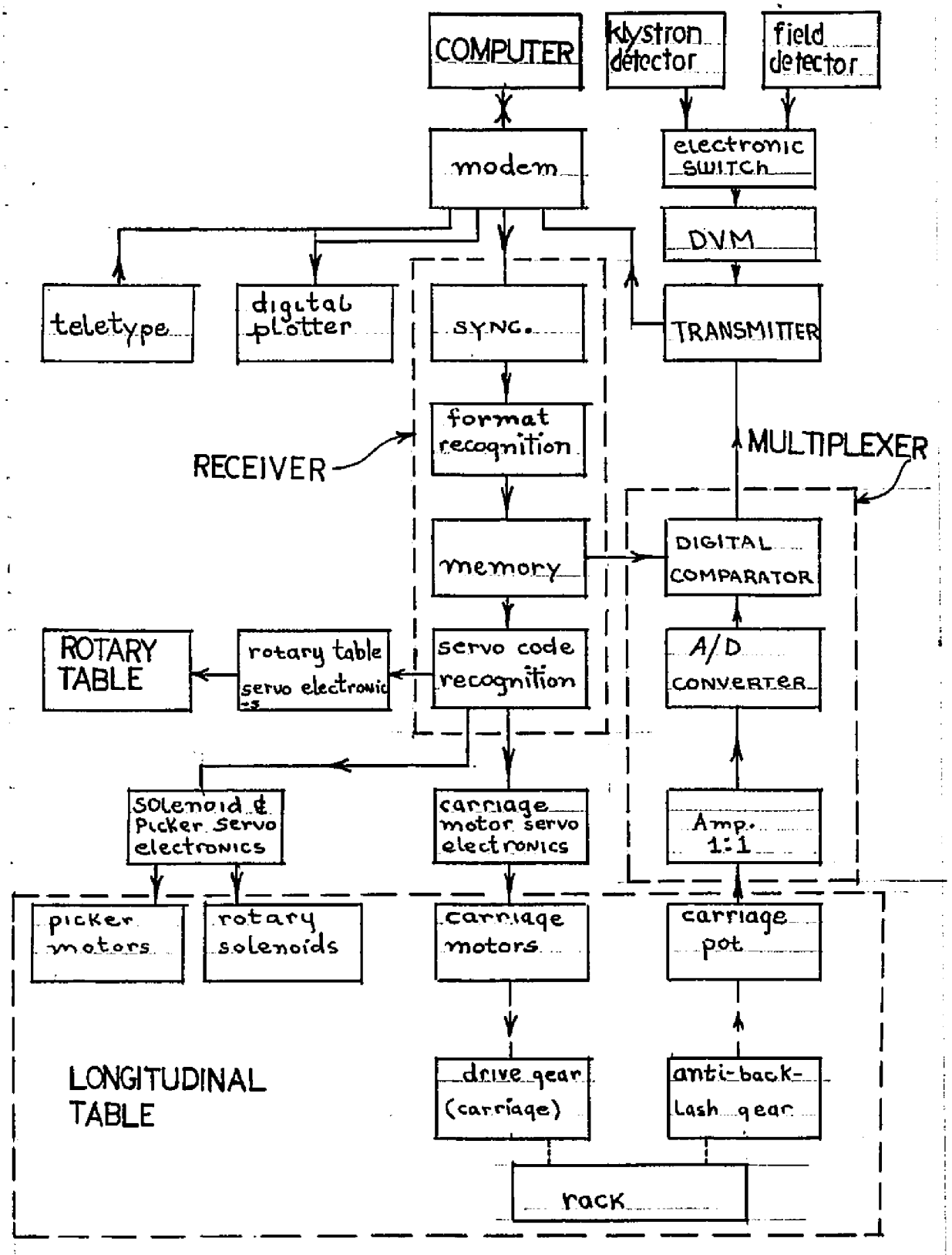
COMPUTER
klystron detector
field detector
modem
electronic switch
DVM
teletype
digital plotter
SYNC.
TRANSMITTER
format recognition
RECEIVER
MULTIPLEXER
memory
DIGITAL COMPARATOR
ROTARY TABLE
rotary table servo electronics
servo code recognition
A/D CONVERTER
solenoid & Picker Servo electronics
carriage motor servo electronics
Amp. 1:1
picker motors
rotary solenoids
carriage motors
carriage pot
LONGITUDINAL TABLE
drive gear (carriage)
anti-back-lash gear
rack

FIGURE. 29b

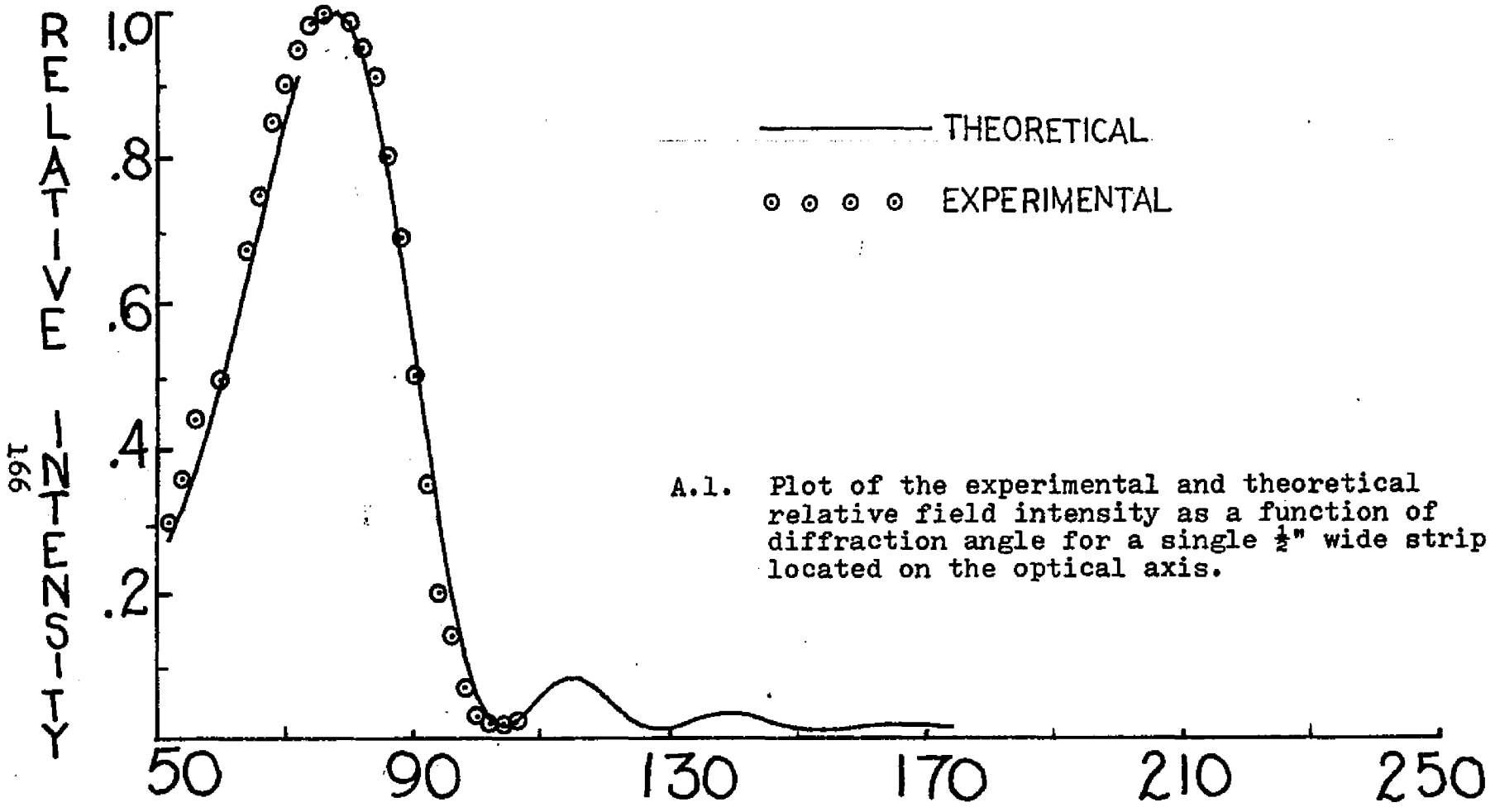

A.1. Plot of the experimental and theoretical relative field intensity as a function of diffraction angle for a single ½" wide strip located on the optical axis.

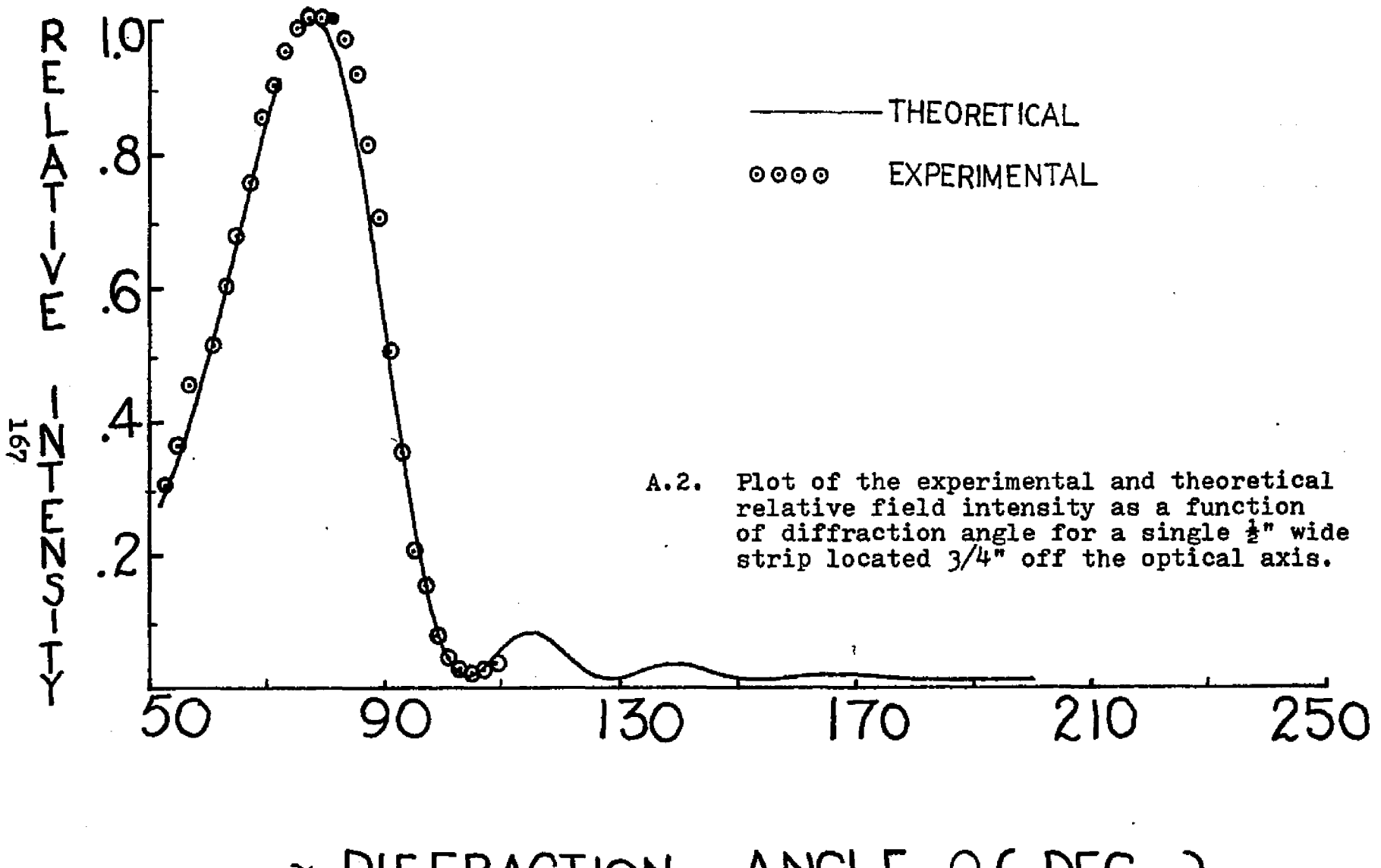

A.2. Plot of the experimental and theoretical relative field intensity as a function of diffraction angle for a single ½" wide strip located 3/4" off the optical axis.

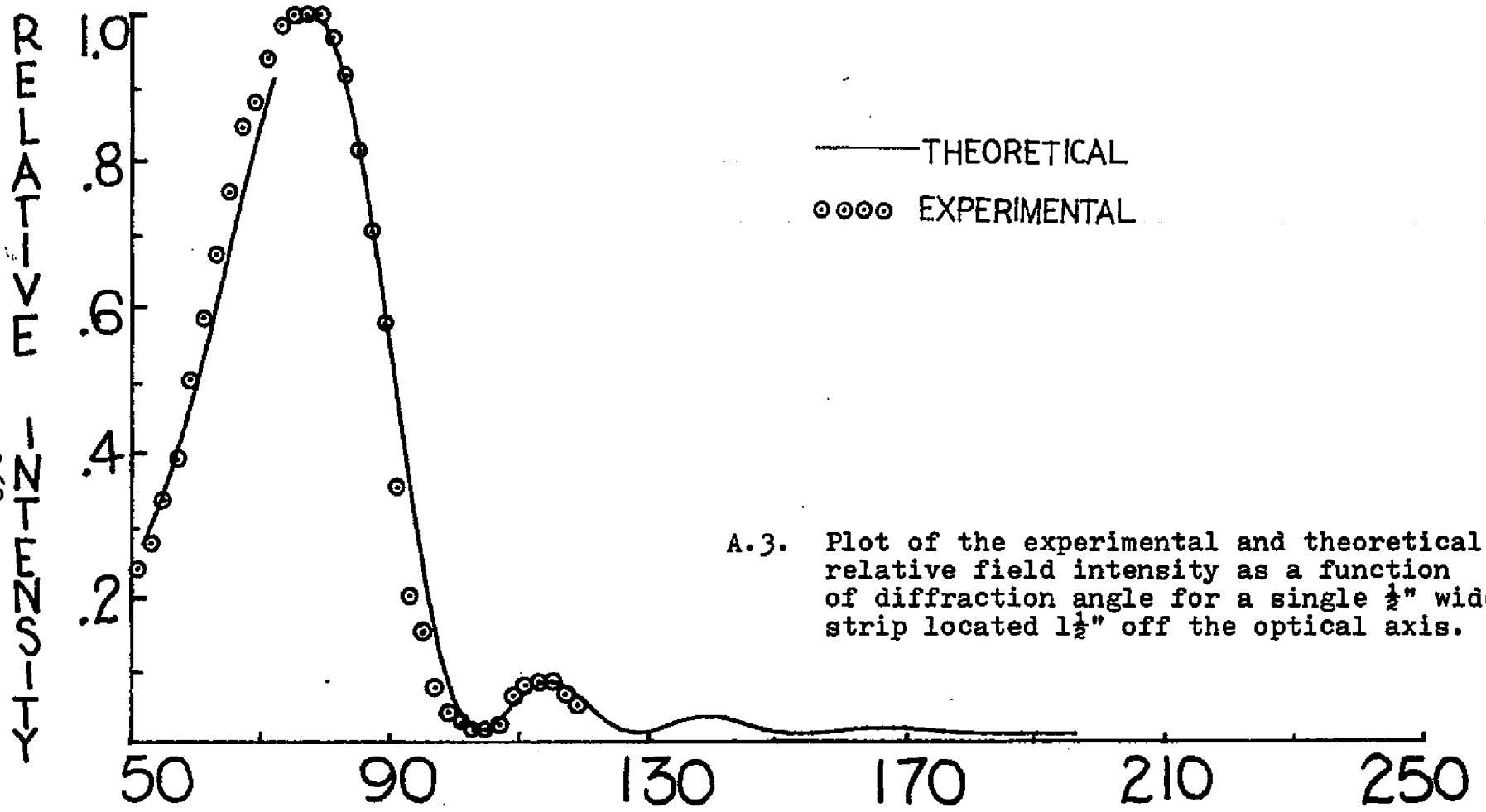

A.3. Plot of the experimental and theoretical relative field intensity as a function of diffraction angle for a single ½" wide strip located 1½" off the optical axis.

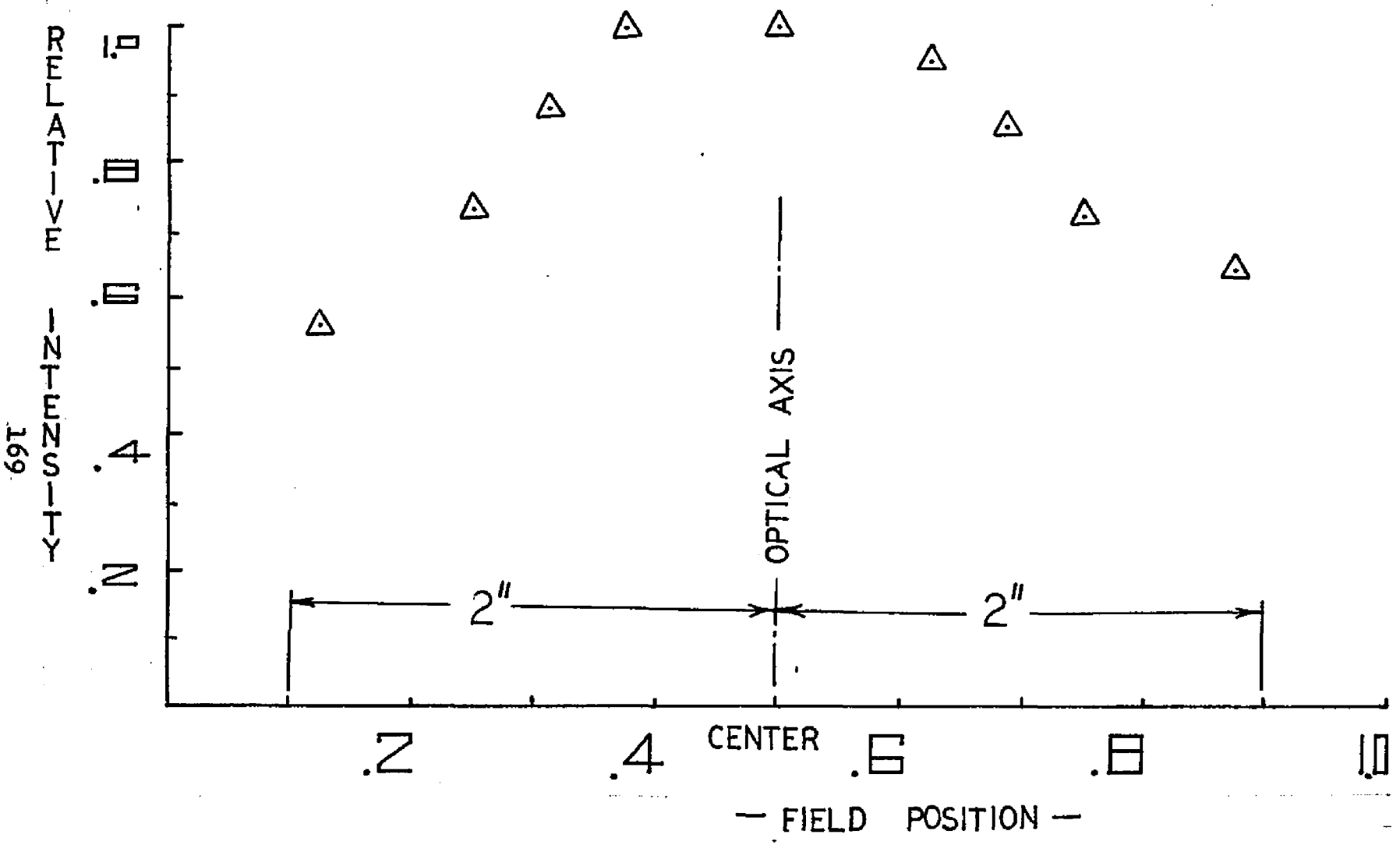

A.4. Plot of the experimental relative field intensity as a function of field position in the incident microwave beam.

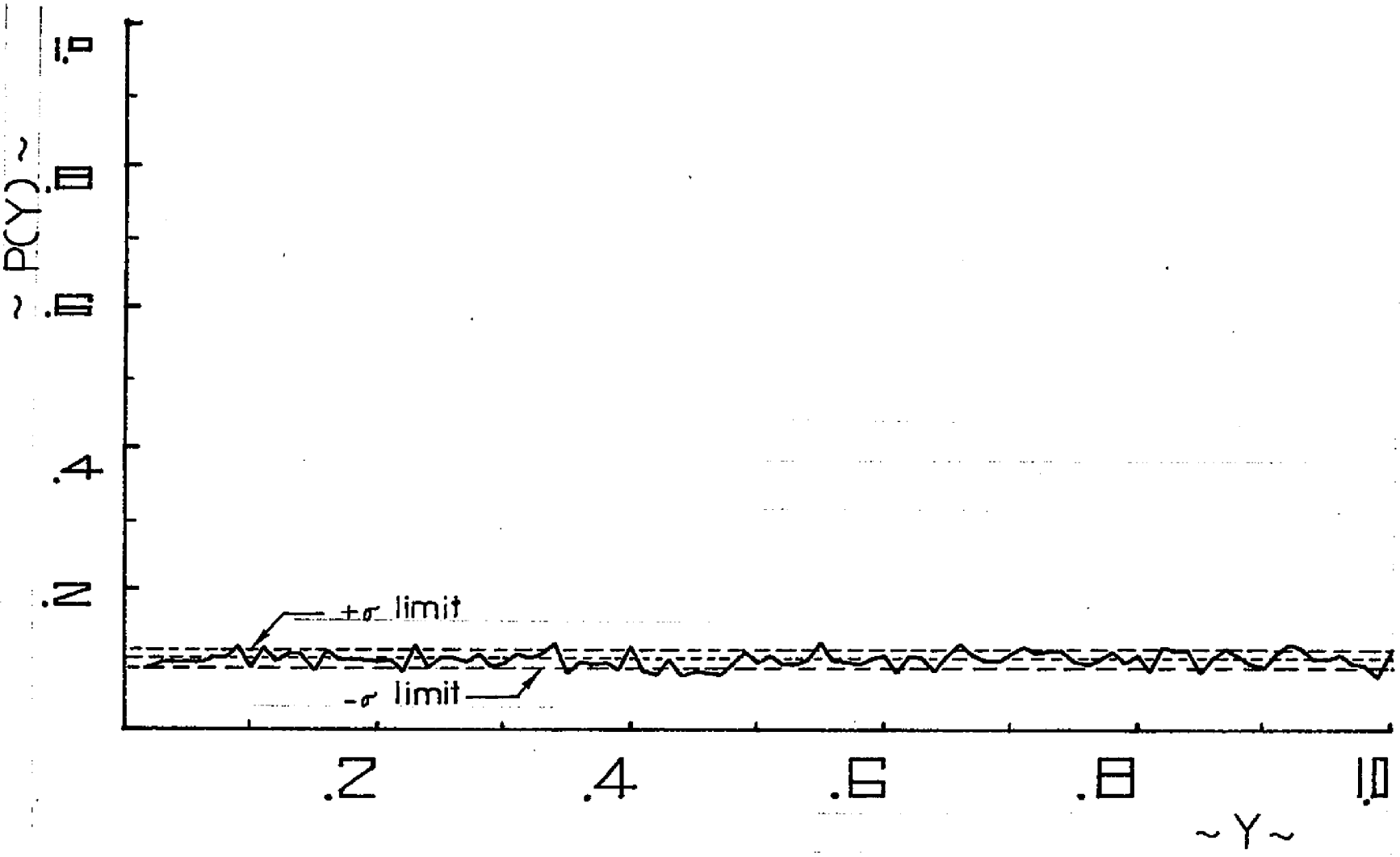

A.5. Plot of random number probability density as a function of random number magnitude for Xerox Sigma 7 Digital Computer random number generator subroutine.

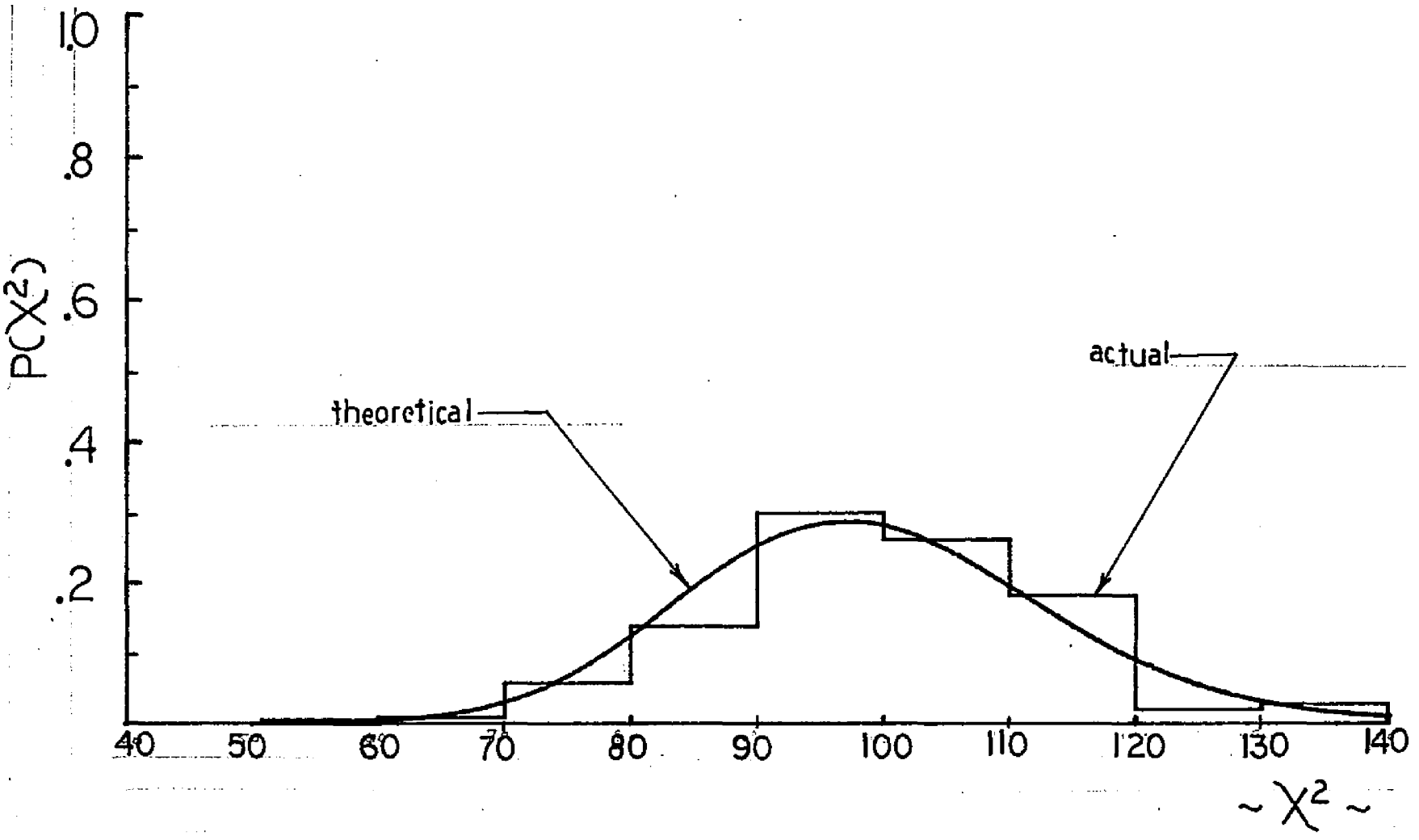

A.6. Plot of actual and theoretical values of the Chi Square probability density as a function of Chi Square for Xerox Sigma 7 Digital Computer random number generator subroutine.

References

1. Adams, R. N., "A Modified Coefficient for Layered Media," Rad. Sci. 3, 299-301, (1968).
2. Salzberg, B., "Propagation of Electromagnetic Waves through a Stratified Medium. I," J. Opt. Soc. Am., 40, 465-470, (1950).
3. Miller, J. C., "Reflection from an Absorbing Multilayer System," J. Opt. Soc. Am., 58, 1604-1606, (1968).
4. Harrison, M., "Scattering Theory for One-Dimensional Problems," J. Acous. Soc. Am., 37, 84-89, (1964).
5. Bennett, H. S., "The Electromagnetic Transmission Characteristics of the Two-Dimensional Lattic Medium, J. Appl. Phys., 24, 785-810, (1953).
6. Ott, R. H., "Scattering by a Two-Dimensional Periodic Array of Narrow Plates," Rad. Sci., 2, 1347-1359, (1967).
7. Waterman, P. C., "Multiple Scattering of Waves," J. Math. Phys., 2, 512-537, (1961).
8. Twersky, V., "On Scattering of Waves by Random Distributions. II Two-Space Scatterer Formalism," J. Math. Phys. 3, 724-734, (1962).
9. Karal, F. C., and Keller, J. B., "Elastic, Electromagnetic, and Other Waves in a Random Medium," J. Math. Phys. 5, 537-547, (1964).
10. Chen, Y. M., "On Wave Propagation in Large Waveguides Containing Random Media," Rad. Sci., 1, 697-708, (1966).
11. Bassanini, P., "Wave Propagation in a One-Dimensional Random Medium," Rad. Sci. 2, 429-436, (1967).

12. Frisch, U., "Wave Propagation in a Random Medium," Probabilistic Methods in Applied Mathematics, Vol. 1, A. T. Bharucha-Reid, ed., (Academic Press, New York, 1968), 75-198.

13. Papanicolaou, G. C., "Wave Propagation in a One-Dimensional Random Medium," Siam. J. Appl. Math. 21, 13-18, (1971).

14. Papanicolaou, G. C., "Stochastic Differential Equations with Application to Random Harmonic Oscillators and Wave Propagation in Random Media," Siam. J. Appl. Math. 21, 287-305, (1971).

15. Morrison, J. A., Papanicolaou, G. C., and Keller, J. B., "Mean Power Transmission Through a Slab of Random Medium," Comm. Pure Appl. Math. 24, 473-489, (1971).

16. Keller, J. B., "Geometrical Theory of Diffraction," J. Opt. Soc. 52, 116-130 (1962).

17. Ref. 13, p. 18.

18. Born, M. and Wolf, E., "Principles of Optics," (Pergamon Press, New York, 1965), 55-70.

19. Sterling, T. D., "Introduction to Statistical Data Processing," (Prentice-Hall, New York, 1968), 287-299.

20. Adams, R. N. and Denman, E. D., "Wave Propagation and Turbulent Media," Modern Analytic and Computational Methods in Science and Mathematics, R. E. Bellman, ed., (American Elsevier, New York, 1966), Appendix 3, p. 54.

21. Ref. 20, p. 56.

22. Bernstein, A., "Handbook of Statistics Solutions for the Behavioral Sciences," (Holt, Rinehart and Winston, New York, 1964), p. 16.

23. Ref. 20, p. 57.

24. De Acetis, L. A., "Kirchhoff Theory and Keller's Geometrical Theory Applied to Experimental Diffraction by Two Long, Thin, Conducting Strips," PH.D. Thesis, City University of New York, Queens College, New York (1969), pp. 4-14.

25. Brekhovskikh, L. M., "Waves in Layered Media," (Academic Press, New York, 1960), pp. 44-50.

26. Ref. 13, p. 18.

27. Papoulis, A., "Probability, Random Variables and Stochastic Processes," (McGraw-Hill, New York, 1965), p. 294.

28. Ref. 27, p. 295.

29. Ref. 13, p. 14.

30. Purcell, E. M., "Measurements of Standing Waves," Technique of Microwave Measurements, C. G. Montgomery, ed., (Boston Technical, Mass., 1964), pp. 478-480.

31. Ref. 30, p. 476.

32. Ref. 13, p. 13.

33. De Wolf, D. A., "Multiple Scattering in a Random Continuum," Rad. Sci. 2, 1379, (1967).

34. Ref. 27, p. 294.

35. Ref. 13, p. 14.

36. Ref. 24, p. 105.

37. Ref. 24, p. 110.

38. Ref. 24, p. 85.

39. Ref. 24, p. 105.

40. See Appendix A. and Ref. 24, p. 87.

41. Ref. 24, p. 11.

42. Ref. 13, p. 13.

43. Hochstim, A. R. and Martens, C. P., "Radar Scattering from a Plane Parallel Turbulent Plasma Slab with Step Function Fluctuations of Electron Density," (Institute for Defense Analysis Contract DAHC1567C0011, 1967), p. 35.

44. Ref. 15

45. Ref. 13, p. 13.

46. Ref. 13, p. 18.

47. Ref. 13, p. 13.

48. Ref. 4.

49. Ref. 33.

50. Ref. 11.

51. Ref. 10.

52. Ref. 8.

53. Ref. 33, p. 1379.

54. Ref. 2.

55. Ref. 25.

56. Ref. 20, pp. 10-29.

57. The program for the Brekhovskikh, equations was written by Professor L. Diesendruck, Queens College, City University of New York, New York.

58. Chernov, L. A., "Wave Propagation in a Random Medium," (Dover, New York, 1960), p. 5.

59. Ref. 19, pp. 338-339.

60. Hemmerle, W. J., "Statistical Computations on a Digital Computer," (Blaisdell, Mass., 1967), p. 103.

61. Lazar, I., and R. D. Hatcher, "Exact Solution and Numerical and Graphical Presentation for Diffraction of Electromagnetic Waves by a Single Strip," unpublished.

62. Ref. 16.

63. Ref. 24, pp. 46-75.

64. Cohn, S. B., "Analysis of a Metal-Strip Delay Structure for Microwave Lenses," Appl. Phys. 20, 257-262, (1948).

65. Ref. 20, p. 11.

66. Ref. 13, p. 14.

67. Ref. 27, pp. 301-302.

68. Private communication with Professor G. C. Papanicolaou, New York University, Courant Institute, New York.

69. Ref. 27, p. 30.

70. Ref. 12, p. 80.

71. Ref. 12, p. 80.

72. Ref. 15.

73. Ref. 14.

74. Ref. 15, p. 475

75. Hashminskii, R. Z., "A Limit Theorem for the Solutions of Differential Equations with Random Right Hand Sides," Theor. Probability Appl., 11, 390-406, (1966).

76. Ref. 14, p. 288.

77. Ref. 15, p. 473.

78. Ref. 14, p. 288.

79. Ref. 27, pp. 510-511, 538-539.

80. Reif, F., "Fundamentals of Statistical and Thermal Physics," (McGraw-Hill Book Company, New York, 1965), pp. 577-582.

81. Breiman, L., "Probability and Stochastic Processes," (Houghton Mifflin Co., New York, 1969), pp. 196-215.

82. Ref. 14, p. 303.